

Kaunas University of Technology
Faculty of Mechanical Engineering and Design

Investigation of Vehicle Muffler Acoustic Transmission Loss

Master's Final Degree Project

Aravind Vimaladass
Project author

Prof. Dr. Vaidas Lukosevicius
Supervisor

Kaunas, 2022



Kaunas University of Technology
Faculty of Mechanical Engineering and Design

Investigation of Vehicle Muffler Acoustic Transmission Loss

Master's Final Degree Project
Vehicle Engineering (6211EX021)

Aravind Vimaladass

Project author

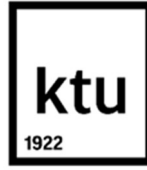
Prof. Dr. Vaidas Lukosevicius

Supervisor

Assoc. Prof. Dr. Robert Kersys

Reviewer

Kaunas, 2022



Kaunas University of Technology

Faculty of Mechanical Engineering and Design

Aravind Vimaladass

Investigation of Vehicle Muffler Acoustic Transmission Loss

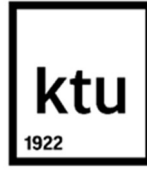
Declaration of Academic Integrity

I confirm the following:

1. I have prepared the final degree project independently and honestly without any violations of the copyrights or other rights of others, following the provisions of the Law on Copyrights and Related Rights of the Republic of Lithuania, the Regulations on the Management and Transfer of Intellectual Property of Kaunas University of Technology (hereinafter – University) and the ethical requirements stipulated by the Code of Academic Ethics of the University;
2. All the data and research results provided in the final degree project are correct and obtained legally; none of the parts of this project are plagiarised from any printed or electronic sources; all the quotations and references provided in the text of the final degree project are indicated in the list of references;
3. I have not paid anyone any monetary funds for the final degree project or the parts thereof unless required by the law;
4. I understand that in the case of any discovery of the fact of dishonesty or violation of any rights of others, the academic penalties will be imposed on me under the procedure applied at the University; I will be expelled from the University and my final degree project can be submitted to the Office of the Ombudsperson for Academic Ethics and Procedures in the examination of a possible violation of academic ethics.

Aravind Vimaladass

Confirmed electronically



Kaunas University of Technology

Faculty of Mechanical Engineering and Design

Study programme: Vehicle Engineering (6211EX021)

Task of the Master's Final Degree Project

Given to the student: Aravind Vimaladass

1. Title of the Project:

Investigation of Vehicle Muffler Acoustic Transmission Loss

Transporto priemonių duslintuvų garso perdavimo nuostolių tyrimas

2. Aim of the Project:

The project aims to find out which parameter affects the transmission loss in the muffler by changing the design framework with the comparison of how efficient these variables play a role.

3. Tasks of the Project:

1. Scientific papers are to be reviewed, to study the engine backpressure and transmission loss of the muffler.
2. A base muffler will be designed, the analytical and theoretical values will be compared with the experimental values to verify the setup for the transmission loss simulation.
3. Three types of mufflers are designed, and simulations must be conducted to calculate the backpressure.
4. Harmonic acoustics must be conducted to find out the transmission loss of all the mufflers.
5. Perforated pipes and baffle plates are included in the previously designed mufflers with variations in design parameters to investigate the significance of transmission loss.

4. Structure of the Text Part:

- I. Introduction
- II. Literature Review
- III. Methodology
- IV. Results and Discussion
- V. Conclusion
- VI. List of reference

5. Consultants of the Project:

Author of the Final Degree Project Aravind Vimaladass 2020-09-15
(name, surname, date)

Supervisor of the Final Degree Project Prof. Dr. Vaidas Lukosevicius 2020-09-15
(abbreviation of the position, name, surname, date)

Head of Study Programmes Assoc. prof. Saulius Japertas 2020-09-15
(abbreviation of the position, name, surname, date)

Vimaladass, Aravind. Investigation of Vehicle Muffler Acoustic Transmission Loss. Master's Final Degree Project/supervisor Dr. Prof. Vaidas Lukosevicius; Faculty of Mechanical Engineering and Design, Kaunas University of Technology.

Study field and area (study field group): Transport Engineering (E12), Engineering Science.

Keywords: Muffler, Back pressure, Transmission loss, CFD analysis, Harmonic acoustics, baffle plates, perforated pipes.

Kaunas, 2022. 82 p.

Summary

Numerous literatures were studied to evaluate the significance of mufflers in the exhaust system. As mufflers are an integral part of the exhaust system, the design parameters must be carefully accessed to obtain the required outcome. Mufflers are often associated with the scope of sound attenuation property. In this research, a base muffler is chosen to evaluate and validate the analysis simulation parameters to establish the test conditions. The process of evaluation was carried out using Solidworks and Ansys software platforms to determine the analysis outcomes to later compare with existing data. A comparison of the experimental and theoretical values is obtained to validate the results. Further optimized design variants of mufflers were designed using the Solidworks platform to determine the effects of different obstructions introduced in the expansion chamber. Three different design variants of these designs were considered for data analysis purposes. The design variants further have design variations with the difference in the obstructions. The initial analysis was to determine the effect of baffle plates and then baffle plates with obstruction and finally baffle plates with perforated pipes. The combinations of these design variants were analyzed to test the effects of these different types of obstructions. These design variants were analyzed using Solidworks to determine the velocity and pressure trajectories. From the results, the surface velocity of the flow was gained which served as the input to determine the transmission loss on each design variant on Ansys. From the analysis, it is evident that the different obstruction design parameters placed in a different position provide different acoustic loss properties to the flow. The laminar flow at the entry is converted into a controlled laminar flow using the obstructions to attenuate acoustics. From the simulation results, a comparison study was created to understand the impact of the design obstructions inserted into the expansion chamber on transmission loss. This study represents that each obstruction creates a significant amount of acoustics loss. Design 1 yields the maximum transmission loss with the design 1.3 variant having 13.21 dB at 1380 Hz. Design 2 yields the maximum transmission loss with the design 2.3 variant having 99.56 dB at 680 Hz. Design 3 yields the maximum transmission loss with the design 3.1 variant having 116.13 dB at 1300 Hz. Irrespective of the shape of the expansion chamber the baffle plate and perforated pipes create an impact. But to conclude, the position, shape, and size of the obstructions and the design of the expansion chamber play a major role in impacting the transmission loss. Even though studies are stating the performance of reactive mufflers under low frequency, it can be seen that the design of the muffler and expansion chamber alters the transmission loss irrespective of the frequency range. Depending on the needs we can design the muffler and the expansion chamber to perform under a specific frequency range.

Vimaladass, Aravind. Transporto priemonių duslintuvų garso perdavimo nuostolių tyrimas. Magistro baigiamasis projektas / vadovas Prof. dr. Vaidas Lukoševičius; Kauno technologijos universitetas, Mechanikos inžinerijos ir dizaino fakultetas.

Studijų kryptis ir sritis (studijų krypčių grupė): Transporto inžinerija (E12), Inžinerijos mokslai.

Reikšminiai žodžiai: duslintuvas, priešslėgis, perdavimo nuostoliai, CFD analizė, harmoninė akustika, pertvaros plokštės, perforuoti vamzdžiai.

Kaunas, 2022. 82 p.

Santrauka

Išnagrinėti literatūros šaltiniai siekiant įvertinti duslintuvų reikšmę išmetimo sistemoje. Kadangi duslintuvai yra neatsiejama išmetimo sistemos dalis, norint gauti reikiamą rezultatą, reikia atidžiai įvertinti konstrukcinius parametrus. Duslintuvai dažnai siejami su garso slopinimo savybių sritimi. Šiame tyrime pasirinktas bazinis duslintuvas, kad būtų galima įvertinti ir patvirtinti analizės modeliavimo parametrus, siekiant nustatyti bandymo sąlygas. Modeliavimas atliktas naudojant "Solidworks" ir "Ansys" programinės įrangos platformas, kad būtų galima nustatyti analizės rezultatus, kuriuos vėliau būtų galima palyginti su esamais duomenimis. Rezultatams patvirtinti gautas eksperimentinių ir teorinių verčių palyginimas. Naudojant "Solidworks" platformą buvo suprojektuoti optimizavimui skirti duslintuvų konstrukciniai variantai, siekiant nustatyti skirtingų išsiplėtimo kameroje įvestų elementų poveikį. Duomenų analizės tikslais nagrinėti trys skirtingi šių konstrukcijų variantai. Iš pradžių analizuota, kaip veikia pertvaros plokštelės, vėliau - pertvaros plokštelės su kliūtimi ir galiausiai - pertvaros plokštelės su perforuotais vamzdžiais. Šių konstrukcinių variantų deriniai buvo analizuojami siekiant patikrinti šių skirtingų tipų kliūčių poveikį. Šie konstrukciniai variantai buvo analizuojami naudojant "Solidworks", siekiant nustatyti greičio ir slėgio trajektorijas. Remiantis rezultatais, buvo gautas srauto paviršinis greitis, kuris buvo naudojamas kaip įvesties duomenys nustatant perdavimo nuostolius kiekviename konstrukciniame variante naudojant "Ansys". Atlikus analizę paaiškėjo, kad skirtingose padėtyse esančios skirtingi kliūtys suteikia srautui skirtingas akustinių nuostolių savybes. Įėjime esantis laminarinis srautas paverčiamas valdomu laminariu srautu, naudojant kliūtis, slopinančias akustinius garsus. Remiantis modeliavimo rezultatais, buvo atliktas lyginamasis tyrimas, siekiant suprasti į išsiplėtimo kamerą įterptų konstrukcinių kliūčių poveikį perdavimo nuostoliams. Šiame tyrime nustatyta, kad kiekviena kliūtis sukelia didelius akustinius nuostolius. Dėl 1 konstrukcijos gaunami didžiausi perdavimo nuostoliai, o dėl 1.3 konstrukcijos varianto - 13,21 dB, esant 1380 Hz dažniui. Pagal 2 konstrukciją didžiausi perdavimo nuostoliai yra 2.3 konstrukcijos varianto, kurio perdavimo nuostoliai yra 99,56 dB, esant 680 Hz dažniui. 3 konstrukcijos atveju didžiausi perdavimo nuostoliai yra 3.1 konstrukcijos varianto - 116,13 dB, esant 1300 Hz dažniui. Nepriklausomai nuo išsiplėtimo kameros formos, pertvaros plokštė ir perforuoti vamzdžiai daro poveikį. Tačiau apibendrinant galima teigti, kad kliūčių padėtis, forma ir dydis bei išsiplėtimo kameros konstrukcija turi didelę įtaką perdavimo nuostoliams. Nors tyrimuose nurodomas reaktyvinių duslintuvų veikimas esant žemam dažniui, matyti, kad duslintuvo ir išsiplėtimo kameros konstrukcija keičia perdavimo nuostolius nepriklausomai nuo dažnių diapazono. Atsižvelgdami į poreikius, galime suprojektuoti duslintuvą ir išsiplėtimo kamerą taip, kad jie veiktų tam tikrame dažnių diapazone.

Table of Contents

List of figures	9
List of tables	11
Introduction	12
1. Literature Survey	14
1.1. Review of Legal Regulations of Car Noise	15
1.2. Review of Exhaust System Control	19
1.3. Review of Reactive Muffler.....	22
1.4. Review of Absorptive Muffler.....	23
1.5. Review of a Computational and Experimental Model in Fluid Dynamics.....	25
1.6. Review of Transmission Loss in a Muffler.....	26
2. Methodology	30
2.1. Base muffler.....	30
2.2. Design 1	35
2.3. Design-2.....	39
2.4. Design-3.....	44
2.5. Solid work Simulation	52
2.6. Backpressure calculation	57
2.7. Ansys Workbench.....	57
2.8. Mesh.....	58
3. Result and Discussions	59
3.1 Results.....	59
3.2. Discussions	75
Conclusions	79
List of references	80

List of figures

Fig. 1. Milton Reeves exhaust muffler for engines [4]	14
Fig. 2. Eugene Houdry catalytic converter [5]	15
Fig. 3. Wireframe model of the circular cross-sectional muffler with single outlet [8].....	20
Fig. 4. Isometric view of the circular cross-sectional muffler with dual outlet [2].....	20
Fig. 5. Reactive Muffler [18].....	22
Fig. 6. Absorptive Muffler [23].....	23
Fig. 7. Absorptive Muffler with Ammonia Pulsator [25].....	24
Fig. 8. Muffler Design-1 [26].....	25
Fig. 9. Muffler Design-2 [26].....	25
Fig. 10. Duct model with one, two, and three baffle plates [30].....	27
Fig. 11. Results comparison [30].....	28
Fig. 12. Base muffler design	30
Fig. 13. Base muffler for ANSYS solver	31
Fig. 14. Base muffler Analytical result graph	32
Fig. 15. Measured experimental values by Seybert and Tao [42].....	32
Fig. 16. Analysis result of base muffler	34
Fig. 17. Comparison of all the results (FEA, Analytical and experimental).....	34
Fig. 18. (a) Design-1 model (b) cut section of the model	35
Fig. 19. Design-1 for ANSYS solver (b) Cut section of the fluid domain.....	36
Fig. 20. (a) Cut section of the design-1.1 with baffle plate 1 in SW (b) Cut section of the solid body for ANSYS simulation.....	36
Fig. 21. Baffle plate 1.1	37
Fig. 22. (a) Cut section of the design-1.2 with baffle plate 2 in SW (b) Cut section of the solid body for Ansys solver.....	37
Fig. 23. Baffle plate 1.2.....	38
Fig. 24. (a) Muffler with baffle plate 1.1&1.2 (b)Cut section of the solid body used for ANSYS simulation	39
Fig. 25. (a) Design-2 model (b) Cut section of the model.....	39
Fig. 26. Design-2 for ANSYS simulation (b) Cut section of the fluid domain.....	40
Fig. 27. (a) Cut section of the design 2.1 (b) fluid domain	41
Fig. 28. (a) Cut section of the design-2.2 muffler model (b) fluid domain.....	41
Fig. 29. (a) Cut section of the design-2.3 muffler model and (b) fluid domain	42
Fig. 30. Perforated pipe 2.1	42
Fig. 31. (a) Cut section of the design-2.4 muffler model and (b) fluid domain	43
Fig. 32. Perforated pipe 2.2	43
Fig. 33. Design-3 muffler model (b) cut section of the model.....	44
Fig. 34. (a) Design-3 muffler model fluid domain (b) cut section of the fluid domain	45
Fig. 35. Perforated pipe 3.1	45
Fig. 36. Perforated pipe 3.2	46
Fig. 37. Cut section of the diesel engine muffler model 3.1 and (b) fluid domain	47
Fig. 38. Perforated pipe 3.3	47
Fig. 39. Perforated pipe 3.4	48
Fig. 40. Cut section of design-3.2 muffler model and (b) fluid domain	48
Fig. 41. Perforated pipe 3.5	49
Fig. 42. Perforated pipe 3.6	49
Fig. 43. Cut section of the design-3.3 muffler model and (b) cut section.....	50

Fig. 44. Cut section of the design-3.4 muffler model and (b) fluid domain.....	51
Fig. 45. Perforated pipe 3.7	51
Fig. 46. Perforated pipe 3.8	52
Fig. 47. Computational Domain of Design -1	53
Fig. 48. Computational Domain of Design 2	54
Fig. 49. Computational Domain of design 3	56
Fig. 50. Mesh pattern for different designs	58
Fig. 51. Velocity trajectories and Pressure contours of design-1	59
Fig. 52. Frequency Vs Transmission loss graph for design-1	59
Fig. 53. Velocity trajectories and Pressure contours of design-1.1	60
Fig. 54. Frequency Vs Transmission loss graph for design-1.1	60
Fig. 55. Velocity trajectories and Pressure contours of design-1	61
Fig. 56. Frequency Vs Transmission loss graph for design-1	61
Fig. 57. Velocity trajectories and Pressure contours of design-1	62
Fig. 58. Frequency Vs Transmission loss graph for design-1	62
Fig. 59. Velocity trajectories and Pressure contours of design-1	63
Fig. 60. Frequency Vs Transmission loss graph for design-1	63
Fig. 61. Velocity trajectories and Pressure contours of design-1	64
Fig. 62. Frequency Vs Transmission loss graph for design-1	64
Fig. 63. Velocity trajectories and Pressure contours of design-1	65
Fig. 64. Frequency Vs Transmission loss graph for design-1	66
Fig. 65. Velocity trajectories and Pressure contours of design-1	67
Fig. 66. Frequency Vs Transmission loss graph for design-1	67
Fig. 67. Velocity trajectories and Pressure contours of design-1	68
Fig. 68. Frequency Vs Transmission loss graph for design-1	68
Fig. 69. Velocity trajectories and Pressure contours of design-1	69
Fig. 70. Frequency Vs Transmission loss graph for design-1	70
Fig. 71. Velocity trajectories and Pressure contours of design-1	71
Fig. 72. Frequency Vs Transmission loss graph for design-1	71
Fig. 73. Velocity trajectories and Pressure contours of design-1	72
Fig. 74. Frequency Vs Transmission loss graph for design-1	72
Fig. 75. Velocity trajectories and Pressure contours of design-1	73
Fig. 76. Frequency Vs Transmission loss graph for design-1	73
Fig. 77. Velocity trajectories and Pressure contours of design-1	74
Fig. 78. Frequency Vs Transmission loss graph for design-1	75
Fig. 79. Frequency vs Transmission loss comparison graph of design (1 – 1.3)	76
Fig. 80. Frequency vs Transmission loss comparison graph of design (2 – 2.4)	77
Fig. 81. Frequency vs Transmission loss comparison graph of design (3 – 3.4)	78

List of tables

Table 1. ISO/TC 43/SC 1 standard directly related to noise emitted by road vehicles	16
Table 2. Limit values of allowed exterior noise emitted by road vehicles in laboratory conditions	19
Table 3. Base muffler dimensions:	30
Table 4. Design-1 dimension:	35
Table 5. Baffle plate 1 dimension	37
Table 6. Baffle plate 1.2 dimensions	38
Table 7. Design-2 dimensions.....	39
Table 8. Perforated pipe 2.1 dimensions.....	42
Table 9. Perforated pipe 2.2 dimensions.....	43
Table 10. Design-3 dimensions.....	44
Table 11. Perforated pipe 3.1 dimensions.....	45
Table 12. Perforated pipe 3.2 dimensions.....	46
Table 13. Perforated pipe 3.3 dimensions.....	47
Table 14. Perforated pipe 3.3 dimensions.....	48
Table 15. Perforated pipe 3.5 dimensions.....	49
Table 16. Perforated pipe 3.6 dimensions.....	50
Table 17. Perforated pipe 3.7 dimensions.....	51
Table 18. Perforated pipe 3.8 dimensions.....	52
Table 19. Engine Specifications:	52
Table 20. Computational Domain dimensions.....	53
Table 21. Engine Specifications	54
Table 22. Computational Domain dimensions.....	55
Table 23. Engine Specifications:	55
Table 24. Computational Domain dimensions.....	56
Table 25. Simulation parameters for design (1-1.3)	76
Table 26. Simulation parameters for design (2-2.4)	77
Table 27. Simulation parameters for design (3-3.4)	78

Introduction

Noise and pollution from the exhaust system and certain large industries are the main concern of the public because they have a significant environmental impact. A muffler is a noise reduction tool that can be used. The performance of the muffler is dependent on certain parameters. The three acoustic performance parameters of the muffler are transmission loss, insertion loss, and level differences. The main parameter that most consider is the transmission loss of these different parameters. A muffler's main purpose is to reduce the anechoic termination of the muffler exhaust. The loss of transmission is therefore the most favorable parameter for this termination. The growth and decrease of the transmission loss vary according to the type of acoustic filters in the muffler. Some of these filters are the Helmholtz resonator, absorbent material, perforated tube, and even tube [1]. There are different types of mufflers used in the automobile industry are:

- Absorptive Muffler
- Resonance Muffler
- Combination of a both absorptive and reactive muffler
- Wave cancellation type muffler
- Baffle type muffler

If an engine runs without a muffler, it makes a huge difference in noise level. It comprises a simple set of tubes with a few holes inside the muffler. The tubes and chambers are as fine as a musical instrument. The sound waves produced by the motor were designed to reflect them so that they partially cancel out.

Automotive mufflers are available in all shapes, designs, and sizes reliant on the application required. It usually consists of an inlet and outlet tube that is oval or geometric round and separated by a larger chamber. Almost all reciprocating internal combustion motors are equipped with mufflers. The silencer installed on an engine is intended to reduce the exhaust gas pressure from the engine cylinders. In general, mufflers for these motors are reactive rather than dissipating devices. Reactive mufflers work on acoustic waves that propagate in them through destructive interference. Absorptive mufflers usually operate in porous fibrous materials by dissipating acoustic energy.

There is also some dissipating function in practical reactive mufflers. An ideal muffler should function as a low-pass filter for a reciprocal internal combustion engine. The continuous or median flow must pass through the muffler unimpeded while preventing the fluctuating flow combined with the fluctuating acoustic pressure. The so-called rear pressure is very low, and the engine is more efficient if the constant flow is not greatly impaired. The pressure drop associated with constant flow through the muffler is desirable to be predictable. Perforated tubes are usually used in car mufflers [2].

The general requirements of the muffler are high performance, less weight, maintenance-free, easy mounting, cost-efficient, easy production, quiet and compact design. The factors recommended for the selection of muffler are size, material, the diameter of the pipes (inlet and outlet), vehicle exhaust system, and acceptable backpressure of the engine. Generally, stainless-steel material is preferred to manufacture the muffler because, of its durability, corrosion resistance, and average life properties.

Novelty of the work

The novelty of the work lies within the scope of introducing different types of obstructions in the expansion chamber whilst similar research on mufflers focuses on the impact of the same obstruction parameter altered slightly.

The tasks:

1. Scientific papers are to be reviewed, to study the engine backpressure and transmission loss of the muffler.
2. A base muffler will be designed, the analytical and theoretical values will be compared with the experimental values to verify the setup for the transmission loss simulation.
3. Three types of mufflers are designed, and simulations must be conducted to calculate the backpressure.
4. Harmonic acoustics must be conducted to find out the transmission loss of all the mufflers.
5. Perforated pipes and baffle plates are included in the previously designed mufflers with variations in design parameters to investigate the significance of transmission loss.

1. Literature Survey

The muffler is a key element of the car's exhaust system. When a small car runs without a muffler, the noise is extremely loud if an engine is large enough to power the system. The larger and stronger the engine would typically be, the louder the sound. To reduce and manage motor noise, mufflers were created [3].

Reeves Automobile

The early automobile pioneers at the Reeves Pulley Co. invented the first generation of the muffler. Milton Reeves is credited with inventing the first muffler for automobile engines. Because early automobiles were so loud, they terrified horses and enraged residents who cherished communities where automobiles were used. In 1896, Reeves created a baffle device to reduce engine noise.

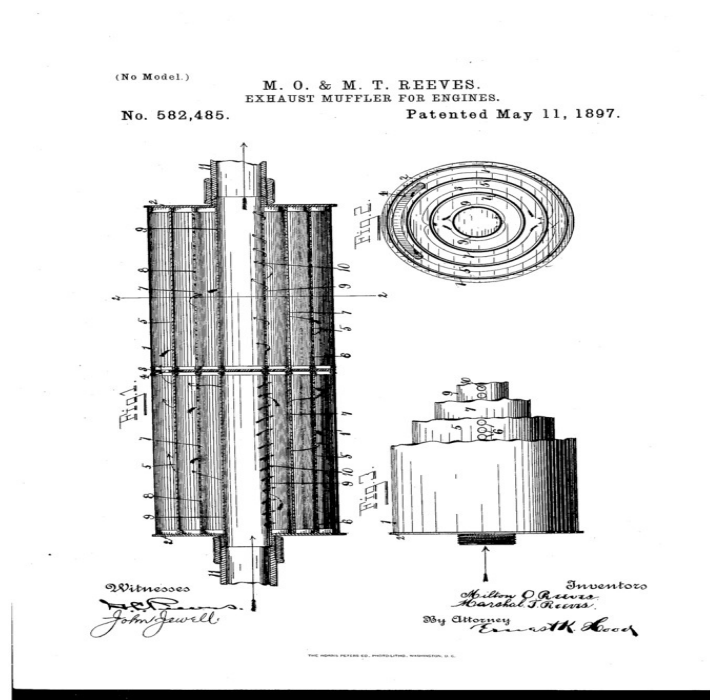


Fig. 1. Milton Reeves exhaust muffler for engines [4]

Eugene Houdry

The contemporary automotive muffler owes its origins to the work of a single man named Eugene Houdry. He witnessed the creation of the automobile personally and was involved in many of its important stages, including contributing to the evolution of both gasoline and aviation fuel. The first patent for a catalytic muffler was filed in 1962. The design of Houdry's forms the basis for most mufflers used after this time.

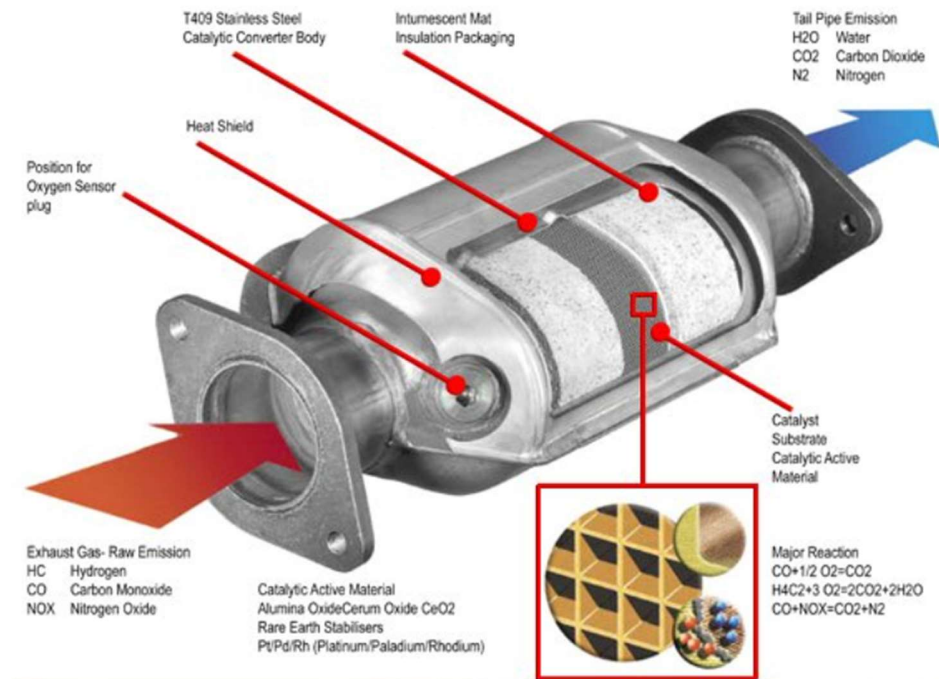


Fig. 2. Eugene Houdry catalytic converter [5]

To silence the engine, the original mufflers utilized baffles. Designers eventually understood that employing a substance to absorb the sound from the engine before it exited the closed system could help to lessen the noise. These two technologies are frequently used in conjunction with current mufflers. Fibreglass is frequently utilized as the absorbent material that dampens sound in mufflers.

The situation with diesel from an engineering point of view was even more interesting as a particulate filter had to be installed. This was an addition to the diesel exhaust fluid that eventually grew into an SCR system, a complicated device with a wide range of sensors and a distinct control unit. Initially, it aimed only at trucks, but also light vehicles in 2015 (with the transition to Euro-6 anti-diesel). No further way to meet the standards set for nitrogen oxides is currently possible [5].

Modern muffler developments:

Since sales of electric vehicles have risen so dramatically, only time will tell whether or not automobile mufflers will disappear from the market. As a result, the exhaust system will have to undergo yet another upgrade soon, as Euro-7 standards are expected to be implemented by the decade's end of the twenty-first century. Even though the standard is still being worked on, developers are almost certainly looking for alternate solutions [6].

1.1. Review of Legal Regulations of Car Noise

International Electrotechnical Commission (IEC) and International Standardization Organization (ISO) are the main international organizations that publish standards for measurement and analysis of noise. IEC is responsible for the design of noise measuring instruments, and ISO is competent for measuring techniques, experimental conditions, measurement parameters, and measuring limitations, as the standardization holder [7].

ISO Standards

ISO is the global federation of national standardization bodies. Many technical committees prepare international standards. The work is carried out in all issues concerning standardization in the field of electrical engineering, ISO cooperates closely with the International Electrical Technology Commission. In 111 published standards and 23 currently under development standards, the ISO and its Technical Committee 43 – Acoustics, Subcommittee 1 – Noise (ISO/TC 43/SC 1) deal with global noise problem [8].

The following standards ISO/TC 43/SC 1 address the impact of roads on-road noise:

- ISO 10844:2014 – Acoustics - The main characteristics of a test surface for the measurement of vehicle and bullet or road-noise emissions are specified.
- ISO 11819-1:1997 – Acoustics - Measuring the impact on traffic noise of road surfaces Part 1: method of statistical pass by.
- ISO/PAS 11819-4:2013 – Acoustics - Method to measure the impact on traffic noise of roads – Part 4: Statistical Pass By method using a backing board.
- ISO 13472-1:2002 – Acoustics - In situ evaluation of road surface sound absorption qualities Part:1 The process of extending the surface is called the extended surface method.
- ISO 13472-2:2010 – Acoustics - Measurement of road surfaces sound absorption properties on the ground — part 2: reflective surface spot procedure.
- ISO/CD 13471-1 – Acoustics - Temperature influence on the measurement of tyre/road noise - Part 1: Temperature correction when tested using CPX.
- ISO 13325:2003 – Tyres - Cost-by methods for measuring sound emissions from tyre to road.
- ISO/TC31 N1129 - ISO/NP 20908 Tyre sound emission test - Methods of a drum.

All the ISO standards on noise related to road transport provide the necessary information on the techniques and equipment to be used, the test conditions to be met, the measuring parameters to be considered, and the limits for the results of the measurement. The ISO/TC 43/SC 1 standards directly related to traffic noise are described briefly in Table 1 [8].

Table 1. ISO/TC 43/SC 1 standard directly related to noise emitted by road vehicles

ISO/TC 43/SC 1 standard	Brief Description
ISO 362-1:2015 - Measurement of road vehicle noise emissions - Engineering method -part 1: M and N categories	Measures road vehicle noise in typical urban traffic using an engineering method that specifies the road vehicle categories M and N
ISO 362-2:2009 - Measurement of road vehicle exhaust noise - Engineering method - Part 2: L category	Under typical urban traffic conditions, this standard specifies an engineering method for evaluating the noise of road vehicles in categories L3, L4, and L5
ISO 362-3:2016 – Measurement of noise emitted by accelerating road vehicles – Engineering method - Part 3: Indoor testing M and N categories	A semi-anechoic chamber can be used to measure the noise of road vehicles in categories M and N
ISO 5128:1980 – Acoustics – Measurement of sound inside motor-powered vehicles	Defines the circumstances under which reliable and comparable measurements of noise levels and spectral characteristics within moving vehicles can be obtained (excluding agricultural tractors and field machinery)

ISO 5130:2007 – Acoustics – Measurement of sound pressure level produced by stationary road vehicles	Sets the circumstances for measuring the exterior sound pressure levels emitted by stationary road vehicles, including a range of engine speeds and a continuous sound pressure level measurement. Only road vehicles of categories L, M, and N with internal combustion engines are covered by this rule.
ISO 9645:1990 – Acoustics – Measurement of noise emitted by two-wheeled scooters in motion – Engineering method	Measures the noise from two-wheeled mopeds moving through an irregular urban traffic flow using an engineering solution that makes full use of the engine power available.
ISO 16254:2016 – Acoustics – Measurement of road vehicle categories M and N noise emissions during a stop and a low-speed run – Engineering method	An engineering method based on ISO 362-1 for measuring the sound output by M and N-category road vehicles in stationary and low-speed vehicle operation situations relevant to pedestrian safety is specified.

European Standard Regulations

Environmental noise reduction activities across Europe often have a distinct priority compared with environmentally friendly issues such as air and water pollution, often because it was believed that such issues were best dealt with at national and local levels. Since noise information is increasingly available on human health, the need for increased levels of protection against noise by EU citizens through a broader framework for actions across Europe is becoming more pronounced [9].

The EU and EFTA have formally recognized the European Standardization Committee (CEN) as one of three European Standardization Organizations in charge of the development of Europe, along with CENELEC—the European Electrotechnical Standardization Committee—and ETSI—the European Telecom Standards Institute, respectively. CEN/TC 301 "Road Vehicles" is developing standards in response to the European Commission's requests for standardization, including M/421 and M/533.

In the electric vehicle industry, CEN/TC 301 'Road Vehicles' is developing a new grade, prEN ISO 19363, on the safety and compatibility requirements for magnet transmission of power in electric vehicles. CEN/TC 268's hydrogen transport application will complete the modification of Standard EN 17124 for Product Specification and Quality Assurance for Proton Exchange Membrane (PEM) Fuel Cell applications on Hydrogen-Powered Road Vehicles [9].

In Europe, external noise control emitted by road vehicles is carried out by using vehicle type-approval procedures. The requirements published in law must be met by each new type of vehicle on the market. In 1970, Directive 70/157/EEC, the former European Economic Community, introduced allowable noise levels for all vehicles operating on at least four wheels at maximum speeds exceeding 25 km/h-1, was adopted (cars, buses, trucks). It is subject to several amendments in noise limits and measuring methods, which have been adapted by Member State laws concerning permissible noise and exhaust systems in the vehicle are [8]:

- 77/212/EEC - Vehicle category change and introduction of reduced noise limits.
- 81/334/EEC - Modifications of the moving and stationary noise measurement method to bring them closer to the real conditions.

- 84/372/EEC - Amendments to the noise measurement method emitted by high-performance vehicles and automated vehicles and vehicles, including manual adjustments, to bring them closer to the actual operating conditions.
- 84/424/EEC - Substitution of lower noise limit values for all vehicle categories.
- Comprehensive amendments by reducing the noise limit for all vehicle categories and improving the test method for large engine-powered vehicles, as this type of vehicle is being increasingly designed so that there is a greater power-to-mass ratio (PTM), and the torque of the engine is changed to create a greater driving force at low engine speeds as a function of motor speed. The use of gear levers in urban transport was increased by new designs and the effect on road noise is significant.

The European Parliament and Council of Europe have repealed Directive 70/157/EEC in 2014 in Regulation EU 540/2014 on sound levels for motor vehicles and substitute silencing systems. The reason behind this event is that EU noise emission limitations have not changed for over 20 years despite increased traffic. To reduce road noise, the European Committee has therefore proposed reducing the quantity of noise generated by passenger cars, light-duty trucks, and coaches by some 25 percent. The new regulation has introduced:

- Additional Provisions on Sound emissions (ASEP) are included as preventive requirements in the type-approval procedure to cover conditions for actual road traffic ensuring that the sound of a vehicle does not substantially differ from the sound of a vehicle when tested.
- specific annex on electric and hybrid vehicle minimum noise and
- noise labeling to foster competition with the sound level of each vehicle displaying manufacturers during sale [8].

Directive 70/157/EEC relates to the United Nations Noise Commission Regulation No 51 and UNECE Regulation No 59, which govern the approval of noise silencing systems and provide the noise emission test technique. A Contracting Party to a UNECE Agreement of March 20, 1958, on the development of universal technical specifications for wheeled vehicles, appliances, and parts to be fitted or used on wheeled vehicles, the Union has chosen to use these standards. [10].

Directive 70/157/EEC was significantly modified on several occasions since its adoption. There have been no expected effects on the most recent reduction in motor vehicle sound levels established in 1995. Studies have shown that the method of testing employed under this directive no longer reflects urban drive behavior. The test approach overstated the contribution of tyre-rolling noise to total noise emissions, according to the Green Paper on Future Noise Policy, issued on November 4, 1996. As a result, Directive 70/157/EEC will be replaced by a new test procedure under this regulation. It is recommended that the new approach be based on UNECE's 2007 noise working group's test protocol, which included a 2007 version of ISO 362. (GRB). New and old techniques of testing were monitored for compliance with regulations.

The new test method is considered in normal circulation of the sound level but is less representative in the worst case of the sound level. Additional sound emission provisions must therefore be set out in this Regulation. These provisions should lay down preventive provisions intended to cover vehicle driving conditions outside the typology approval cycle in real traffic and to prevent cycles from being beaten. These driving situations are environmentally related, and it is essential not to distinguish the sound emission of a vehicle from the type-app under road driving conditions.

The sound level limit should also be further reduced in this Regulation. The European Parliament and Council Reg. (EC) No 661/2009 should consider a new stronger noise requirement for vehicle tyres. Studies to show that road traffic noise, as well as the costs and advantages related to it, have adverse health effects and annoyance should also be considered. Considering the pneumatic offering to noise reduction declared in Regulations (EC) No 661/2009, overall limits should be reduced in all motor vehicle noise sources, including air intake over the power train and exhaust [10].

Table 2. Limit values of allowed exterior noise emitted by road vehicles in laboratory conditions

Motor vehicles with at least four wheels	
Vehicle category	Limit value of noise in dB(A)
M1, K5a, L6, and L7	87
M2 and N1	88
M3, N2, and N3 and with an engine rated power not higher than 147 kW	92
M3, N2, and N3 and with an engine rated power higher than 147 kW	95

1.2. Review of Exhaust System Control

For carrying unburnt gasses from the combustion chamber to the surrounding environment, the exhaust system is used. NOX and CO are gases that are harmful to society. The car industry is dynamic and changing rapidly [11]. A successful muffler design, therefore, needs to meet a relatively high number of exacting requirements, and it is not strange that many prototypes can be constructed and tested, and alternative methods and procedures can be used to predict the accurate performance of the muffler. Automotive research NVH has moved from noise control to the new scene emphasizing the design of noise and sound quality; a traditional search for sound pressure noise in vehicles can no longer meet today's demands [12].

Hanida Abdullah, et al [13] presented a numerical analysis by the transfer matrix method of transmission loss for exhaust mufflers. This research focused on predicting the loss of muffler transmission and determining the various other factors such as the diameter of the muffler and its location and the thickness of the baffle. To conclude the transmission loss of muffler computer program was developed. The performance of the expansion chamber silencer was found by using the approach of transmission matrix and the coding was verified by test results. The analyzes of the mufflers with different baffle thickness and locations are carried out. Test outcomes show that the most important factors for noise reduction are thickness and location.

K.Sri Rama Murthy, et al [2] investigated enhancing the noise level in the muffler. The main motive of this research was to model a muffler that dampens the noise levels. The model was designed and tested with all the essential parameters in consideration. The main principle behind the researcher's work was the concept resistance muffler to decrease the levels of noise emitted from the engine. Designing a muffler requires a certain set of criteria to be followed. They are geometrical, mechanical,

aerodynamical, acoustical, and economical criteria. The least noise attenuation that was required from the muffler as a function of frequency was given by the acoustical criterion. The material that was chosen to manufacture the muffler was determined based on the mechanical criterion. While designing and fabricating the muffler, the benefit of the material is very important as it should last longer and does not need frequent maintenance. This ensures a good economical criterion was adhered to.

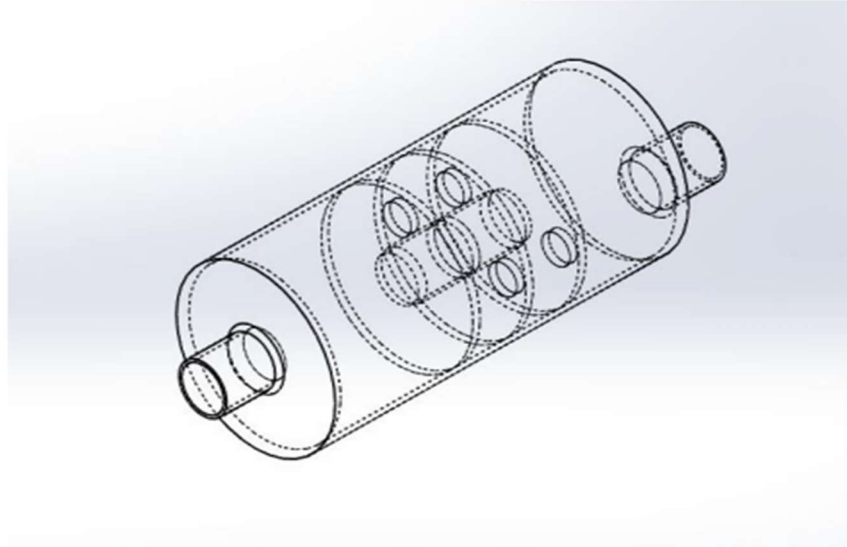


Fig. 3. Wireframe model of the circular cross-sectional muffler with single outlet [8]

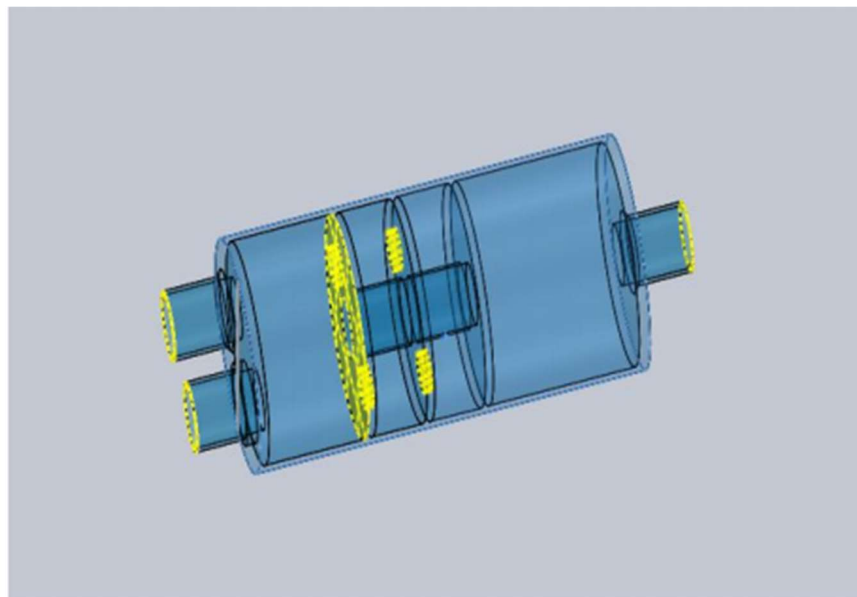


Fig. 4. Isometric view of the circular cross-sectional muffler with dual outlet [2]

Based on the principles of reactive type mufflers, the researcher designed several muffler types. Among the various types of mufflers that were designed, it was determined that circular cross-sectional muffler which has single and dual exhaust outlets has higher levels of noise attenuation. A noise attenuation test was performed, and the results obtained were compared with the theoretical results. The results were:

- 5.19 – Theoretical transmission loss.

- 6.06 – Practically obtained transmission loss (single outlet)
- 6.44 – Practically obtained transmission loss (dual outlet)

Vinod Sherekar, et al [14] proposed a paper on the fundamentals of muffler design. The researcher listed the basic functional requirements that have to be considered while designing the muffler. The important functional requirements include insertion loss, backpressure, weight, size, and cost. This paper sets out appropriate guidelines for the selection of muffler grade, length, and diameter, tailpipe length according to the cubic capacity of the engine, and the calculation of the exhaust gas pressure drop based on the flow rate. The test criteria for muffler suitability for specific applications are also explained.

Fundamentals of Muffler Design

When designing a muffler for an automotive application, different requirements are to be considered. These functional requirements may involve sufficient insertion loss, backpressure, size, the durability of sound, cost, weight, compact form, and style. Some of them are provided in detail below.

- **Sufficient Insertion Loss**÷
The sound pressure of the noise source is reduced to the expected levels by an effective muffler. The noise produced by the engine in the case of a vehicle muffler is reduced in the exhaust system. Regarding insertion loss or transmission loss, a muffler performance or attenuating function is generally defined. Insertion loss shall be defined as the difference among radiated acoustic forces without and fitted with a muffler [15].
- **Selection of size**÷
It is extremely important that the silencer is properly selected and dimensions to ensure that pressure drop, acoustic performance, and other specific design criteria have been met. The correct type of exhaust silencer is selected depending on the type of engine, end-usage of the engine, and the attenuation required. The selected silencer size must also consider the specified volume of exhaust gas flow that maintains the rear pressure within the specified limits. The space available influences the dimensions and thus the type of silencer that can be used. If the muffler does not meet the space restrictions, however, its geometry may be designed for the highest attenuation [16].
- **Backpressure**÷
Backpressure signifies the additional static pressure the muffler exerts on the engine by limiting exhaust gas flow. A muffler with better attenuation will yield higher backpressure. A reactive muffler where the exhaust gasses are attenuated requires many geometry changes and a considerable number of backpressures can be produced that reduce the engine's output. To avoid power losses especially for improved vehicle performance, backpressure should be kept at a minimum.
- **Cost and Weight**÷
The larger a muffler is generally, the more it weighs and the higher the production costs. Each saved gram is crucial to its performance. Supporting a silencer effectively is always a problem with the design and the bigger a muffler is, the harder it is. Vibration insulation is needed in addition to the muffler's weight to keep the exhaust system's acoustic energy from being transmitted to the chassis and passengers. Vibration from the muffler can be dampened with the use of rubber inserts and brackets. For this, a small, lightweight muffler is preferable. [17].

1.3. Review of Reactive Muffler

Reactive muffler consists of resonant chambers which are separated by various plate and pipe systems. Tubes of different lengths and with perforating devices direct the gas flow from the engine. The exhaust gas is distributed in the resonant chambers. The reactive muffler functions according to the concept of Helmholtz. The muffler reflects the 180° pressure wave from the noise supply, which ultimately calls it down by destruction. In lower and medium-sized engine firing or harmonic frequencies, the reactive muffler works well, with an acoustic performance ranging from 30 to 700 Hz, in reactive mufflers. Exhaust gasses expand to reduce their pressure amplitude in the muffler chamber. The reactive muffler also lowers the rate of slowing down high-speed gasses and reduces flux-oriented noises and creates a high back pressure, the only disadvantage of using a reactive muffler. The optimum rear pressure is controlled by the proper construction of the perforation in the baffle plates and pipes and the selection of the pipe diameter. Drawing on the size of the engine, the volume of the muffler is generally selected to reduce the pressure amplitude effectively by 10 to 12 times the engine size. The main advantage of the reactive muffler is that the system is longer in life because it does not contain any non-degradable materials. Proper choice of sheet metal materials will be running without rusting for a longer time [18].

The noise of vehicles and other ventilation systems is often attenuated by a reactive muffler. Acoustic behavior is one of the main clues for assessing a muffler's performance. Transmission loss (TL) is often used to assess muffler acoustics. For the fuel cell car's exhaust output, flow limitations aren't necessary. Rather, the muffler's acoustic conduct should be as good as possible to reduce the noise spread to the air [19].

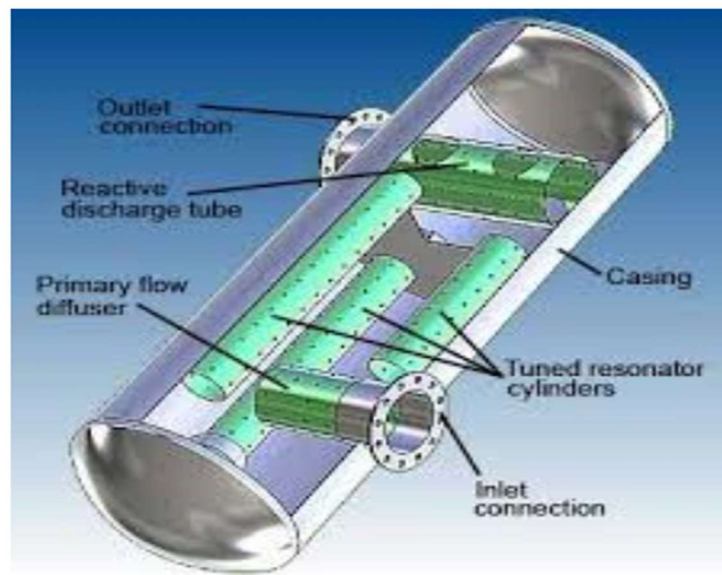


Fig. 5. Reactive Muffler [18]

Nitin Kumar Anekar et al. studied vibration and noise in the reactive mufflers. The paper focused on reactive muffler acoustic performance with side outlet based on the principles of Finite Element Analysis and analytical approach. For the experimental part, two load method was carried out and the results were compared with the finite element method and analytical approach in the aspect of transmission loss [20].

Another researcher proposed a study to optimize the noise levels and backpressure of a muffler. A muffler was designed with a new set of parameters defined by the author. This model was designed and analyzed in Solidworks. A muffler was developed that satisfies requirements that probably produce a reasonable loss of insertion, minimum backpressure, space constraints, and long life. The muffler should therefore be designed to provide the best reduction of noise. Maximum insertion loss of 3500 rpm and 16.2 dB. A new muffler installation can be equipped with a maximum sound level of 80.5 dBA at 3500 rpm. The minimum loss of insertion of the old and new muffler is 10.7 dBA at 2500 rpm. The designed muffler can attenuate at both high and low-frequency noise. The muffler attenuates the noise from 200 Hz to 500 Hz in the low-frequency range. In comparison to Mahindra Maxx Mdi 3200 Di, the muffler must be replaced with existing models [21].

1.4. Review of Absorptive Muffler

Absorptive mufflers use materials that absorb sound to attenuate sound waves. In HVAC duct systems it is commonly used. In the parallel configuration, typical absorptive mufflers are configured. A dissipative muffler consists of pipes and chambers that are lining up with sound-absorbing materials that absorb and convert acoustic energy to heat. These mufflers are helpful for high-frequency broadband. The benefit of this muffler is that the system's pressure drop is comparatively low since flow reversals, twisting, and turning inside the muffler do not significantly change the flow path. The downside of the dissipative muffler is that the wavelength is too big to be damped at low frequencies. But an absolute thickness of absorbent material could be used to overcome it [22].

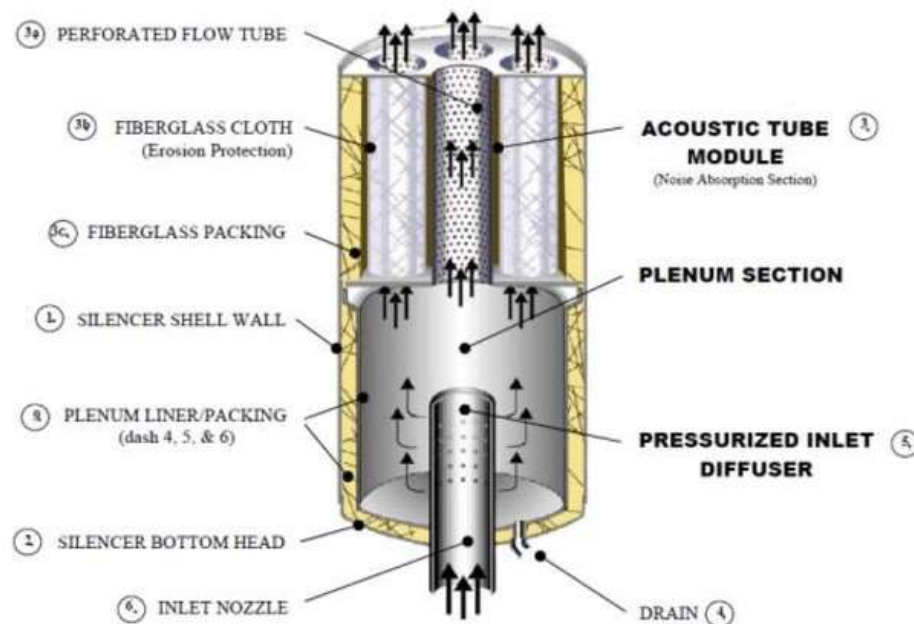


Fig. 6. Absorptive Muffler [23]

Mostafa Ranjbar et al. [24] investigated the development of noise transmission in the muffler. The muffler structure is modeled with the shell elements and its sound-absorbing layer. This model examines the muffler structure that affects the loss of transmission (TL). The results are evaluated with a model without absorption. It specifies that absorbing layer thickness and material character has distinctive effects over a wide frequency range on muffler noise loss. Absorbent mufflers achieve better performance at high frequency, maximizing noise loss transmission was discussed in this paper.

In addition, as the muffler's absorbent layer thickness increases, so does TL at higher frequencies and even RMSL over the whole frequency range.

However, it resulted in a heavy structure of the muffler to use denser absorbent materials. In addition, it reduced the natural frequencies of the muffler structure therefore, it is possible to see more resonance in the muffler. For future works, a full connection between the structure and the acoustic medium is recommended. It increases the time and complexity of the problem, however. To reduce the impact of air contamination of absorbent mufflers, more environmentally friendly absorption materials should be considered. New forms of absorbing mufflers should be considered with well-designed absorbing layer forms [24].

Jayashri P et al. [25] designed and developed an absorptive type muffler with an ammonia pulsator which was analyzed using UG NX-8.0 and ANSYS workbench. This new design and development solved problems that were faced by traditional designs. The results showed that the test was done at the maximum theoretical stress on the tubes and the engine without an ammonia pulsator (cased tube and charcoal pipes). The results for the comparison with von-mises stress (von-mises stress), maximum stress using theoretical methods, and von-mises are well below the allowable limit. The box and the charcoal pipe which is deformed by the action of the force system. The new ammonia-pulsator-optimized absorptive muffler is designed for stationary engines and is suitable for minor modifications in automotive exhaust.

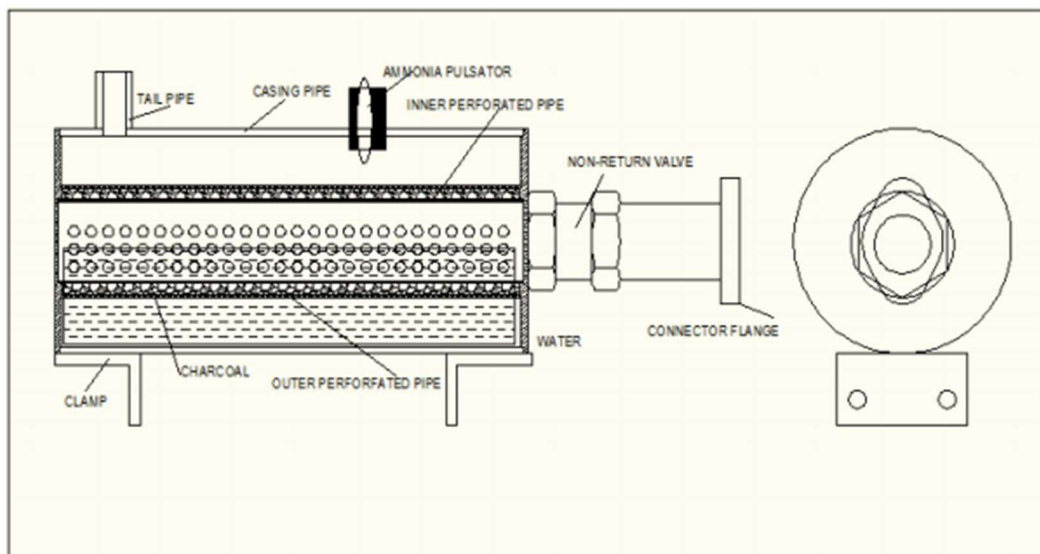


Fig. 7. Absorptive Muffler with Ammonia Pulsator [25]

Ujjal Kalita et al. [26] investigated the maximum possible attenuation levels in the muffler by using various absorptive materials. Airflow resistivity was taken to calculate transmission loss in the muffler. COMSOL Multiphysics software was used to design and analyze two different size mufflers at different frequencies. In this research three materials were used as absorptive material: polyester, rock wool, and ceramic acoustic absorber. The analysis showed that for different materials the loss of transmission of sound varied based on the material used. From the various analysis that was performed, it is evident that transmission loss is least for an empty chamber in the range of 15 to 30 dB. When a layer of absorptive material is used as lining in the muffler the transmission loss is increased by 30 to 40 dB which improves the efficiency of the vehicles. The loss of transmission with polyester lining, rock wool lining, and ceramic acoustic absorber with Sic fibres lining is almost the

same in both designs, however, the variation in the loss is less than 10 dB (in Design 1) and less than 5 dB (in Design 2) by using ceramic acoustic Absorber for the low-frequency range (i.e., below 500 Hz), but the high-frequency range (i.e., 1800 Hz to 2200 Hz). It may therefore be concluded that the ceramic acoustic absorber can be used in the muffler as an absorbent material.



Fig. 8. Muffler Design-1 [26]

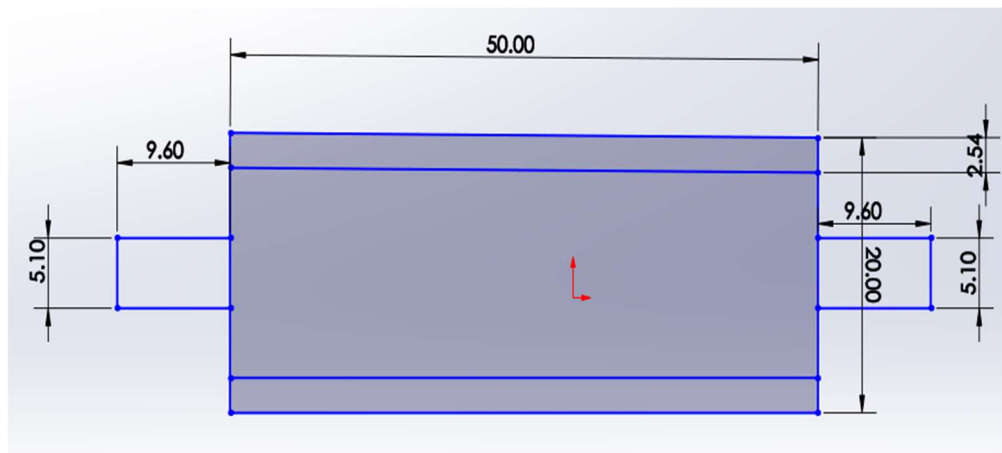


Fig. 9. Muffler Design-2 [26]

It was found that the heat can be resistant to polyester at around 250 °C or Rockwool at 1000 °C, whilst the light ceramic acoustic weight absorbers can be resistant to a temperature between 1800 C and 2300 C. Thus, the polyester muffler could be replaced with ceramic acoustic absorber lining by the rock wool lining since it is high in terms of heat absorption and can be exposed to heat directly for many years. It also assessed that transmission loss increases with an increase in airflow resistivity. The analysis showed that design 2 offered more transmission loss than design 1. Therefore, it is possible to conclude that design 2 is the most suitable muffler for automotive applications [26].

1.5. Review of a Computational and Experimental Model in Fluid Dynamics

Computational fluid dynamics makes use of computers to solve problems numerically in order to model or predict the fluid flow. In most cases, the flow is divided down into "discrete" cells, which create a grid, to better understand it ("the meshes"). The Navier-Stokes equations (continuum equations) can be altered in a variety of methods, including using finite differences, finite quantities, finite elements, or spectral processes. To arrive at a set of algebraic, discrete equations, each one has a different philosophy and programming approach. A suitable numerical approach is used to compute

the flow field's evolution by solving discrete equations under well-defined initial and limiting conditions. This was done in a controlled environment where the variables could be monitored and adjusted as needed. The computer's solution is often represented to make it easier for the user to understand the flow characteristics. There are three stages to the computer modeling process: physical modeling, numerical approximation, and mapping. Models such as the Lattice-Boltzmann category, based on particles and mobile automation, combine the first and second stages in a novel way.

The growing use of computer models has several reasons. The approximate solutions to Navier-Stokes's equations are provided; the period for variation, design, and development of parameters is reduced; the flow conditions are cheaper than experimental modeling and cannot be simulated for the experimental testing. Error sources for computer models may be due to numerical instabilities, with smaller errors accumulating at each step, in the low accuracy or imperfect verification or validation of the model. "Verification" means the analysis of the model against existing analytical solutions or a known solution, which is used as a reference point, encapsulating as far as possible the physics of the problems solved. "Validation" by experimental means, on the other hand, is confirmation. Since any computer model needs to be idealized to be efficient, which is a tedious experiment.

A special case in all of this is turbulent flow. It cannot be analytically approached. Special terms that are often based on pure empirical knowledge must be established if these are to be made up. Insight into turbulence seems so far limited to experimentation (by physical or numerical means). Due to its large costs direct numerical simulation (DNS) was achieved only with a Reynolds-number of 1410, which includes the simulation for vanishing cells, but without average. For simulating a complete airplane using DNS, a supercomputer with 10^{18} floating points operations is required. (Gad-el-Hak, 182ff. 1998). Currently, there are still 10^{12} flops to be overcome [27].

1.6. Review of Transmission Loss in a Muffler

The combined decrease in waveform intensity as a wave propagates out of a source or through a specific area or structure type is referred to as transmission loss. It is a term that is frequently used in optical and acoustic terminology. Acoustic equipment, such as mufflers and sonars, rely heavily on TL measurements. Transmission loss can be expressed in decibels. Transmission loss in dB scale is measured mathematically and can be described generally using the following formula:

$$TL = 10 \log_{10} (W_i/W_t) \text{ dB.} \quad (1)$$

If: W_i – the power of incident wave striking towards a defined structure.

W_t – Power of transmitted wave going away from the defined structure.

Transmission loss in duct acoustics was defined as the difference between the power transferred into an anechoic termination and the power transmitted into a muffler. The source does not affect transmission loss, which is based on an anechoic downstream termination. When operating in an anechoic environment, the transmission loss reveals the difference between the acoustic energy which is incident and also that which is being transferred. [28].

Amit et al. proposed that TMM, FEA (Wave 1-D & COMSOL), and an experimental method (two loading methods) for TL measurement of a muffler for a centralized inlet and lateral outlet position were used in this paper. The analysis for convergent and divergent cylindrical ducts is done with the

help of proven results. COMSOL and Wave 1-D also is used for validating and comparing results using FEA-based tools. An FEA tool has already been validated for virtual prototyping in various case studies [29].

Sachin Jha et al. [30] performed acoustical transmission loss by using various absorptive materials. The work aimed to validate, model, and analyze all the mufflers. The model is prepared in PRO-E software. FEA software was used to calculate the transmission loss, sound pressure level, and acoustic pressure. The expansion chamber muffler's dimensions are taken from the various research papers for validation by the existing FEA system of transmission loss measured. The expansion chamber dimension is mathematically calculated by keeping the volume constant. Models have been developed using dimensions and coordinates in the PTC software wave build 3D.

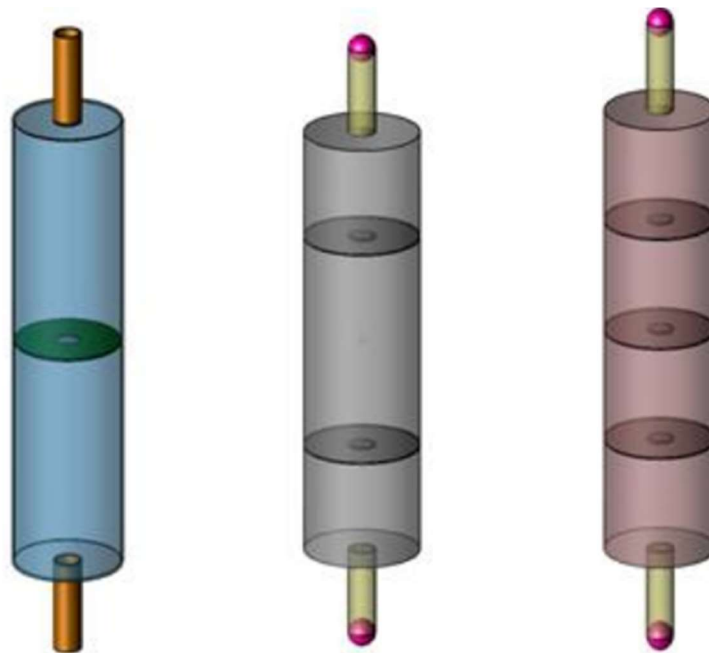


Fig. 10. Duct model with one, two, and three baffle plates [30]

The results of the validation are demonstrated by the experimental method and the 1-D wave transmission loss measurement simulations (TL) in the central outlet muffler with a packing density of 60 kg/m^3 glass wool and rock wool. Comparing rock and glass wool as absorbing materials demonstrates that the greatest loss of transmission in terms of all packaging density is achieved with rock wool. The curve of attenuation under four design observations, i.e., empty expansion room, single platform expansion room, two double platform expansion room, three-plate expansion room. In single plate (empty, rock wool, and glass wool), the mean loss of transmission is 17dB, 29dB, 21dB. The average transmission loss for the double baffle plate is 23.99dB, 32.02dB, and 26.62dB. The average loss of transmission is 27.23dB, 35.32dB, 29.23dB on a triple plate. Thus, the design of a three-blank expansion chamber is best suited to a high loss in transmission. With glass wool and rock wool, the work was proposed to evaluate the loss of muffler transmission. First The increased perforation rate only increases transmission loss to a certain frequency range as per the observation.

PERFORATION RATE	SINGLE BAFFLE PLATE (Avg. TL in dB)	DOUBLE BAFFLE PLATE (Avg. TL in dB)	THREE BAFFLE PLATE (Avg. TL in dB)
With 5%	23.99	26.02	35.02
With 10%	27.05	31.26	40.08
With 15%	30.28	39.56	45.83

Fig. 11. Results comparison [30]

A single baffle plate with 5% perforation on rock wool has a maximum transmission loss of 65 dB, while a double baffle plate with 5% perforation provides the optimal combination of transmission loss and perforation rate. The power of the empty duct is adequate while the frequency is constant, i.e., 2700 Hz, but it is not suitable when the frequency is dynamic.

Sibin babu et al. [31] designed and optimized the hybrid muffler and predicted the acoustic transmission loss. The main purpose of the work was to design a hybrid muffler with good performance. performed acoustic analysis to show how pressure changed when it passes through the muffler. The design and analysis were carried out in ANSYS software. This study selected two production mufflers. Mufflers both contain complex barriers, one of which is filled with absorbent material. ' FEA models have been verified experimentally using a two-source method. Sensitivity analyses on design parameters were conducted after the models had been verified to minimize transmission loss (TL). Perforated holes, partitions, and absorbent material inserts are all included in the analysis. From the study, the result shows that maximum transmission loss was achieved using glass fibre as an absorptive material. The maximum loss of transmission is observed when the outlet chamber length is 0.045 inlet and porosity is equal to the inlet chamber length. There was an increase in TL. This is due to a combination of the absorptive muffler, resonant behavior muffler, and reactive muffler. Maximum Transmission Loss (TL), 43,5901 dB and Transmission Loss (TL) Average at 1484,9943Hz, 32,6161 dB. This work will provide a new method of analysis using ANSYS for the hybrid muffler design.

A Four-pole matrix was used for analyzing and increasing numerically the acoustic features of a muffler in the small space range. A genetic algorithm was applied by M.C. Chiu used to derive a sound transmission loss and to find the optimum form for a separate numerical process. [32]. The results presented a TL numerical analysis for the muffler exit pipe using a transfer matrix approach. The study tried to expand the written program to prophesy the TL of the muffler in this case study [33].

Milad Kermani [34] designed a muffler to maximize the transmission loss. Three approaches for maximizing noise transmission losses in mufflers using a concept for shape changes are followed in this research. For a muffler, the transmission loss is calculated using a three-point method. The impact of muffler geometry on noise transmission loss maximization above the 1/3 octave band and hole frequency range is examined. The same procedure is used for the calculation of loss of noise transmission by the Transfer-Matrix Method. The design variables shall be considered as the diameters and lengths of in, out, and silencer. Finally, the genetic algorithm approach is applied to

analyze the optimal muffler form based on the design variables for a maximum loss of sound transmission.

Puneetha C.G et al. [35] carried out backpressure analysis for four different muffler designs with perforated pipe were studied for the CFD analysis using Acoustic virtual simulation for the Diesel engine (cylinder – 1). Design 1 with 4 holes on the baffle circulated the gas without any perforated pipe. Comparatively the design 1 shows the better backpressure drop.

SY Bhosle et al. [36] Muffler without and with perforation was compared. The velocity at the outlet was higher (4196 Pa). The inlet pipe on which the perforations were made at 3 mm size with 165 mm baffle spacing bend perpendicular to the outlet pipe. Here, the backpressure was 3833 pa which is 8.7% less than the base model.

The exhaust geometry was modified and compared with the old design under the same conditions. The 4 inlet and single outlet with a pipe diameter of 4.2 cm and length of 60 cm was the exhaust geometry. The analysis results were compared with the older ones at the pressure of 1.35 bar and 4 different engine speeds (1300, 1700, 1800, and 1900 rpm). Comparatively the modified one decreased the back pressure and increased the efficiency of the engine [38].

Malaysian researchers modified the exhaust pipe to release gases silently. The 1150 cm pipe was changed to 1350 cm in length, and it has 2 pipes that bend and are located 1000 cm from the header exhaust. Initially, it was located at 1000 cm from the header. The changes affect the performance of the engine (4 stroke Yanmar diesel engine). The analysis was carried out at the speed of 1500 rpm. The modified design shows that the outlet pressure of 9.405×10^4 Pa which is less than the old design (1.021×10^5). The old design with the result of fluctuation in the pressure and the new one shows a gradual reduction in pressure inside the silencer from inlet to outlet [39].

The study shows a methodology for designing a muffler in a practical approach to evaluating the correct formula with time reduction for a 4 stroke 3-cylinder engine. 3 formulas were used to calculate the backpressure. By comparing the error % of CFD and 20% below the theoretical value, it is found that the 2nd Formula is to be finalized for reducing the time consumption [40].

2. Methodology

This chapter will discuss in detail about the parameters which affect the muffler. To narrow down the analysis settings for acoustics a base muffler design was compared with experimental and analytical results with a help of literature. Various designs were incorporated in the base muffler, various other muffler designs, and the acoustics results were obtained for all the designs. The designs that were considered were remodelled by changing different parameters such as baffles, perforations, and diameter change. Solidworks software was used to design the models and Computational Fluid Dynamics (CFD) flow simulation was performed to find the back pressure and the velocity of the mufflers. The inlet velocity obtained in flow simulation is used in ANSYS for acoustic analysis in which the operating frequency is also added in the simulation settings to obtain the transmission loss.

2.1. Base muffler

A simple muffler was designed (Fig.12) using boss extrude and cut extrude options in SW. For harmonic acoustics analysis, only the fluid domain can be used. Hence to attain the fluid domain the model was re-designed in Solidworks using the combine and keep/body delete option and the model was imported into ANSYS in IGES format for analysis.

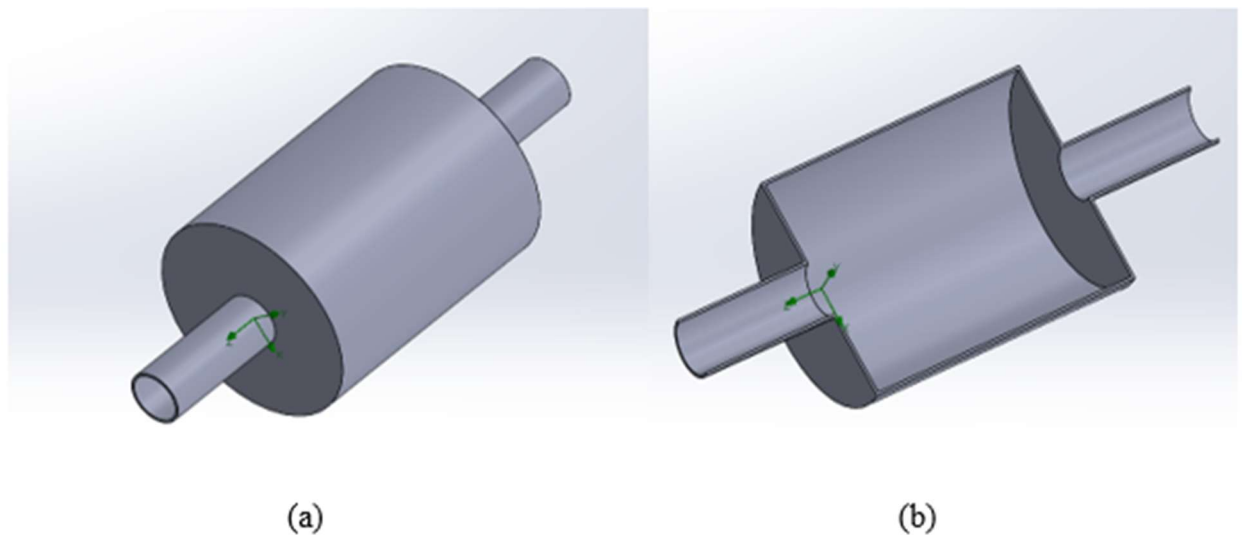


Fig. 12. Base muffler design

Table 3. Base muffler dimensions

No.	Dimensions	Unit(mm)
1.	Inlet & Outlet diameter	41
2.	Expansion chamber length	209
3.	Expansion chamber diameter	159
4.	Inlet & Outlet length	103
5.	Thickness	2

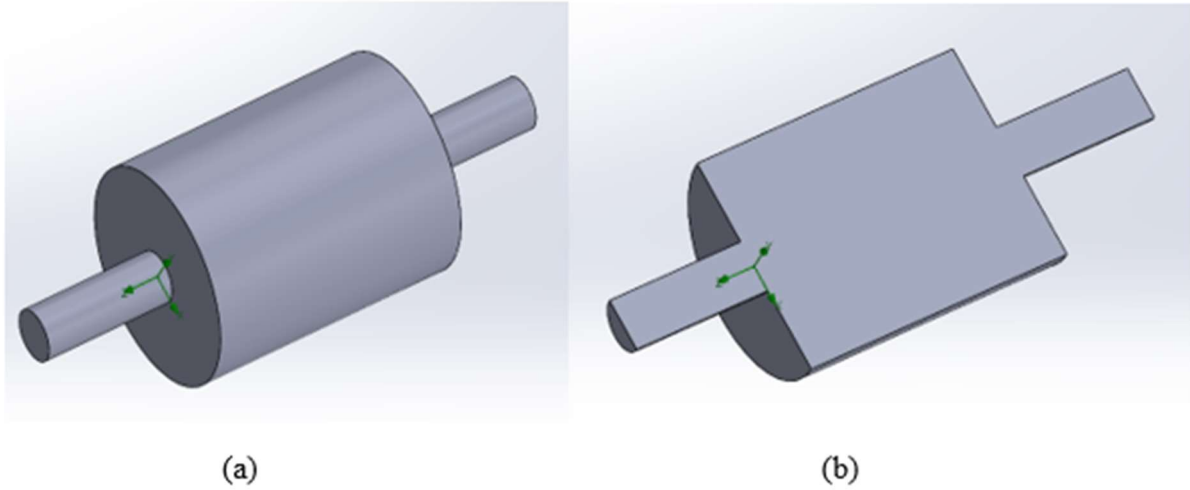


Fig. 13. Base muffler for ANSYS solver

2.1.1. Analytical solution

Numerical solution of the muffler:

$$\text{Transmission Loss (TL)} = 10 \log_{10} \left[1 + \frac{1}{4} \left(m - \frac{1}{m} \right)^2 \sin^2 kL_c \right] \quad (2)$$

$$\text{Area ratio (m)} = \frac{\text{cross-section area of the expansion chamber}}{\text{The cross-section area of the inlet circular pipe}}$$

$$m = \frac{\frac{\pi D^2}{4}}{\frac{\pi d^2}{4}} = \frac{D^2}{d^2} = (0.155)^2 / (0.0037)^2 = 17.54$$

$$\therefore m = 17.54 \text{ mm.}$$

L_c – Chamber length

$$\text{Sound wave number (k)} = 2\pi f/c$$

f- frequency

c- sonic speed

$$k = 2\pi f/ 346.24$$

$$\text{For frequency 650, } k_{650\text{Hz}} = 2(3.14)(650) / 346 \cdot 24 = 11.78$$

$$\text{TL for 650 Hz} = 10 \log_{10} \left[1 + \frac{1}{4} \left(17.54 - \frac{1}{17.54} \right)^2 \sin^2 (11 \cdot 78 \times 2 \cdot 41) \right] = 15.38 \text{ dB.}$$

The calculated value of transmission loss for 650 Hz is 15.38 dB. The maximum frequency range of 2000 Hz with an interval of 50 Hz had been plotted and the resultant graph is shown in the below Fig.14.

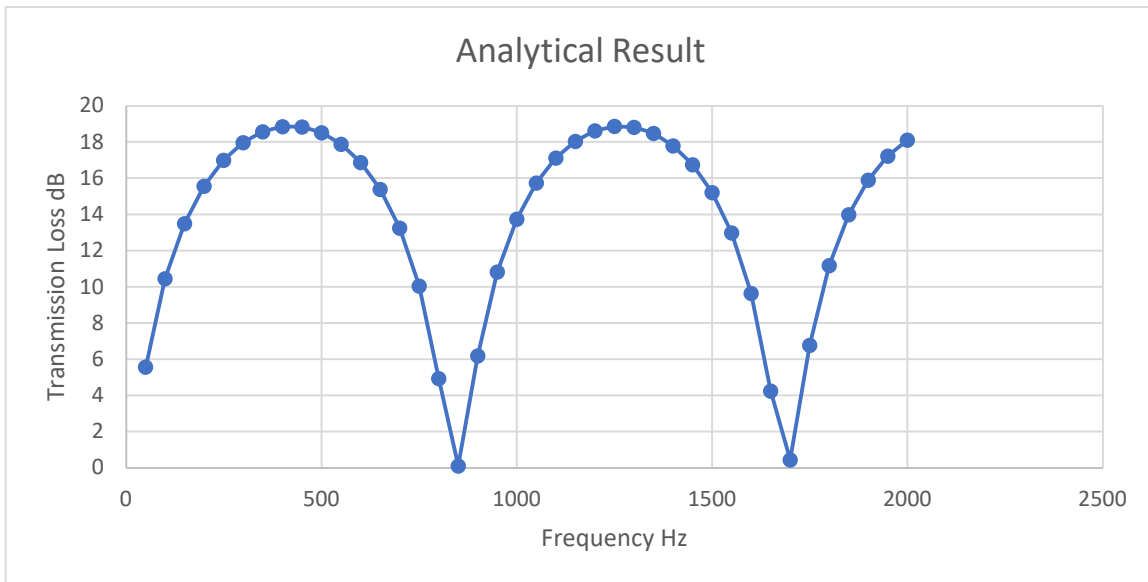


Fig. 14. Base muffler Analytical result graph

2.1.2. Experimental solution

Seybert and Tao experimentally analyzed the acoustic properties, and their results are given below Fig.15.

	Hz	TL	Hz	TL	Hz	TL	Hz	TL
	50	6.3	550	19.1	1050	17.2	1550	15.7
	100	11.5	600	18.3	1100	18.5	1600	12.8
	150	14.6	650	16.3	1150	19.6	1650	8.3
	200	16.5	700	14.3	1200	20.2	1700	0.9
	250	18	750	11.1	1250	20.7	1750	7.6
	300	19.3	800	5.4	1300	20.4	1800	12.4
	350	19.8	850	0.4	1350	20.2	1850	15.7
	400	20.4	900	7.8	1400	19.6	1900	18
	450	20.2	950	12.6	1450	18.5	1950	19.6
	500	19.8	1000	15.4	1500	17	2000	20.9

Fig. 15. Measured experimental values by Seybert and Tao [42]

The obtained analytical value of transmission loss at a frequency of 650 Hz is almost equal to the experimental value which is shown in the above figure.

2.1.3. Ansys workbench

The muffler design was created in Solidworks, and the muffler cavity part was imported in ANSYS as IGES format for the analysis. The simulation was conducted using the Harmonic analysis tool to calculate the transmission loss of the muffler. For the analysis of the fluid domain, Air was used as a material. Patch confirming algorithm with method tetrahedron and for element order global setting was used for meshing.

Mesh size calculation

The maximum frequency, f is 2000 Hz. And the sonic speed of air, C is 346.24 m/s.

To calculate the Wavelength, $\lambda = C/f$.

$$\lambda = 346.24/2000$$

$$\therefore \lambda = 0.173\text{m.}$$

Using the smallest wavelength, the mesh size is calculated. It is recommended that in one wavelength minimum of 6 elements should be there. To calculate the element size using the formula $\lambda/6$.

$$\therefore \text{Element size} = \lambda/6 = 0.173/6 = 0.028\text{m.}$$

$$\therefore \text{Element size} = 0.028\text{m.}$$

The maximum mesh size is up to 28mm but to get accurate results the used value is 0.1m.

Analysis settings

The minimum and maximum range provided here is between 0 Hz to 2000 Hz with a solution interval of 40. So, the result is calculated at every 50 Hz. The only method which can be used for the acoustic analysis is the Full Harmonic method which is used here.

Acoustic Region

In the geometry section, the full body is selected, and the fluid behavior is compressible.

Mass source

- Incident pressure = 1 Pa. (Assumed)
- Mass source = $2/\text{sonic speed}$
 $\therefore \text{Mass source} = 0.005826 \text{ kg/m}^3$

Radiation Boundary

Both the inlet and the outlet faces are selected for the radiation boundary.

Port definition

Two ports were assigned for this analysis.

- Port 1 – Inlet face
- Port 2 – Outlet face.

Solution

After adding all the inputs of harmonic acoustics, the transmission loss was added in the solution section. In the solver section, the input port provided is port-1 and the output port is port-2. [42]

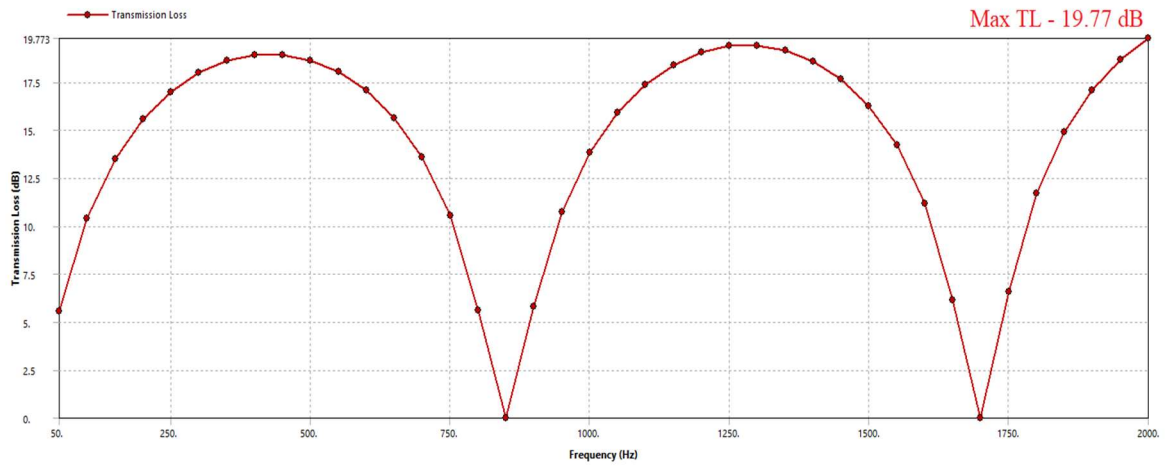


Fig. 16. Analysis result of base muffler

The resultant graph of the transmission loss from ANSYS was shown in the above Fig.16. The maximum transmission loss obtained is 19.77 dB at the frequency of 2000 Hz.

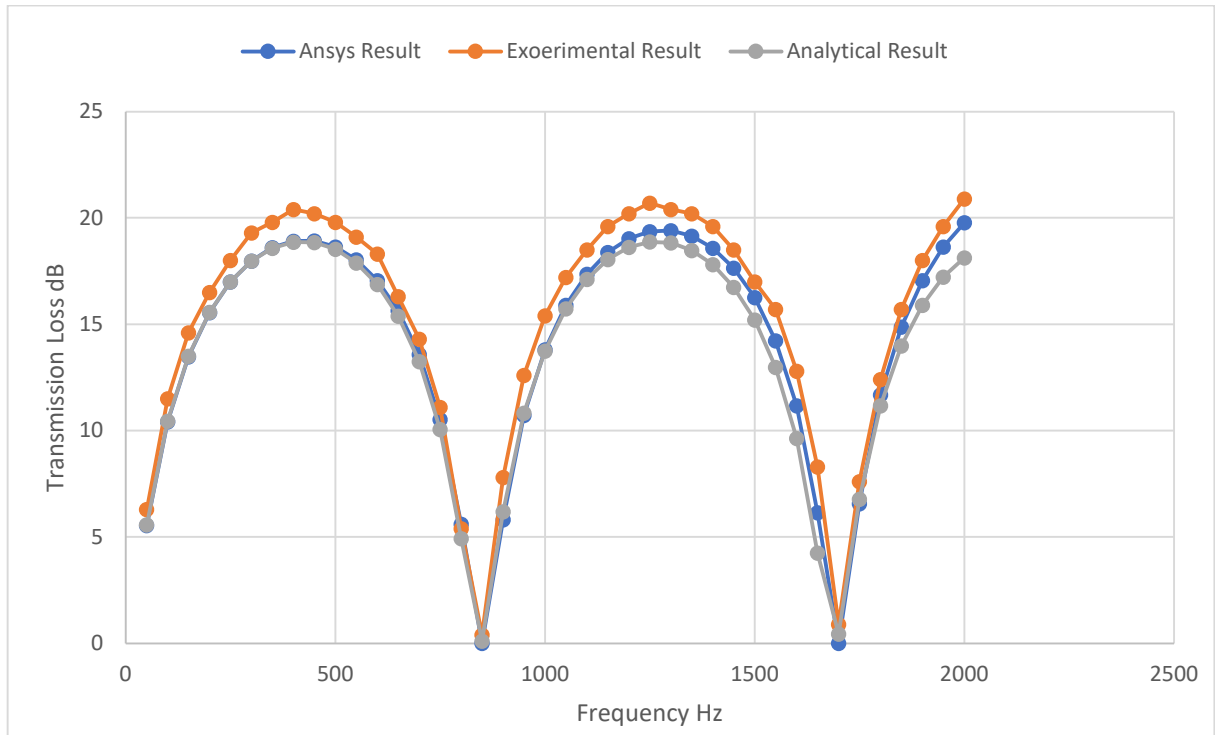


Fig. 17. Comparison of all the results (FEA, Analytical and experimental)

Fig.17 represents comparing the result of Analytical, Experimental, and Finite Element Analysis. It looks like the analysis result (15.3) and experimental result (16.3) are almost equal. So, for my designs, this method was used to calculate the transmission loss. Instead of mass source, surface velocity was considered in the analysis.

2.2. Design 1

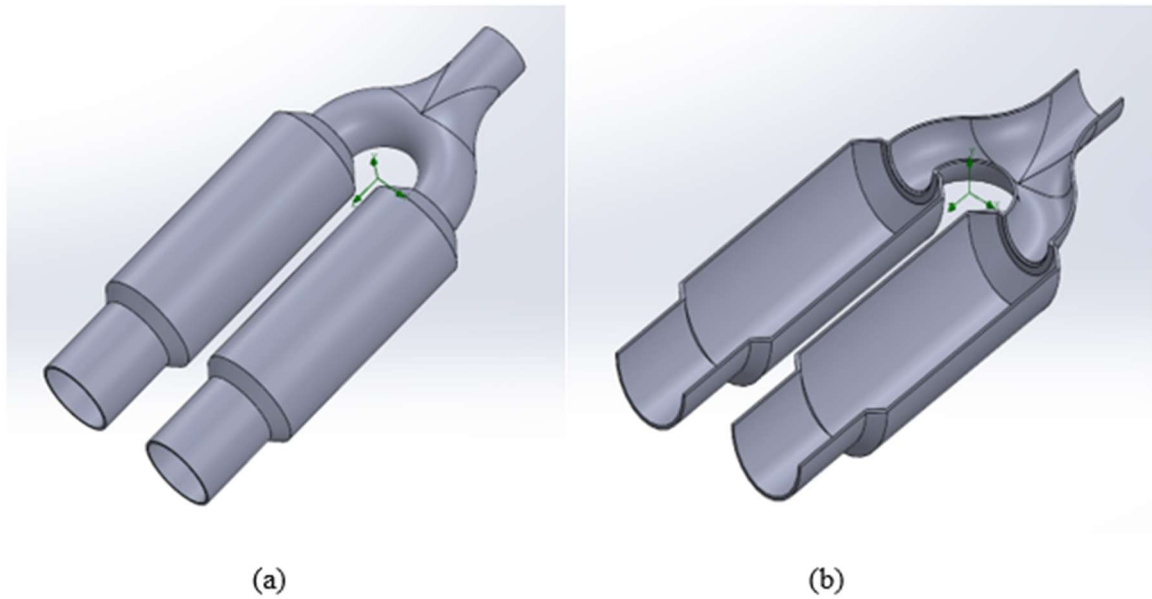


Fig. 18. (a) Design-1 model (b) cut section of the model

Table 4. Design-1 dimension

No.	Dimensions	Unit (mm)
1.	Inlet diameter	70
2.	Expansion chamber length	264
3.	Expansion chamber diameter	120
4.	Thickness	3 (dia)
5.	Outlet diameter	90

The above fig.18. (a) design-1 model with two exhaust pipes and fig.19. (b) represents the cut section of the model. The dimensions given here are within the permissible limit which is mentioned in the above table. This model was designed in Solidworks. To find the transmission loss, harmonic acoustic analysis was carried out in ANSYS software. For harmonic acoustics, only the fluid domain should be used. To get the fluid domain, a rectangle is a boss extruded over the body and Boolean subtraction is used to separate the parts. To get the fluid domain the rectangle body was deleted. Then the solid body was imported to ANSYS for Harmonic acoustic analysis in IGES format.

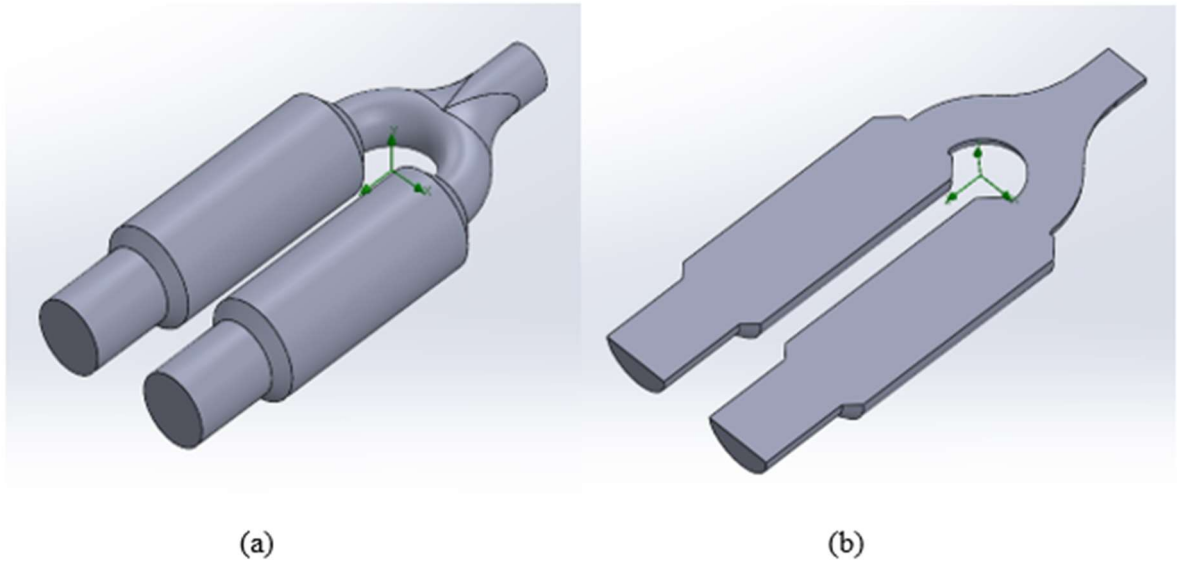


Fig. 19. Design-1 for ANSYS solver (b) Cut section of the fluid domain

The above fig.19 represents a fluid domain of design-1 which was used for the ANSYS simulation. Here the inlet diameter is 64mm and the outlet diameter is 84mm and the diameter of the expansion chamber is 114mm.

2.2.1. Design-1.1

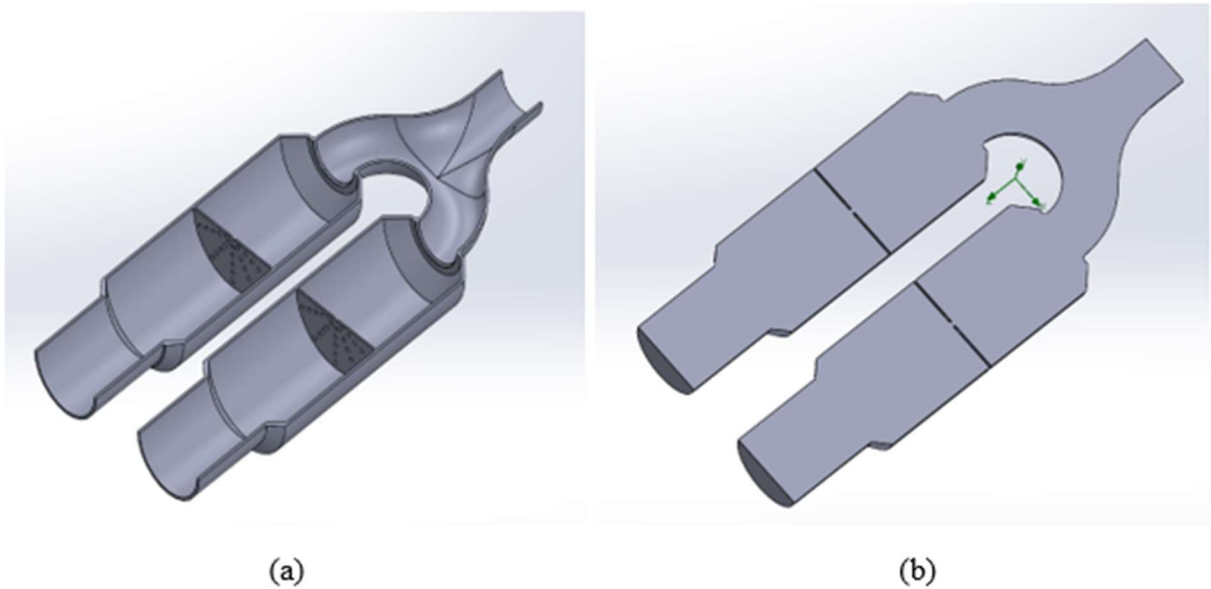


Fig. 20. (a) Cut section of the design-1.1 with baffle plate 1 in SW (b) Cut section of the solid body for ANSYS simulation

The fig.20. signifies the cut section of the muffler with baffle plate 1 which was designed inside the universal muffler. A baffle plate was designed at the center of the expansion chamber and reusing the design-1 procedure to attain the fluid domain model. The solid-body obtained was imported to ANSYS for Harmonic acoustic analysis in IGES format.

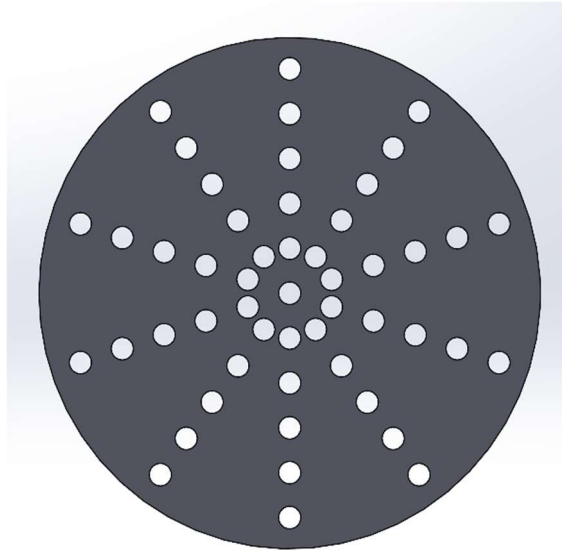


Fig. 21. Baffle plate 1.1

Table 5. Baffle plate 1 dimension

No.	Dimensions	Unit(mm)
1.	Hole diameter	5
2.	Plate Thickness	2
3.	Baffle plate diameter	114

This fig.21. denotes the baffle plate 1.1 which was designed inside the muffler. The dimensions of the baffle plate are mentioned in the above table. The baffle plate was designed using a linear and circular pattern with a hole diameter of 5mm.

2.2.2. Design-1.2

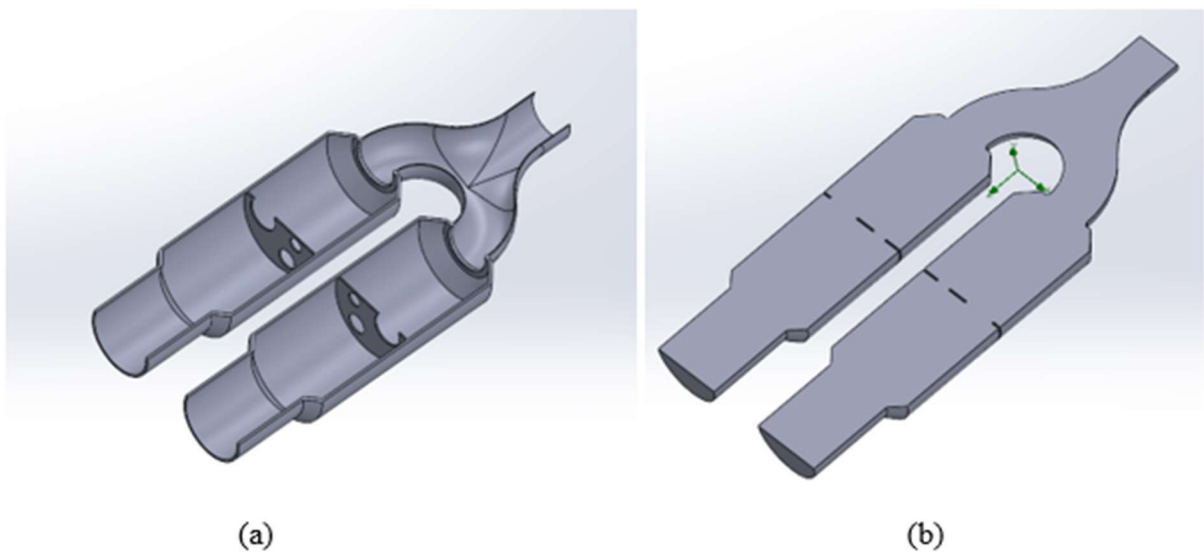


Fig. 22. (a) Cut section of the design-1.2 with baffle plate 2 in SW (b) Cut section of the solid body for Ansys solver

The fig.22. represents the cut section of the muffler with baffle plate 2 which was designed inside the design-1. The baffle plate was designed at the center of the expansion chamber with a diameter of 114mm. The design-1 procedure was reused to attain the solid body for this model. Then the solid body was imported to ANSYS for acoustic analysis in IGES format.

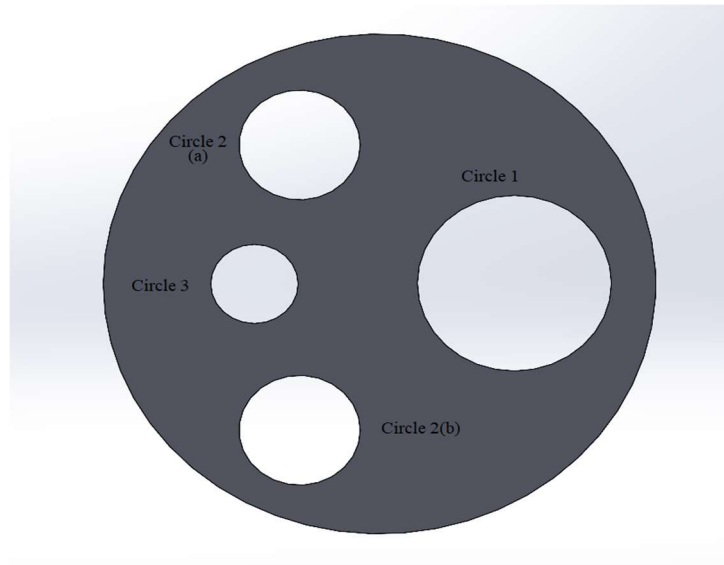


Fig. 23. Baffle plate 1.2

Table 6. Baffle plate 1.2 dimensions

No.	Dimensions	Unit(mm)
1.	Plate Thickness	2
2.	Baffle plate diameter	114
3.	Circle 1 diameter	40
4.	Circle 2 (a & b) diameter	25
5.	Circle 3 diameter	18

This fig.23.represents the baffle plate 1.2 which is designed inside the muffler. The dimensions of the baffle plate are mentioned in the above table. The baffle plate contains four circles with two circles (2 a & b) having the same diameter and the remaining circles having different diameters each.

2.2.3. Design-1.3

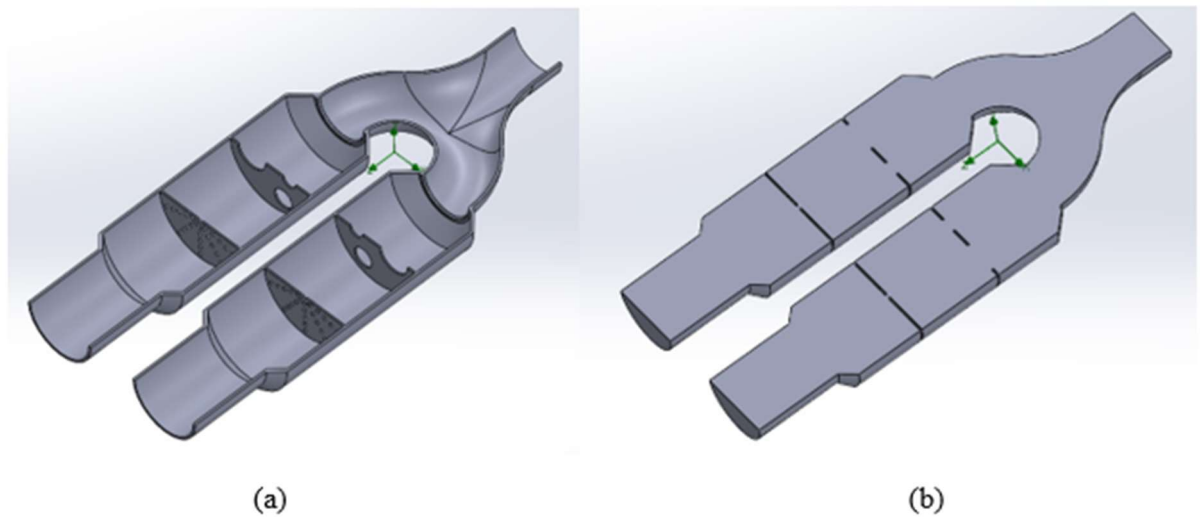


Fig. 24. (a) Muffler with baffle plate 1.1&1.2 (b)Cut section of the solid body used for ANSYS simulation

The fig.24. represents a cut section of the muffler with baffle plates 1.1&1.2. Both the baffle plates have been placed inside the expansion chamber. The baffle plate 1.1 was placed at 100mm from the starting point of the expansion chamber. The baffle plate 1.2 was placed 200mm from the chamber.

2.3. Design-2

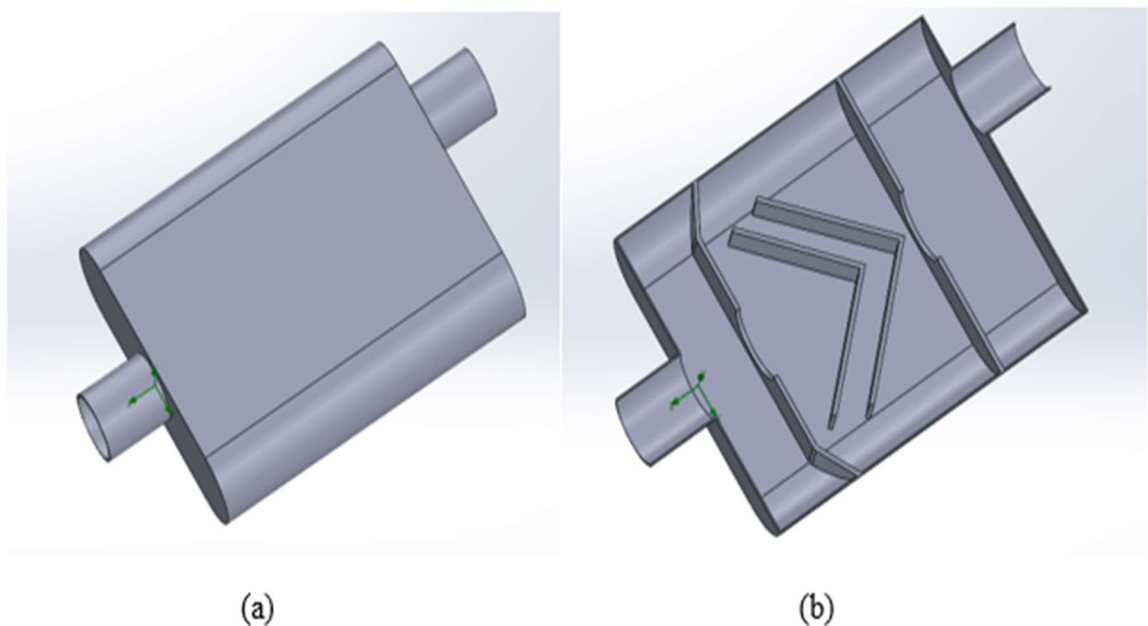


Fig. 25. (a) Design-2 model (b) Cut section of the model

Table 7. Design-2 dimensions

No.	Dimensions	Unit(mm)
1.	Expansion chamber length	434
2.	Inlet & outlet diameter	75
3.	Chamber diameter	104

4.	Chamber width	250
5.	Baffle plate diameter	100
6.	Thickness	2
7.	Baffle hole diameter	80
8.	Baffler plate thickness	5
9.	Inlet & Outlet pipe length	90

The above figure.25 (a) represents the design-2 muffler model and (b) represents the cut section of the model. The dimensions given here are within the permissible limit as per flow master values which are mentioned in the above table. This model has also been designed in Solidworks with 3 chambers. These 3 chambers are divided by two baffle plates with a hole in the center having a diameter of 80mm. In chamber 2 V-shaped perforation was designed with an angle of 90 degrees concerning the inlet origin. The second baffle plate was placed at 315mm from the inlet origin. To find transmission loss, harmonic acoustic analysis was carried out in ANSYS software.

The procedure to get the fluid domain from this model, a rectangle is a boss extruded over the body and the Boolean subtraction is used to separate the parts. To get the fluid domain the rectangle body was deleted. Then the solid body was imported to ANSYS for Harmonic acoustic analysis in IGES format.

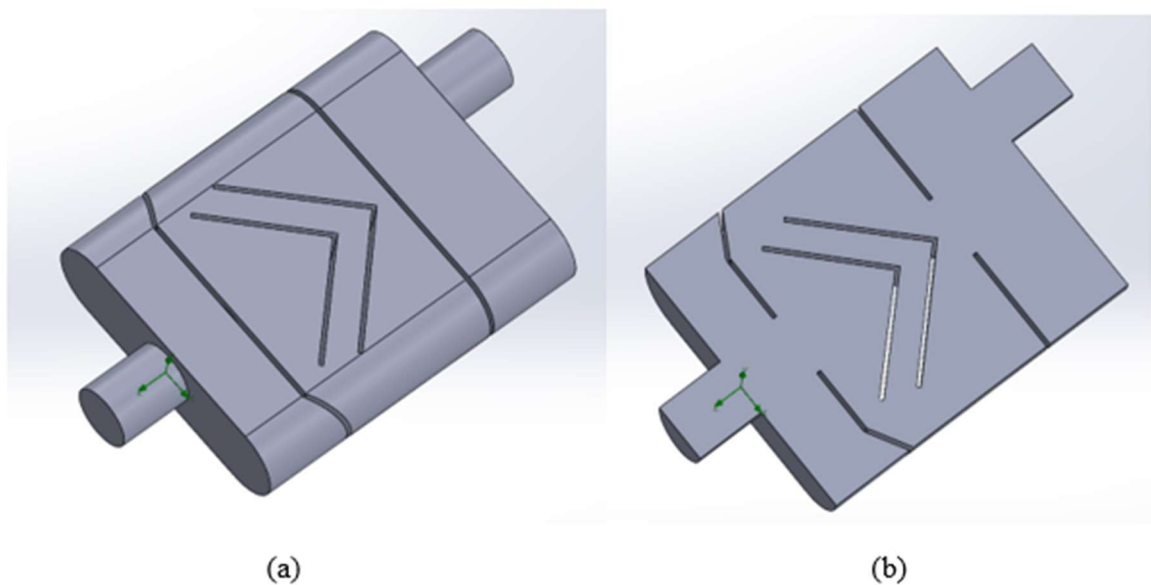


Fig. 26. Design-2 for ANSYS simulation (b) Cut section of the fluid domain

The fluid domain model has an inlet and outlet diameter of 71mm, expansion chamber diameter of 100mm, and length of 430mm. Fig. 26. shows the fluid domain of the chambered muffler which was used for the harmonic acoustic analysis.

2.3.1. Design-2.1

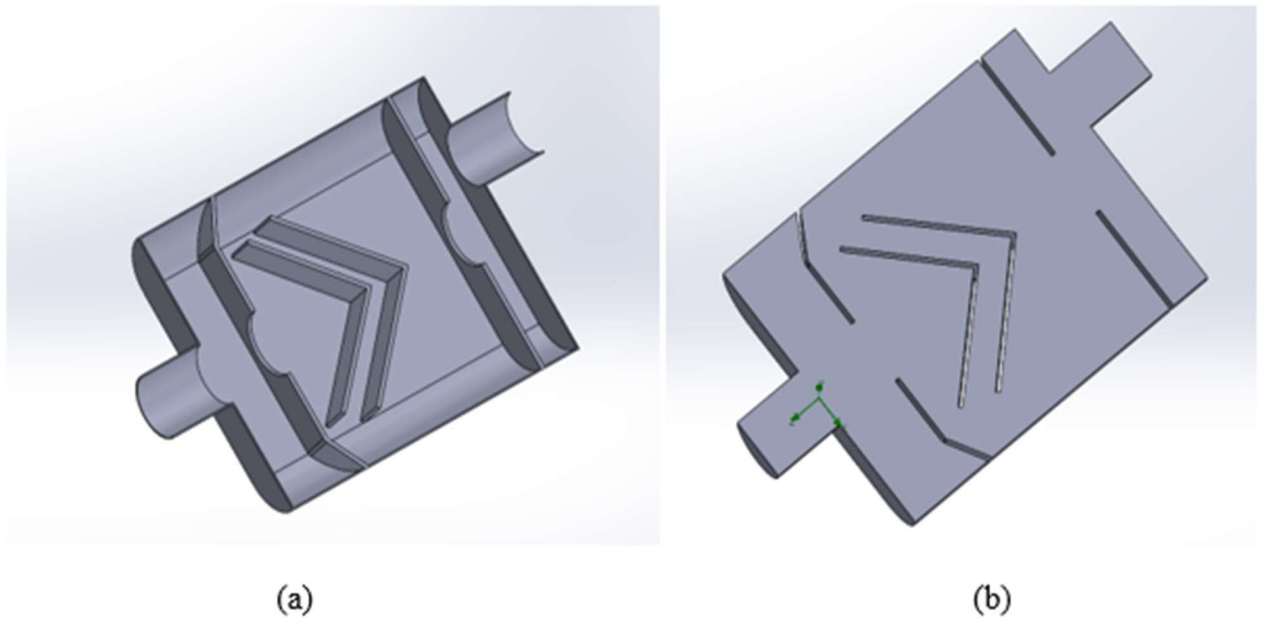


Fig. 27. (a) Cut section of the design 2.1 (b) fluid domain

The above fig.27. represents the design-2.1 muffler model in which the second baffle plate was placed at 380mm from the inlet origin. The steps used to get the fluid domain of the muffler design 2 has been followed for this model as well.

2.3.2. Design-2.2

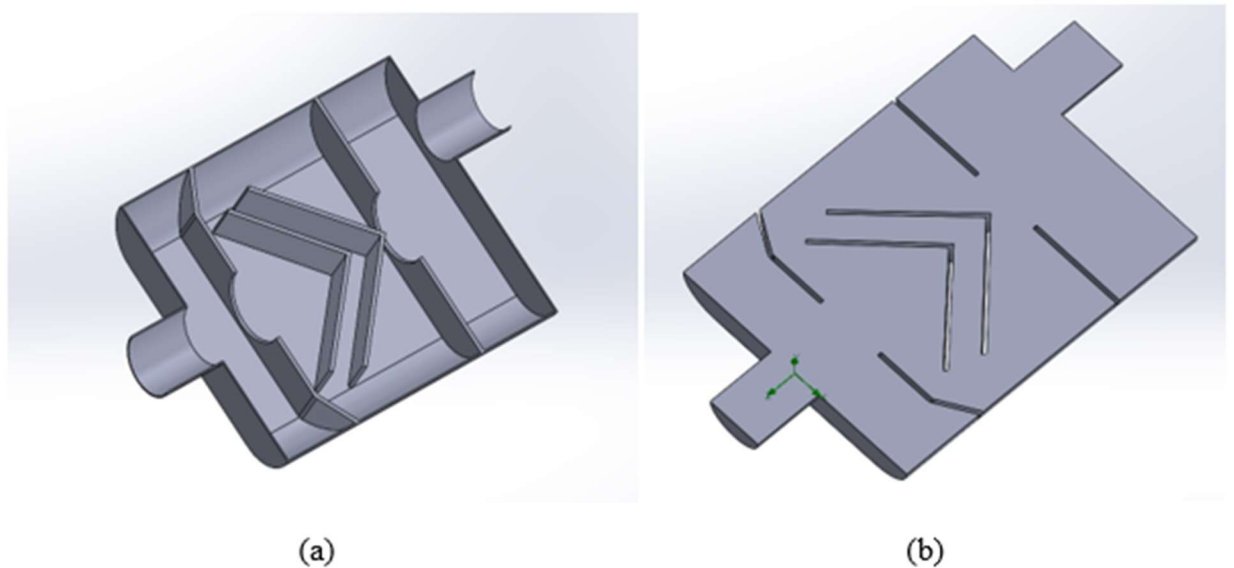


Fig. 28. (a) Cut section of the design-2.2 muffler model (b) fluid domain

The procedure used for design 2.2 reuses the steps of design 2 with an increase in the baffle plate hole diameter from 80mm to 90mm as shown in fig.28.

2.3.3. Design-2.3

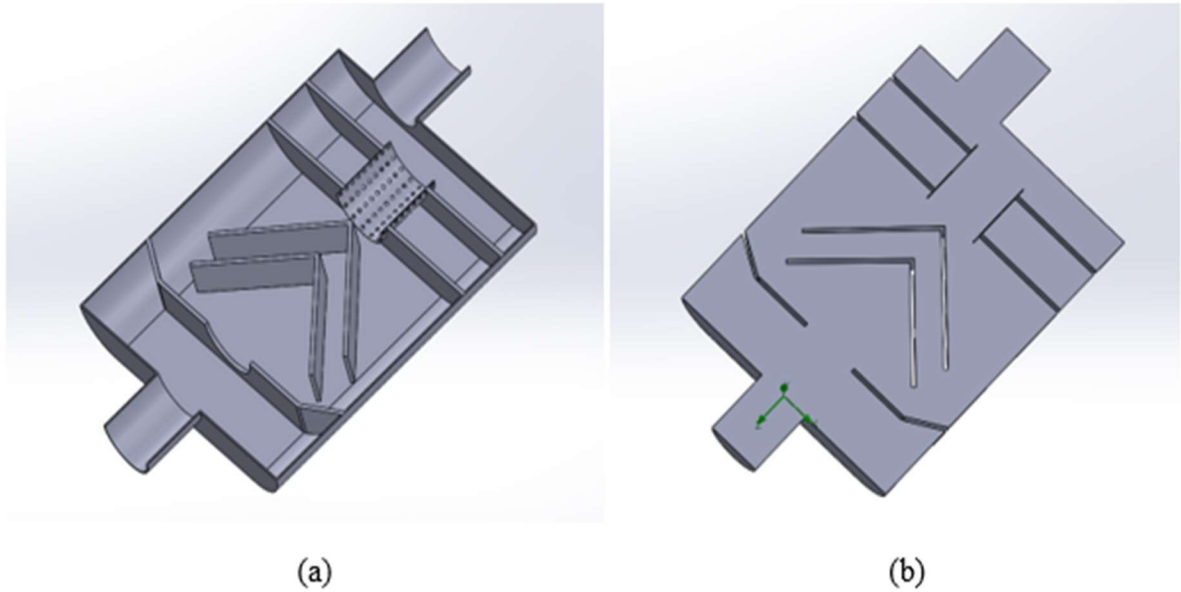


Fig. 29. (a) Cut section of the design-2.3 muffler model and (b) fluid domain

The above fig.29.(a) represents the design-2.3 muffler model and (b) represents the cut section of the model. This model was designed like design-2 with an additional chamber totaling 4 chambers. These four chambers are divided by three baffle plates with a hole in the center having a diameter of 80mm. In between chamber 3, a perforated pipe with an external diameter of 80mm was inserted in between the second and third baffle plates. The second baffle plate was placed at 315mm from the inlet origin. And the third baffle plate was placed at 380mm from the inlet origin. The remaining procedure for this model is the same as the muffler design 2.

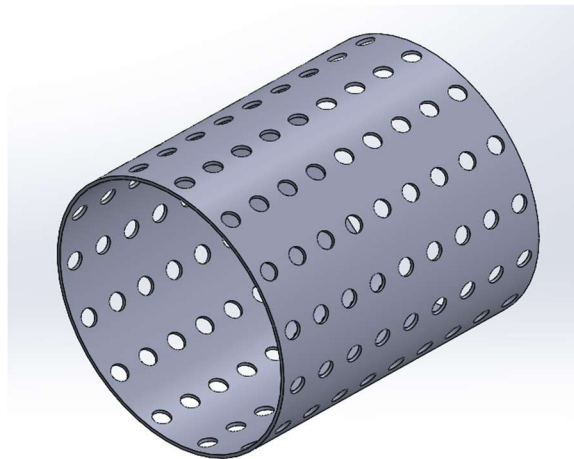


Fig. 30. Perforated pipe 2.1

Table 8. Perforated pipe 2.1 dimensions

No.	Dimensions	Unit(mm)
1.	Pipe length	90
2.	Hole diameter	5
3.	Thickness	2
4.	External diameter	80

Fig.30. represents the perforated pipe with an external diameter of 80mm which was placed in between the baffle plates 2 and 3 in design 4. A circle was extruded at the center of the pipe and then the linear patter option was used for 10mm spacing on both sides with 5 instances. The circular pattern option was used with equal spacing for 360 degrees for 15 instances.

2.3.4. Design-2.4

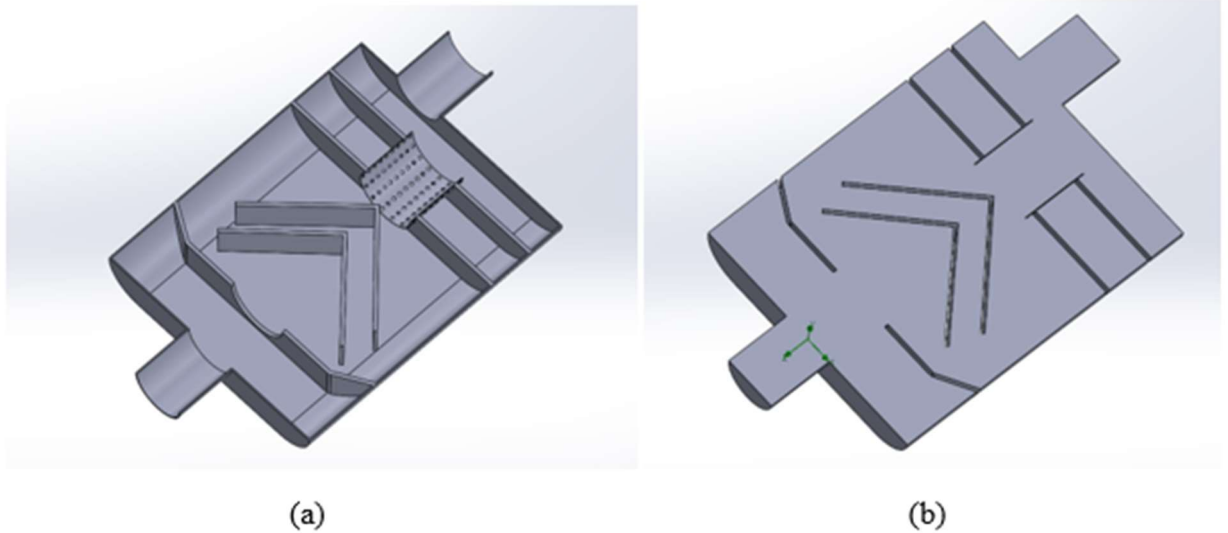


Fig. 31. (a) Cut section of the design-2.4 muffler model and (b) fluid domain

The procedure used for design 2.4 reuses the steps of design 2.3 with an increase in the baffle plate hole diameter from 80mm to 90mm as shown in fig. The perforated pipe 2.2 shown in fig.32 was placed between the baffle plates 2 and 3.

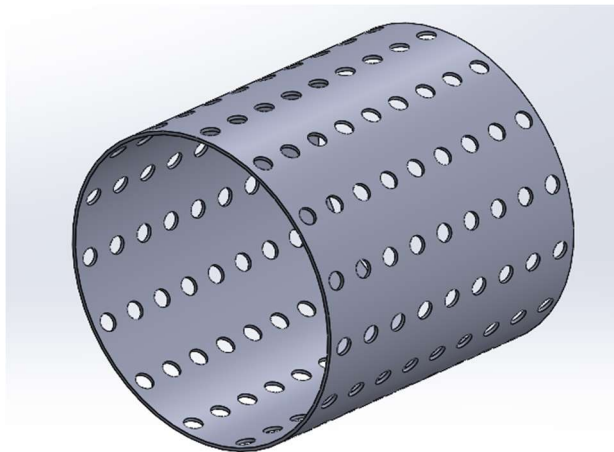


Fig. 32. Perforated pipe 2.2

Table 9. Perforated pipe 2.2 dimensions

No.	Dimensions	Unit(mm)
1.	Pipe length	90

2.	Hole diameter	5
3.	Thickness	2
4.	External diameter	90

The above fig.32. represents the perforated pipe with an external diameter of 90mm which was placed in between the baffle plates 2 and 3 in chambered muffler design 2.4 as mentioned above.

2.4. Design-3

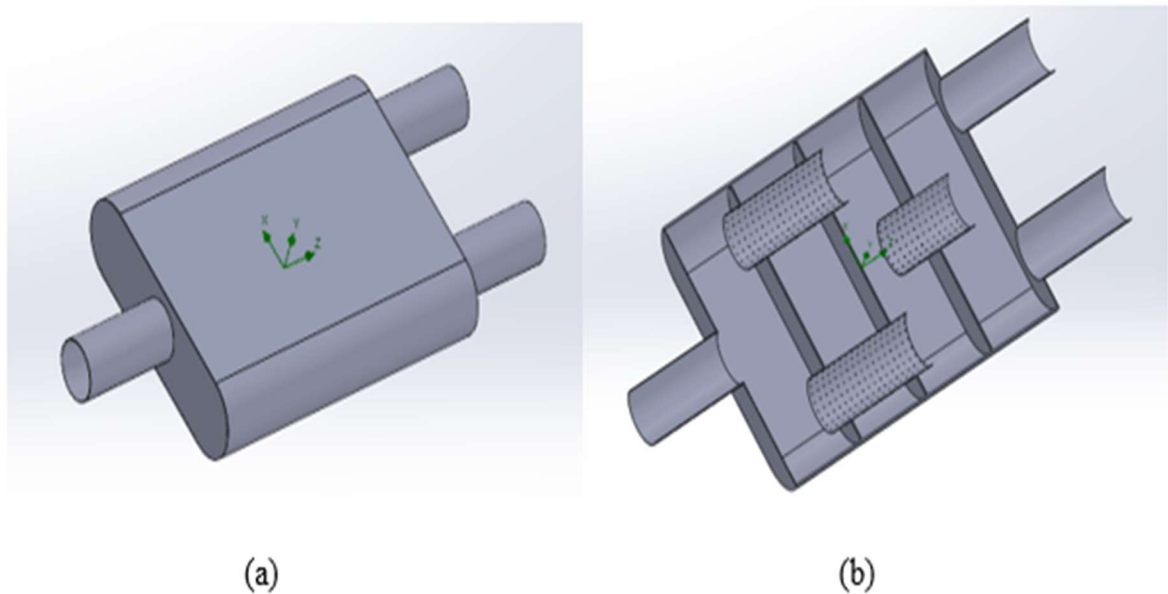


Fig. 33. Design-3 muffler model (b) cut section of the model

Table 10. Design-3 dimensions

No.	Dimensions	Unit(mm)
1.	Expansion chamber length	450
2.	Expansion chamber diameter	100
3.	Inlet & Outlet diameter	70
4.	Thickness	3
5.	Inlet & Outlet pipe length	150
6.	Expansion Chamber width	250
7.	Baffle plate diameter	96
8.	Baffle plate hole diameter	70
9.	Baffle plate thickness	2

Fig. 33. represents the design-3 muffler model and the cut section of the model. The dimension of the model is mentioned in the above table. This model has also been designed in Solidworks with 4 chambers. These four chambers are divided by three baffle plates which have a hole in the center with a diameter of 70mm. In between the baffle plate 1 and 2, a set of perforated pipes (3.1) was placed inside the muffler with an external diameter of 70mm and length of 168mm. And a small, perforated pipe (3.2) was placed at the center of the baffle plate 3 with an external diameter of 70 mm and length

of 120mm. The spacing between the three baffle plates is 112mm from the inlet origin. To find the transmission loss, harmonic acoustic analysis was carried out in ANSYS software.

The procedure to get the fluid domain from this model, a rectangle is a boss extruded over the body and the Boolean subtraction is used to separate the parts. To get the fluid domain the rectangle body was deleted. Then the solid body was imported to ANSYS for Harmonic acoustic analysis in IGES format.

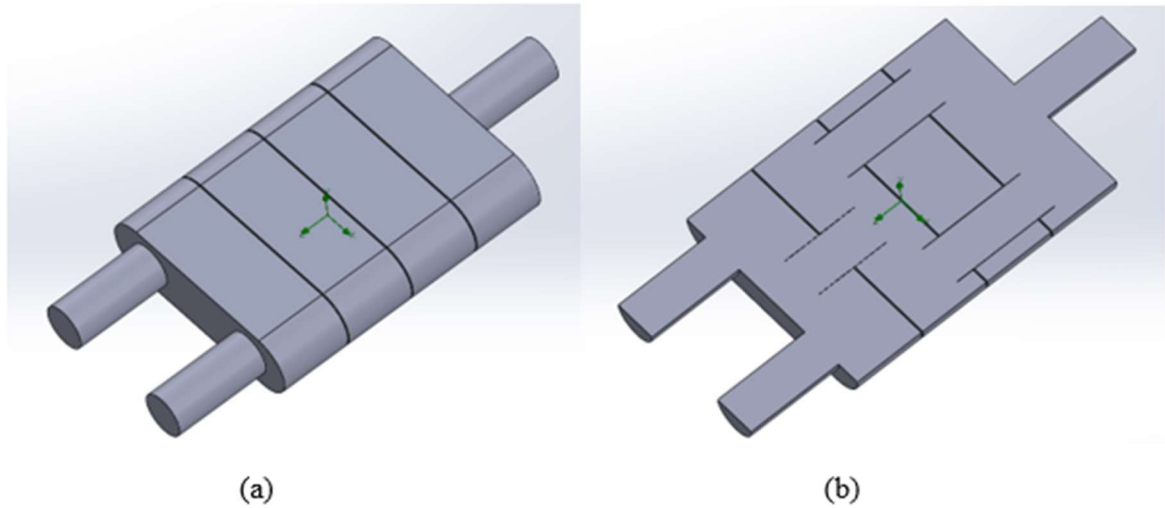


Fig. 34. (a) Design-3 muffler model fluid domain (b) cut section of the fluid domain

The above fig.34. represents the fluid domain of the diesel engine muffler which was used for the Harmonic acoustic analysis in ANSYS software. The inlet and outlet diameter for this fluid domain are 64mm and the expansion chamber diameter is 94mm.

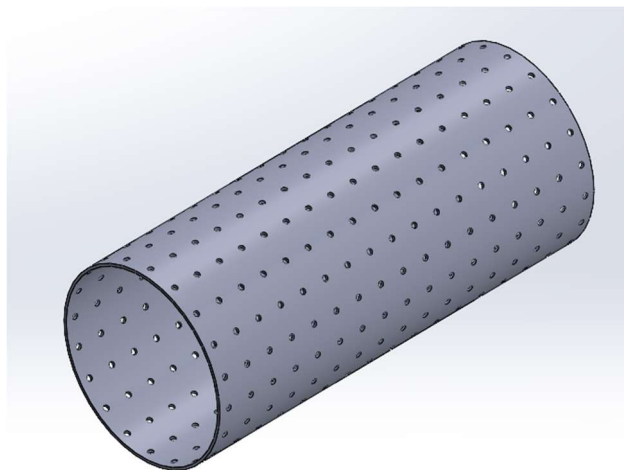


Fig. 35. Perforated pipe 3.1

Table 11. Perforated pipe 3.1 dimensions

No.	Dimensions	Unit(mm)
1.	Pipe length	168

2.	Hole diameter	2
3.	Thickness	2
4.	External diameter	70

The above fig.35. shows a perforated pipe with an external diameter of 70mm that has a length of 168mm with a hole diameter of 2 mm was designed between the baffle plate 1 and 2. A circle was extruded at the center of the pipe from the top plane and a linear patter option was used for 10mm spacing on both sides with a total of 17 instances. Additionally, the circular pattern option was used with equal spacing for 360 degrees for 20 instances.

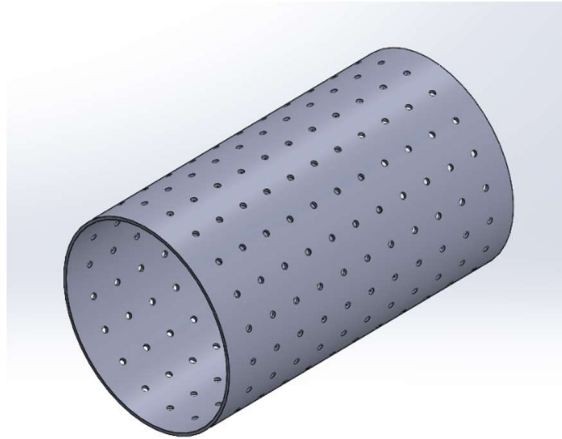


Fig. 36. Perforated pipe 3.2

Table 12. Perforated pipe 3.2 dimensions

No.	Dimensions	Unit(mm)
1.	Pipe length	120
2.	Hole diameter	2
3.	Thickness	2
4.	External diameter	70

In the above fig.36. is the perforated pipe with an external diameter of 70mm with a length of 120mm and a hole diameter of 2 mm was designed at the center of the baffle plate 3. A circle was extruded at the center of the pipe from the top plane and a linear patter option was used for 10 mm spacing on both sides with a total of 13 instances. And then circular pattern option was used with equal spacing for 360 degrees for 20 instances.

2.4.1. Design-3.1

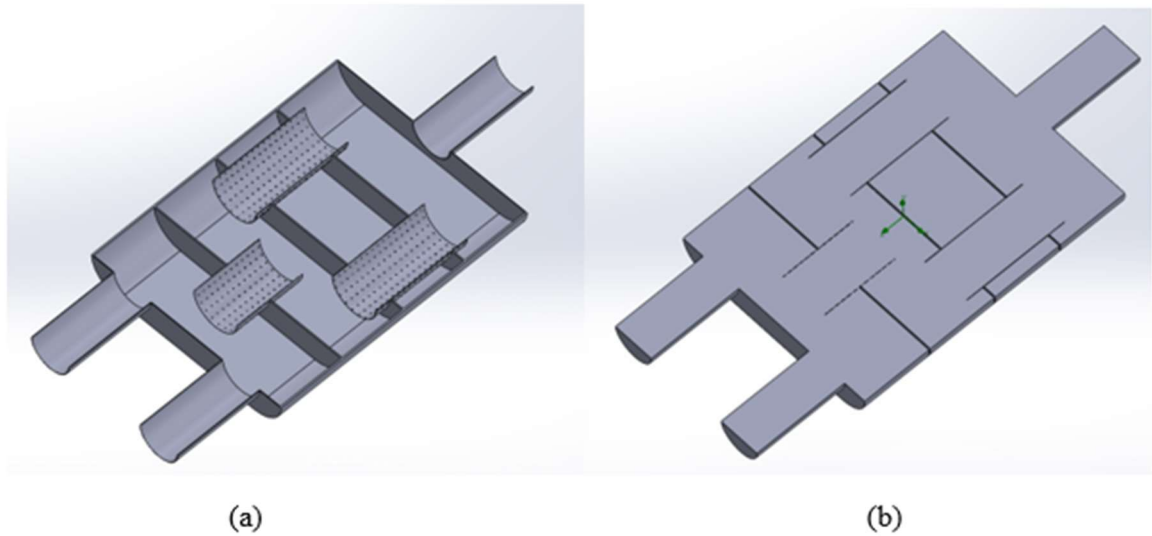


Fig. 37. Cut section of the diesel engine muffler model 3.1 and (b) fluid domain

Fig. 37. represents the same as the design-3 muffler model, but the baffle plate hole diameter was changed to 80mm in this design for all three baffle plates. In between the baffle plate 1 and 2, a set of perforated pipes (3.3) was placed inside the muffler with an external diameter of 80mm and length 168mm with a hole diameter of 2mm. And a small, perforated pipe (3.4) was placed at the center of the baffle plate 3 with an external diameter of 80 mm and length of 120mm. The same procedure as design 3 was followed for ANSYS simulation.

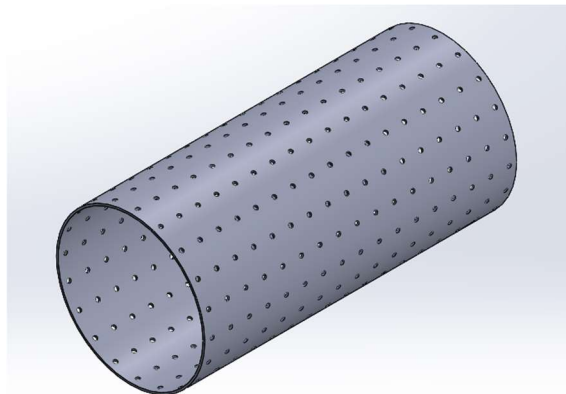


Fig. 38. Perforated pipe 3.3

Table 13. Perforated pipe 3.3 dimensions

No.	Dimensions	Unit(mm)
1.	Pipe length	168
2.	Hole diameter	2
3.	Thickness	2
4.	External diameter	80

In the above fig.38. is the perforated pipe with an external diameter of 80mm with a length of 168mm and a hole diameter of 2mm was designed between the baffle plate 1 and 2. A circle was extruded at

the center of the pipe from a top plane and a linear patter option was used for 10mm spacing on both sides with a total of 17 instances. And then circular pattern option was used with equal spacing for 360 degrees for 20 instances.

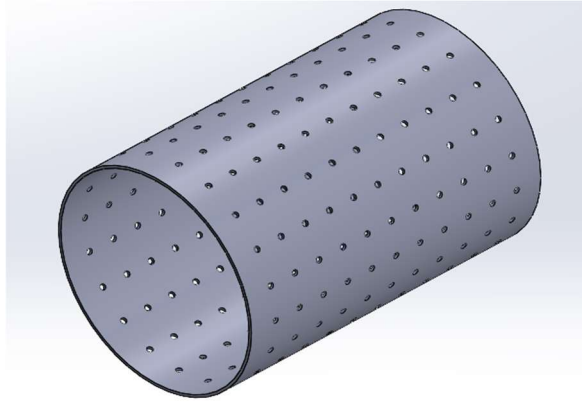


Fig. 39. Perforated pipe 3.4

Table 14. Perforated pipe 3.3 dimensions

No.	Dimensions	Unit(mm)
1.	Pipe length	120
2.	Hole diameter	2
3.	Thickness	2
4.	External diameter	80

In the above fig.39. is the perforated pipe with an external diameter of 80mm with a length of 120mm and a hole diameter of 2mm was designed at the center of the baffle plate 3. A circle was extruded at the center of the pipe from the top plane and a linear patter option was used for 10 mm spacing on both sides with a total of 13 instances. And then circular pattern option was used with equal spacing for 360 degrees for 20 instances.

2.4.2. Design-3.2

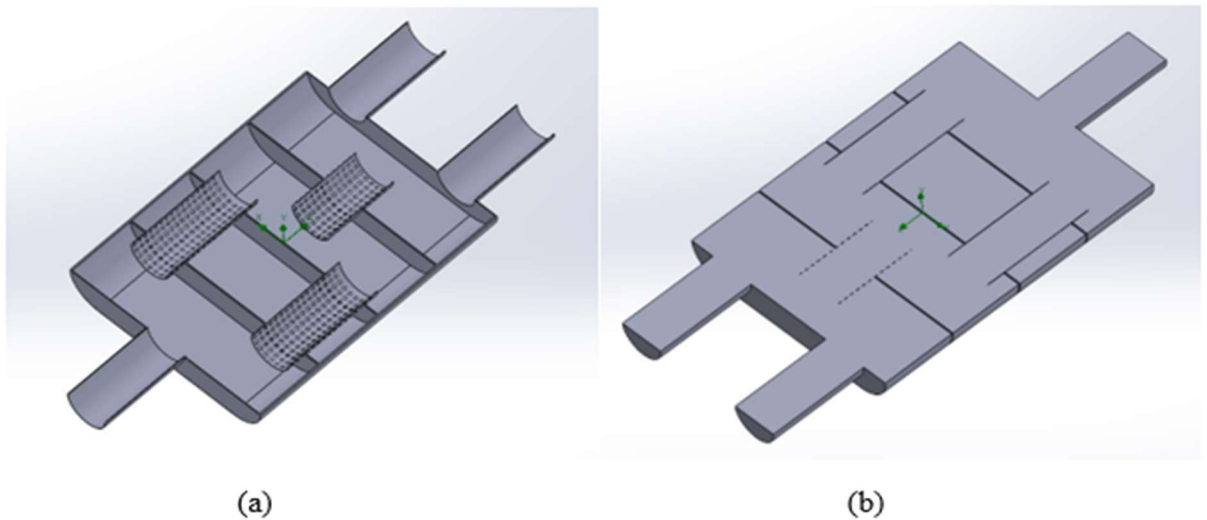


Fig. 40. Cut section of design-3.2 muffler model and (b) fluid domain

Fig. 40. shows the same model as design-3 but the perforated pipe hole diameter was changed to 5mm for this model. The rest of the dimensions and procedures are the same as in design-3.

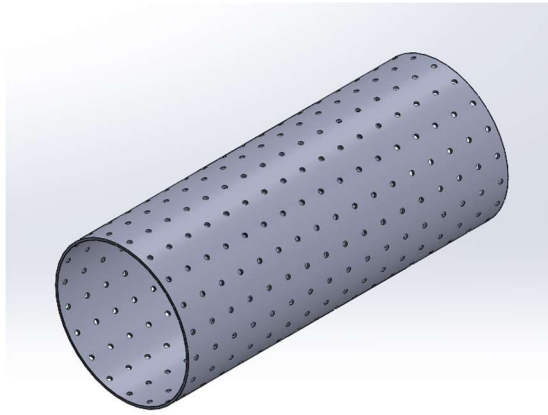


Fig. 41. Perforated pipe 3.5

Table 15. Perforated pipe 3.5 dimensions

No.	Dimensions	Unit(mm)
1.	Pipe length	168
2.	Hole diameter	5
3.	Thickness	2
4.	External diameter	70

In the above fig.41. is the perforated pipe with an external diameter of 70mm with a length of 168mm and a hole diameter of 5mm was designed between the baffle plate 1 and 2. A circle was extruded at the center of the pipe from the top plane and a linear patten option was used for 10mm spacing on both sides with a total of 17 instances. And then circular pattern option was used with equal spacing for 360 degrees for 20 instances.

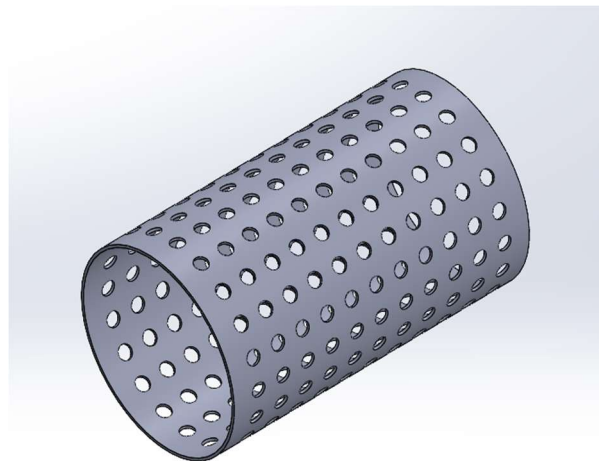


Fig. 42. Perforated pipe 3.6

Table 16. Perforated pipe 3.6 dimensions

No.	Dimensions	Unit(mm)
1.	Pipe length	120
2.	Hole diameter	5
3.	Thickness	2
4.	External diameter	70

In the above fig.42. is the perforated pipe with an external diameter of 70mm with a length of 120mm and a hole diameter of 5mm was designed at the center of the baffle plate 3. A circle was extruded at the center of the pipe from the top plane and a linear pattern option was used for 10 mm spacing on both sides with a total of 13 instances. And then circular pattern option was used with equal spacing for 360 degrees for 20 instances.

2.4.3. Design-3.3

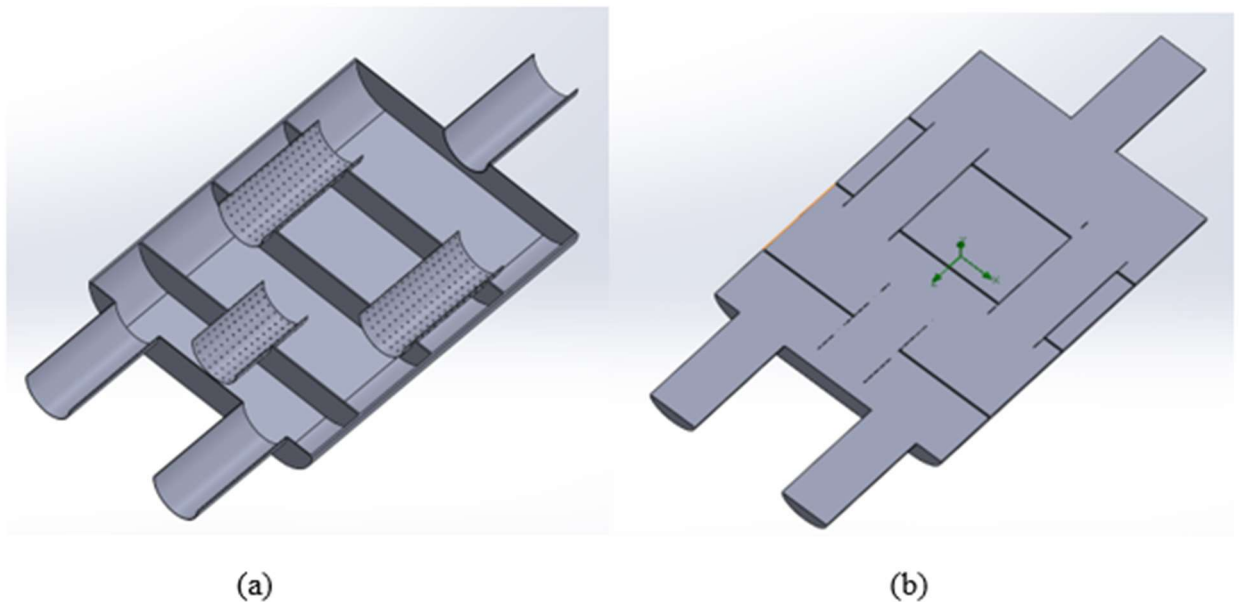


Fig. 43. Cut section of the design-3.3 muffler model and (b) cut section

The above fig.43. was designed with the same dimension as design 3. The only difference in this model is the spacing between the three baffle plates was changed to 122mm from the inlet origin as opposed to design 1 where the distance was 112mm. The perforated pipes 3.1 and 3.2 have been designed in between the baffle plates. The same procedure followed in design-3 was repeated here for ANSYS simulation.

2.4.4. Design-3.4

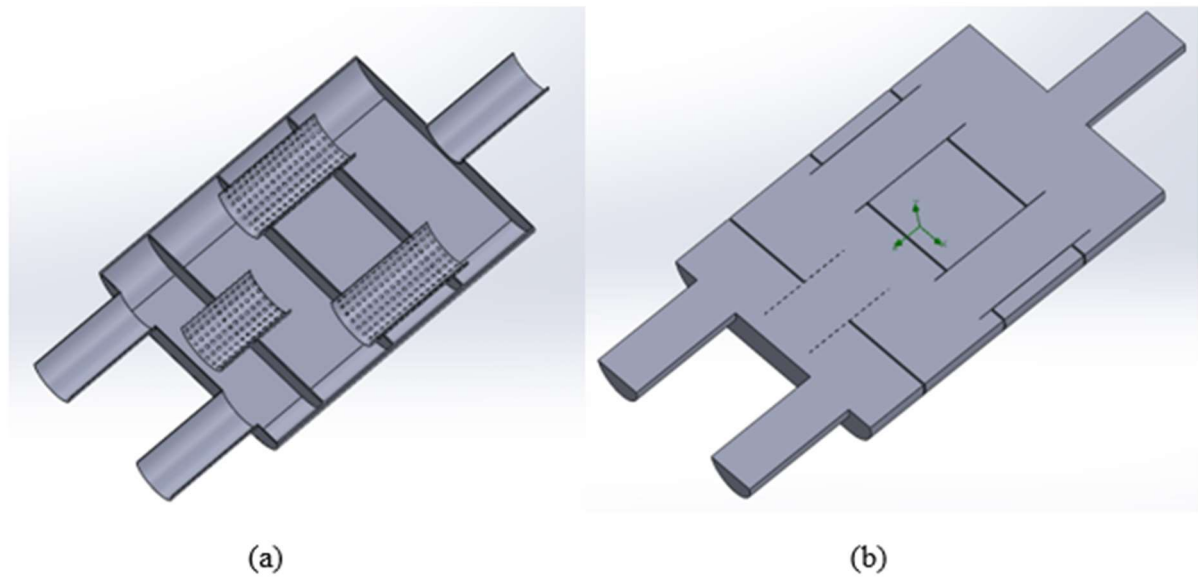


Fig. 44. Cut section of the design-3.4 muffler model and (b) fluid domain

All the design changes which have been done in the previous models have been implemented in this model fig.44. The baffle plate hole diameter was changed to 80mm for all the baffle plates and the perforated pipe hole diameter was changed to 5mm for all the pipes. The spacing between the three baffle plates was changed to 122mm from the inlet origin.

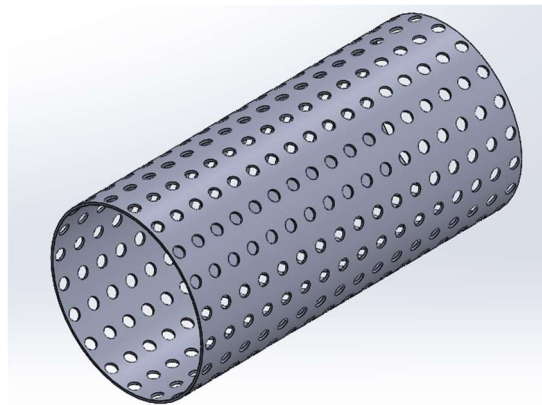


Fig. 45. Perforated pipe 3.7

Table 17. Perforated pipe 3.7 dimensions

No.	Dimensions	Unit(mm)
1.	Pipe length	168
2.	Hole diameter	5
3.	Thickness	2
4.	External diameter	80

In the above fig.45. is the perforated pipe with an external diameter of 80mm with a length of 168mm and a hole diameter of 5mm was designed between the baffle plate 1 and 2. A circle was extruded at

the center of the pipe from the top plane and a linear patter option was used for 10mm spacing on both sides with a total of 17 instances. And then circular pattern option was used with equal spacing for 360 degrees for 20 instances.

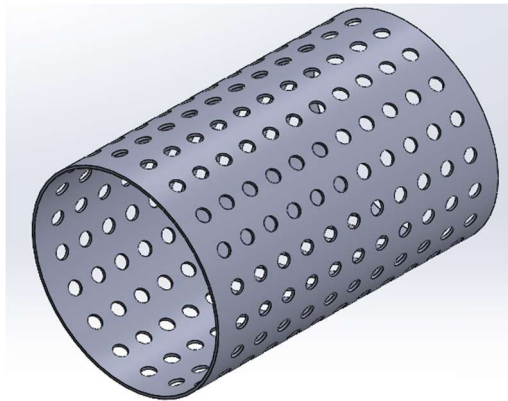


Fig. 46. Perforated pipe 3.8

Table 18. Perforated pipe 3.8 dimensions

No.	Dimensions	Unit(mm)
1.	Pipe length	120
2.	Hole diameter	5
3.	Thickness	2
4.	External diameter	80

In the above fig.46. is the perforated pipe with an external diameter of 80mm with a length of 120mm and a hole diameter of 5mm was designed in the baffle plate 3. A circle was extruded at the center of the pipe from the top plane and a linear patter option was used for 10 mm spacing on both sides with a total of 13 instances. And then circular pattern option was used with equal spacing for 360 degrees for 20 instances.

2.5. Solid work Simulation

Design-1

Mazda 3 2017 SKYACTIV-G 1.5 100HP

Table 19. Engine Specifications:

Parameter	Value
Number of cylinders	4
Displacement	1496 cc
Maximum Torque	150 Nm at 4000 rpm
Maximum Power	101 PS at 6000 rpm
Bore*Stoke	74.5*85.8 mm

Calculation of exhaust flow rate

$$L = \text{displacement (m}^3\text{)} = 0.001496$$

$$R = \text{Revolution per minute (RPM)} = 4000$$

For a 4 – stroke engine the exhaust flow rate is:

$$Q = L * \frac{R/2}{60} \text{ (m}^3\text{/s)} \quad (3)$$

$$\therefore Q = 0.001496 * (4000/2)/60$$

$$\therefore Q = 0.049.$$

Flow Simulation in Solidworks

The simulation must be run only in closed conditions. So, for that, the inlet and outlet have been closed with lids. The additional change in the parameter was listed in the table -. Stainless steel alloy 321 material was applied for all the designs. The computational domain was set up for the model which is shown in figure -. The computational domain was the same for all the designs (1-1.3)

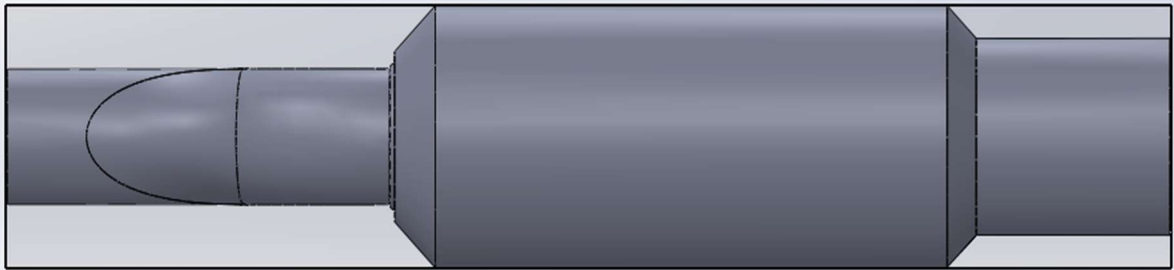


Fig. 47. Computational Domain of Design -1

Table 20. Computational Domain dimensions

Axis	Size
+X	0.1352
-X	-0.1352
+Y	0.0601
-Y	-0.0601
+Z	0.4006
-Z	-0.2006

Inlet Condition

Volume flow rate	0.049 m ³ /s
Temperature	600 °C

Outlet Condition

Environment Pressure	20 °C
----------------------	-------

Substance concentrations

Components	Volume percentage (petrol engine)
Water	3.55
Oxygen	0.3-8

Carbon dioxide	5-12
Nitrogen	74-77

The substance concentration of the gasoline engine was taken from the journal [41]. The same condition and volume flow rate have been applied for design (1 – 1.3).

Design-2

Hyundai Sonata VII.5 1.6T

Table 21. Engine Specifications

Parameter	Value
Number of cylinders	4
Displacement	1591 cc
Maximum Torque	264 Nm 4500rpm
Maximum Power	180 PS at 5500rpm
Bore*stroke	77*85 mm

Calculation of exhaust flow rate

$L = \text{displacement (m}^3) = 0.001591$

$R = \text{Revolution per minute (RPM)} = 4500$

For a 4 – stroke engine the exhaust flow rate is:

$$Q = L * \frac{R/2}{60} \text{ (m}^3/\text{s)}$$

$$\therefore Q = 0.001591 * (4500/2)/60$$

$$\therefore Q = 0.059.$$

Flow Simulation in Solidworks

The simulation must be run only in closed conditions. So, for that, the inlet and outlet have been closed with lids. The additional change in the parameter was listed in the table -. Stainless steel alloy 321 material was applied for all the designs. The computational domain was set up for the model which is shown in figure -. The computational domain was the same for all the designs (2-2.4)

Computational Domain

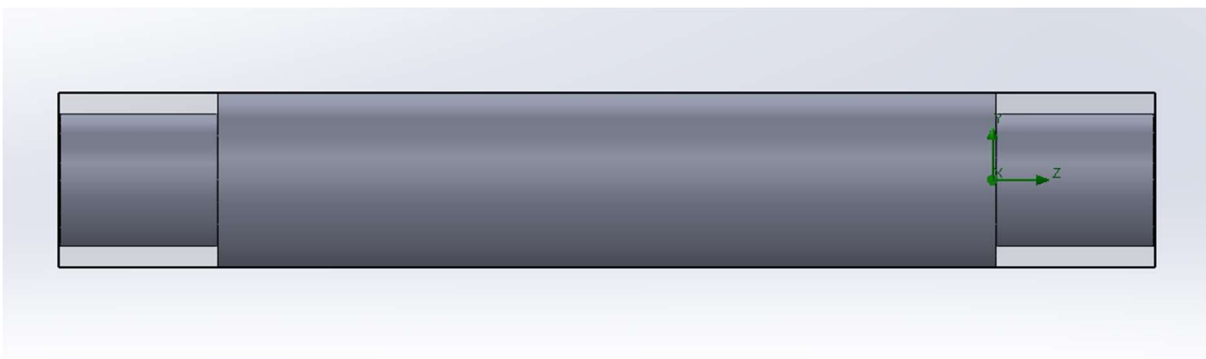


Fig. 48. Computational Domain of Design 2

Table 22. Computational Domain dimensions

Axis	Size
+X	0.1773
-X	-0.1773
+Y	0.0521
-Y	-0.0521
+Z	0.0906
-Z	-0.5206

Inlet Condition

Volume flow rate	0.059 m ³ /s
Temperature	600 °C

Outlet Condition

Environment Pressure	20 °C
----------------------	-------

Substance concentrations

Components	Volume percentage (petrol engine)
Water	3.55
Oxygen	0.3-8
Carbon dioxide	5-12
Nitrogen	74-77

The same condition and volume flow rate have been applied for design (2 – 2.4).

Design-3

Honda Accord 10 Sedan 2.0T 256HP

Table 23. Engine Specifications:

Parameter	Value
Number of cylinders	4
Displacement	1996 cc
Maximum Torque	370 Nm 4000rpm
Maximum Power	256 PS at 6000rpm
Bore*stroke	86*58.9 mm

Calculation of exhaust flow rate

$L = \text{displacement (m}^3) = 0.001996$

$R = \text{Revolution per minute (RPM)} = 4000$

For a 4 – stroke engine the exhaust flow rate is:

$$Q = L * \frac{R/2}{60} \text{ (m}^3\text{/s)}$$

$$\therefore Q = 0.001996 * (4000/2)/60$$

$$\therefore Q = 0.066.$$

Flow Simulation in Solidworks

The simulation must be run only in closed conditions. So, for that, the inlet and outlet have been closed with lids. The additional change in the parameter was listed in the table -. Stainless steel alloy 321 material was applied for all the designs. The computational domain was set up for the model which is shown in figure -. The computational domain was the same for all the designs (3-3.4)

Computational Domain

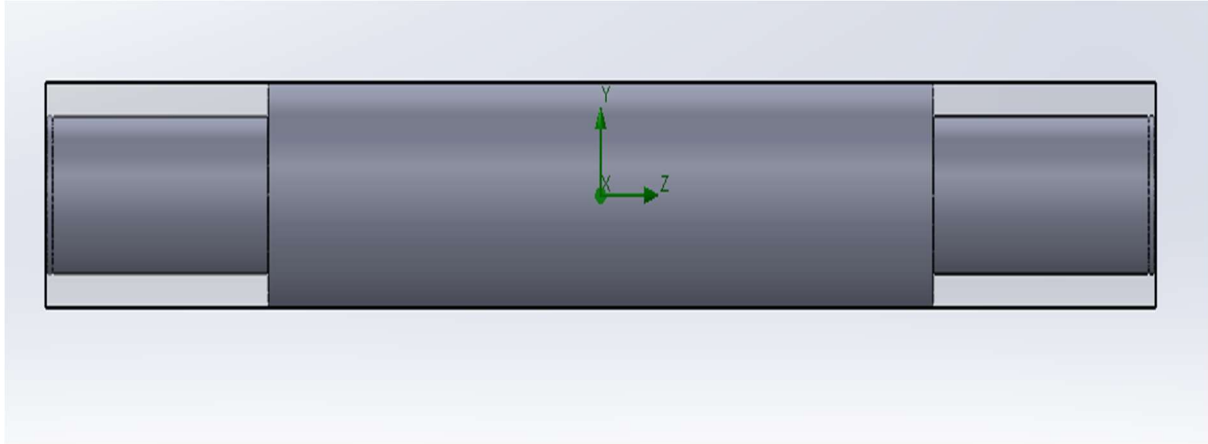


Fig. 49. Computational Domain of design 3

Table 24. Computational Domain dimensions

Axis	Size
+X	0.1753
-X	-0.1755
+Y	0.0501
-Y	-0.0501
+Z	0.3757
-Z	-0.3757

Inlet Condition

Volume flow rate	0.066 m ³ /s
Temperature	600 °C

Outlet Condition

Environment Pressure	20 °C
----------------------	-------

Substance concentrations

Components	Volume percentage (petrol engine)
Water	3.55
Oxygen	0.3-8
Carbon dioxide	5-12
Nitrogen	74-77

The same condition and volume flow rate have been applied for design (3 – 3.4). The velocity and pressure have been calculated using these conditions.

2.6. Backpressure calculation

$$P(kPa) = \frac{L*S*Q^2*3.6*10^6}{D^5} + P_s \quad (4)$$

Where,

P = Backpressure in (kPa)

L = Total Equivalent of the pipe (m)

Q = Exhaust gas flow (m³/min)

D = Inside diameter of pipe (mm)

S = Density of gas (kg/m³)

P_s = Pressure drop of silencer (kPa)

By using this formula, the backpressure was calculated for all the designs. [40]

2.7. Ansys Workbench

The muffler design was created in SOLIDWORKS, and the muffler fluid domain was imported in ANSYS as IGES format for the analysis. The simulation was conducted using the Harmonic analysis tool to calculate the transmission loss of the muffler. For the analysis of the fluid domain, Air was used as a material. Patch confirming algorithm with method tetrahedron and for element order global setting was used for meshing. For sizing different mesh size was given for the designs. For design (1-1.3) the mesh size is 10mm, design (2-2.4) 15mm and design (3-3.4) 20mm. The mesh size was varied for the designs due to size limitations in the Ansys student version.

Analysis settings

The cut-off frequency is calculated for 2000 Hz, which is acquired using the equation $f_c = 1.84c/(\pi d)$, where c is the sound speed and d is the diameter of the silencer [38]. The solution interval of 200 and the result is calculated at every 10 Hz. The only method which can be used for the acoustic analysis is the Full Harmonic method which was used here.

Acoustic Region

In the geometry section, full-body was selected, and the fluid behavior is compressible.

Surface velocity

The value of inlet velocity from Solidworks was considered here.

Radiation Boundary

Both the inlet and the outlet faces are selected for the radiation boundary.

Port definition

Two ports were assigned for this analysis.

- Port 1 – Inlet face
- Port 2 – Outlet face.

Solution

After adding all the inputs of harmonic acoustics, the transmission loss was added in the solution section. In the solver section, the input port provided is port-1 and the output port is port-2.

The same settings have been used for all the designs (1-3). Only the mesh size was changed for these designs which are mentioned above.

2.8. Mesh

The muffler design has complex structures, it is important to choose the correct mesh type to obtain accurate results. The tetrahedron mesh type is chosen to gain accurate results for the complex placements of baffle plates and perforated pipes. Thus, the designed muffler's fluid domain is imported in ANSYS and meshed using the patch-dependent algorithm. The obtained number of nodes and elements for the different designs of mufflers is as shown in fig.50 and stated below,

1. For designs 1-1.3, the mesh size was 10mm. After meshing there are 110118 nodes, and 75347 elements approximately are shown in fig.50 (a).
2. For designs 2-2.4, the mesh size was 15mm. After meshing there are 62410 nodes, and 40644 elements approximately are shown in fig.50 (b).
3. For designs 2-2.4, the mesh size was 15mm. After meshing there are 253333 nodes, and 165648 elements approximately are shown in fig.50 (c).

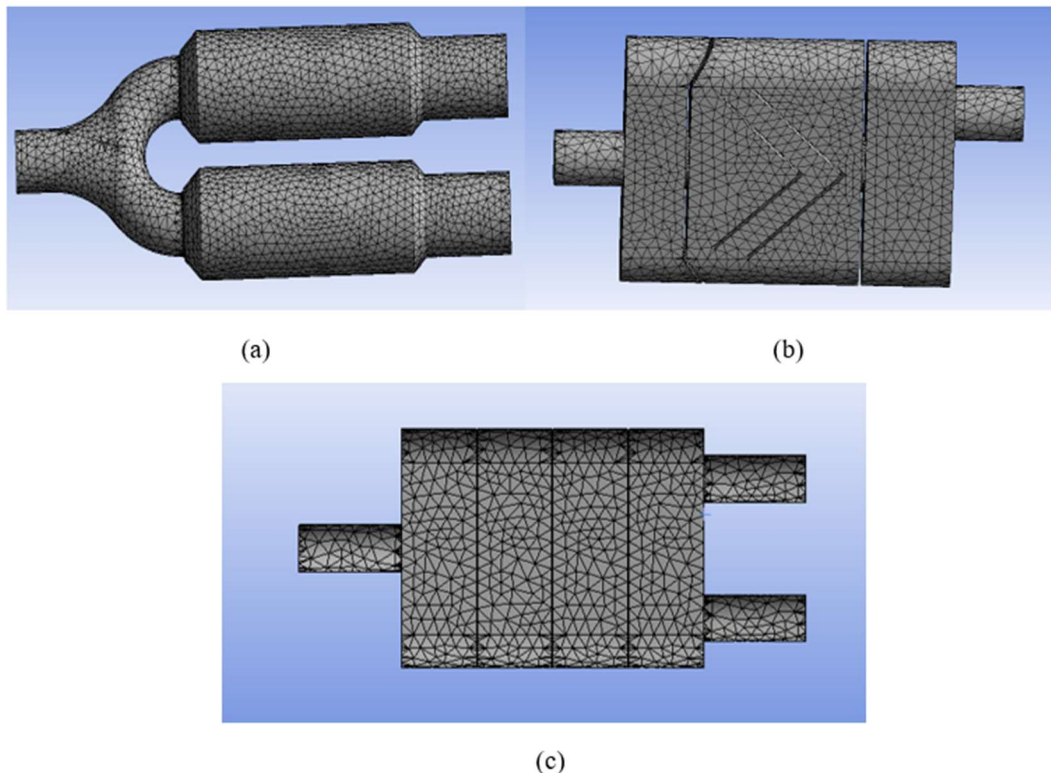


Fig. 50. Mesh pattern for different designs

3. Result and Discussions

3.1 Results

A solid work simulation and analysis were performed for all the designs. Each design was modelled with different design parameters and compared to find out the best and efficient design for transmission loss.

Design-1

This model was designed without any perforations and once the computational domain is set up the simulation for this design is performed on Solidworks which is shown in fig.51 denotes the velocity trajectories and pressure contours. The exhaust gas is a laminar flow till it enters the muffler where the muffler design alters the flow of the exhaust gas further. The flow is altered due to the design of the muffler to create a controlled laminar flow pattern. As we can see the velocity decreases while the trajectory of the flow is diverted into two sections on a U shape design of the muffler. Proportional to the design of the muffler, the pressure of the flow is intense in the obstruction region where the muffler design splits into two separate sections as clearly shown in the figure below.

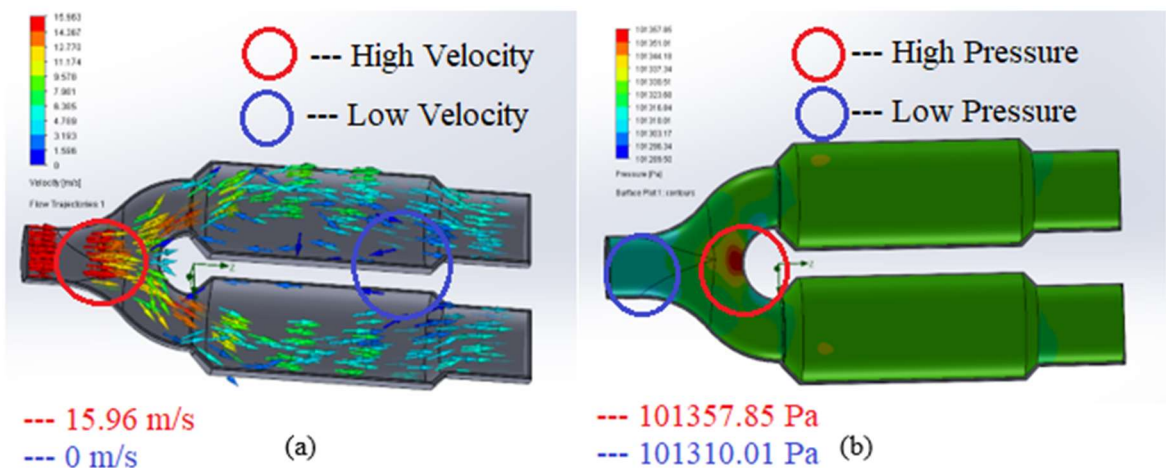


Fig. 51. Velocity trajectories and Pressure contours of design-1

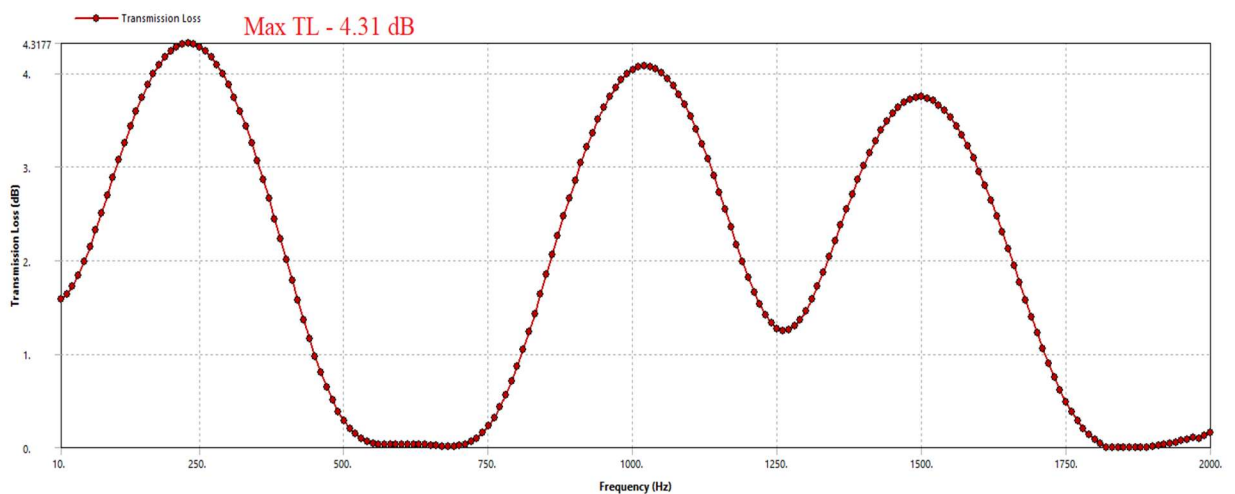


Fig. 52. Frequency Vs Transmission loss graph for design-1

Fig. 52 represents the frequency and transmission loss graph that was performed in Ansys software. The maximum transmission loss is 4.31dB and it is obtained at the frequency range of 230Hz, and this is achieved due to the attenuation of the acoustics transmission in the U-shaped section where the expansion chamber divides into two sections.

Design-1.1

Design 1.1 was modelled with a baffle plate 1.1 at the center of the expansion chamber and once the computational domain is set up the simulation for this design is performed on Solidworks which is shown in fig.53 denotes the velocity trajectories and pressure contours. The exhaust gas is a laminar flow till it enters the muffler where the muffler design alters the flow of the exhaust gas further. The flow is altered due to the design of the muffler to create a controlled laminar flow pattern. As we can see the velocity decreases while the trajectory of the flow is diverted into two sections on a U shape design of the muffler and decreases to a minimum on the addition of the baffle plate at the center of the expansion chamber. Proportional to the design of the muffler, the pressure of the flow is intense in the obstruction region where the muffler design splits into two separate sections as clearly shown in the figure below. Further, the pressure drops beyond the baffle plate in the expansion chamber towards the outlet.

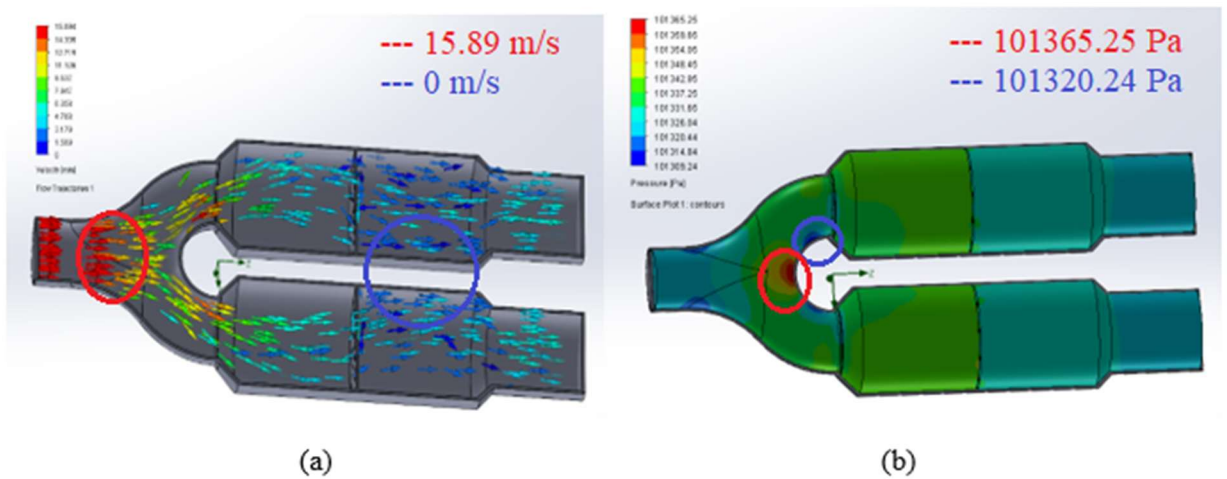


Fig. 53. Velocity trajectories and Pressure contours of design-1.1

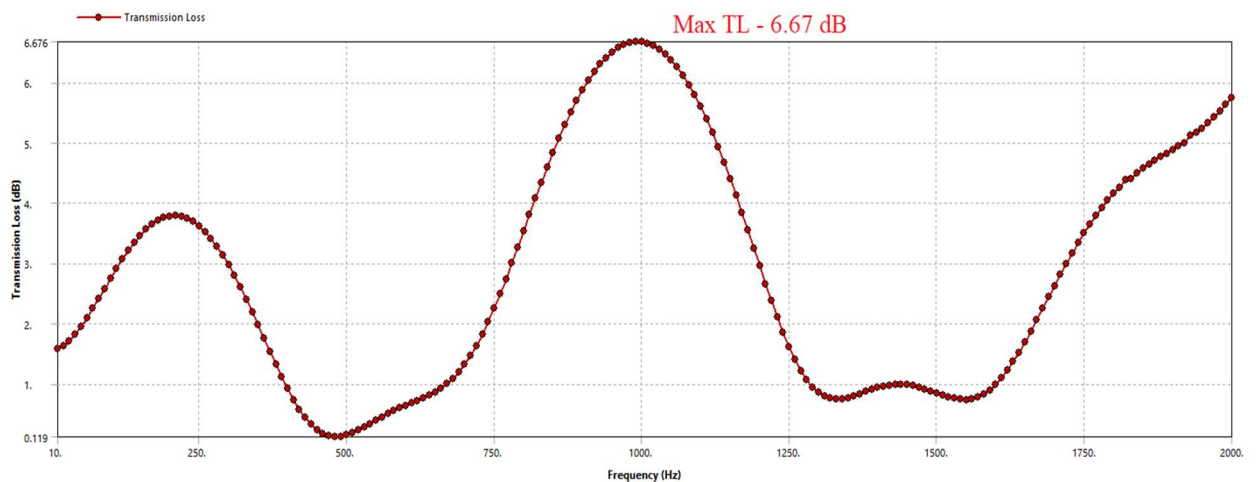


Fig. 54. Frequency Vs Transmission loss graph for design-1.1

Fig. 54 represents the frequency and transmission loss graph that was performed in Ansys software. The maximum transmission loss is 6.67 dB, and it is obtained at the low-frequency range of 990 Hz, and this is achieved due to the attenuation of the acoustics transmission in the U-shaped section where the baffle plate 1.1 is mounted.

Design-1.2

Design 1.2 was modelled with a baffle plate 1.2 at the center of the expansion chamber and once the computational domain is set up the simulation for this design is performed on Solidworks which is shown in fig.55 denotes the velocity trajectories and pressure contours. The exhaust gas is a laminar flow till it enters the muffler where the muffler design alters the flow of the exhaust gas further. The flow is altered due to the design of the muffler to create a controlled laminar flow pattern. As we can see the velocity decreases while the trajectory of the flow is diverted into two sections on a U shape design of the muffler and decreases to a minimum on the addition of the baffle plate at the center of the expansion chamber. Proportional to the design of the muffler, the pressure of the flow is intense in the obstruction region where the muffler design splits into two separate sections as clearly shown in the figure below. Further, the pressure drops beyond the baffle plate in the expansion chamber towards the outlet.

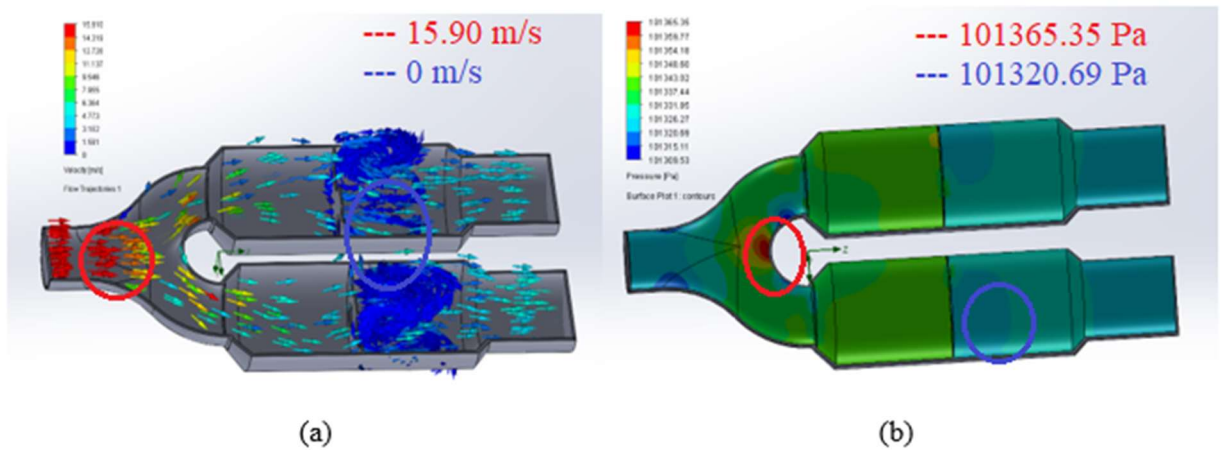


Fig. 55. Velocity trajectories and Pressure contours of design-1

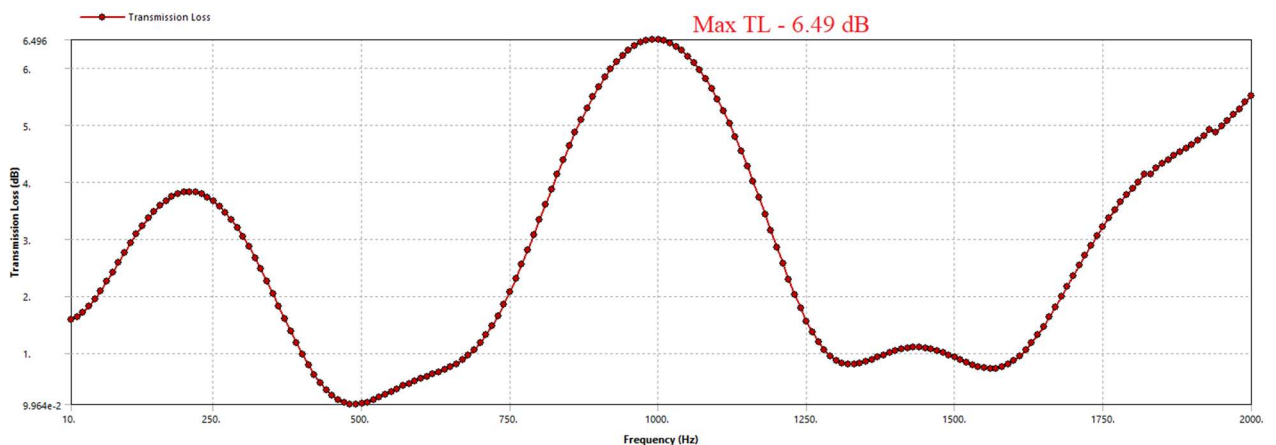


Fig. 56. Frequency Vs Transmission loss graph for design-1

Fig. 56 represents the frequency and transmission loss graph that was performed in Ansys software. The maximum transmission loss is 6.49 dB, and it is obtained at the low-frequency range of 990 Hz,

and this is achieved due to the attenuation of the acoustics transmission in the U-shaped section where the baffle plate 1.2 is mounted.

Design-1.3

Design 1.3 was modelled with a baffle plate 1.1 and 1.2 at equidistance from the center of the expansion chamber and once the computational domain is set up the simulation for this design is performed on Solidworks which is shown in fig.57 denotes the velocity trajectories and pressure contours. The exhaust gas is a laminar flow till it enters the muffler where the muffler design alters the flow of the exhaust gas further. The flow is altered due to the design of the muffler to create a controlled laminar flow pattern. As we can see the velocity decreases while the trajectory of the flow is diverted into two sections on a U shape design of the muffler and decreases to a minimum between the two-baffle plates 1.1 and 1.2. Proportional to the design of the muffler, the pressure of the flow is intense in the obstruction region where the muffler design splits into two separate sections as clearly shown in the figure below. Further, the pressure drops beyond the baffle plate in the expansion chamber towards the outlet.

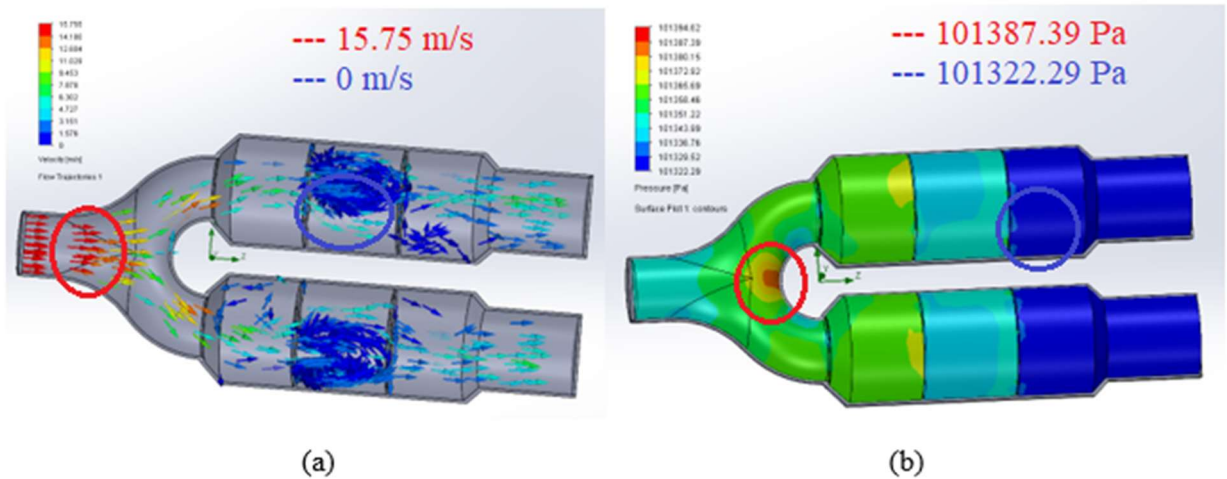


Fig. 57. Velocity trajectories and Pressure contours of design-1

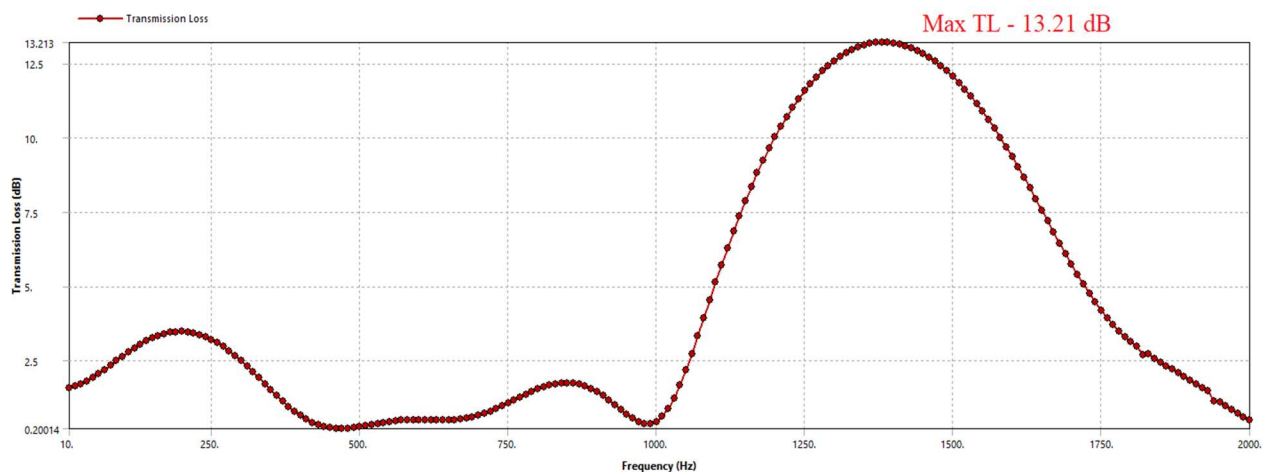


Fig. 58. Frequency Vs Transmission loss graph for design-1

Fig. 58 represents the frequency and transmission loss graph that was performed in Ansys software. The maximum transmission loss is 13.21 dB, and it is obtained at the frequency range of 1380 Hz,

and this is achieved due to the attenuation of the acoustics transmission in the U-shaped section beyond the baffle plates 1.1 and 1.2 in the expansion chamber.

Design-2

Design 2 was modelled with a baffle plate at either end of the expansion chamber along with V-shaped perforation plates between them and once the computational domain is set up the simulation for this design is performed on Solidworks which is shown in fig.59 denotes the velocity trajectories and pressure contours. The exhaust gas is a laminar flow till it enters the muffler where the muffler design alters the flow of the exhaust gas further. The flow is altered due to the design of the muffler to create a controlled laminar flow pattern. As we can see the velocity decreases while the trajectory of the flow is diverted into two sections on a V-shaped perforation plate design of the muffler and decreases to a minimum between the V-shaped perforation plates. Proportional to the design of the muffler, the pressure of the flow is intense in the obstruction region where the V-shaped perforation plate that is placed is clearly shown in the figure below. Further, the pressure drops beyond the baffle plate in the expansion chamber towards the outlet.

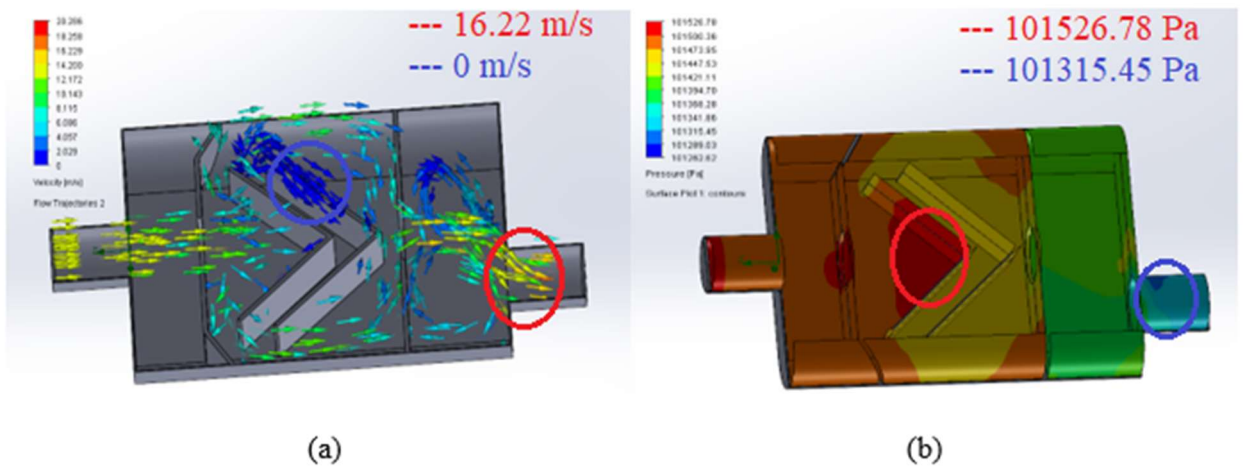


Fig. 59. Velocity trajectories and Pressure contours of design-1

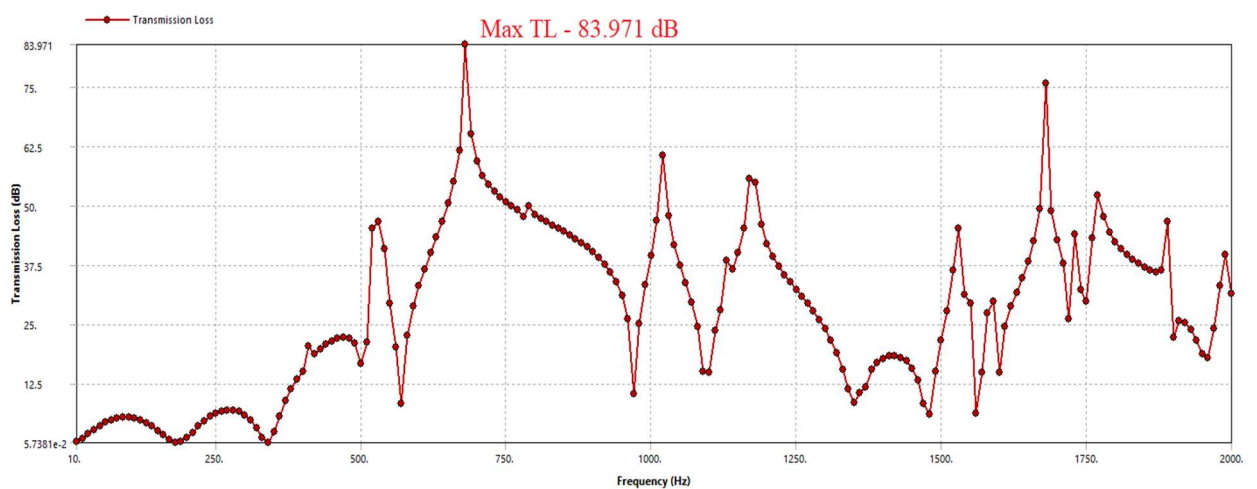


Fig. 60. Frequency Vs Transmission loss graph for design-1

Fig. 60 represents the frequency and transmission loss graph that was performed in Ansys software. The maximum transmission loss is 83.97 dB, and it is obtained at the frequency range of 680 Hz, and

this is achieved due to the attenuation of the acoustics transmission in the V perforation plate in the expansion chamber.

Design-2.1

Design 2.1 was modelled with a baffle plate at either end of the expansion chamber at a different distance as explained in the methodology section. Along with the baffle plates V-shaped perforation plates are placed between them. Once the computational domain is set up the simulation for this design is performed on Solidworks which is shown in fig.61 denotes the velocity and pressure contours. The exhaust gas is a laminar flow till it enters the muffler where the muffler design alters the flow is the exhaust gas further. The flow is altered due to the design of the muffler to create a controlled laminar flow pattern. As we can see the velocity decreases while the trajectory of the flow is diverted into two sections on a V-shaped perforation plate design of the muffler and decreases to a minimum between the V-shaped perforation plates. Proportional to the design of the muffler, the pressure of the flow is intense in the obstruction region where the V-shaped perforation plate that is placed is clearly shown in the figure below. Further, the pressure slightly increases before entering the hole in the last baffle plate and drops beyond the baffle plate in the expansion chamber towards the outlet.

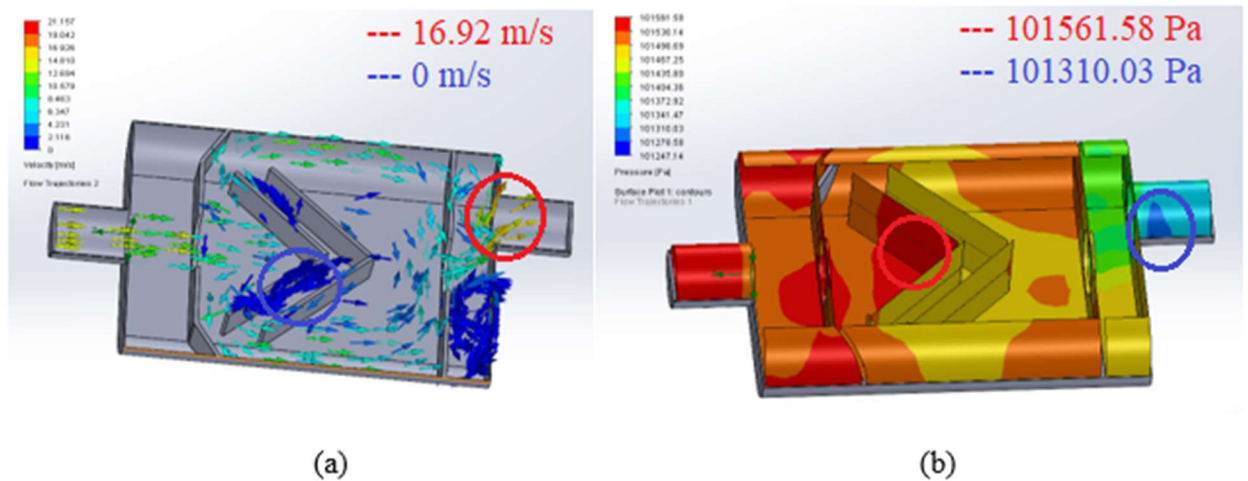


Fig. 61. Velocity trajectories and Pressure contours of design-1

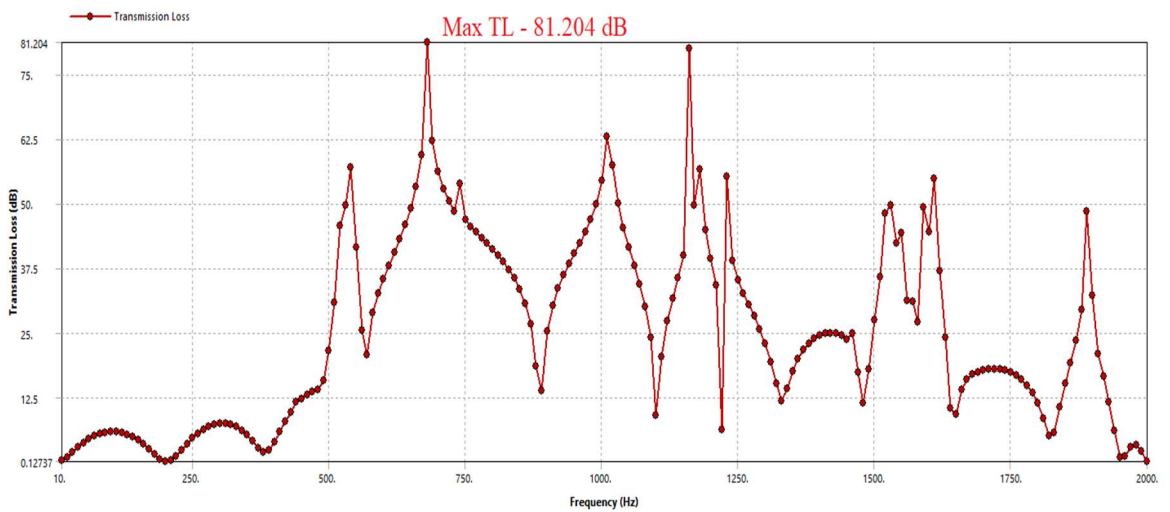


Fig. 62. Frequency Vs Transmission loss graph for design-1

Fig. 62 represents the frequency and transmission loss graph that was performed in Ansys software. The maximum transmission loss is 81.20 dB and 80.11 dB at the frequency range of 680 Hz and 1160 Hz respectively, this is achieved due to the attenuation of the acoustics transmission in the V perforation plate in the expansion chamber at 680 Hz and in the V end of the perforation plate at 1160 Hz.

Design-2.2

Design 2.2 was modelled with a baffle plate at either end of the expansion chamber along with V-shaped perforation plates between them. This design has a different hole diameter for the baffle plate while the rest remains the same as design 2. Once the computational domain is set up the simulation for this design is performed on Solidworks which is shown in fig.63 denotes the velocity trajectories and pressure contours. The exhaust gas is a laminar flow till it enters the muffler where the muffler design alters the flow of the exhaust gas further. The flow is altered due to the design of the muffler to create a controlled laminar flow pattern. As we can see the velocity decreases while the trajectory of the flow is diverted into two sections on a V-shaped perforation plate design of the muffler and decreases to a minimum between the V-shaped perforation plates. Proportional to the design of the muffler, the pressure of the flow is intense in the obstruction region where the V-shaped perforation plate that is placed is clearly shown in the figure below. Further, the pressure drops beyond the baffle plate in the expansion chamber towards the outlet.

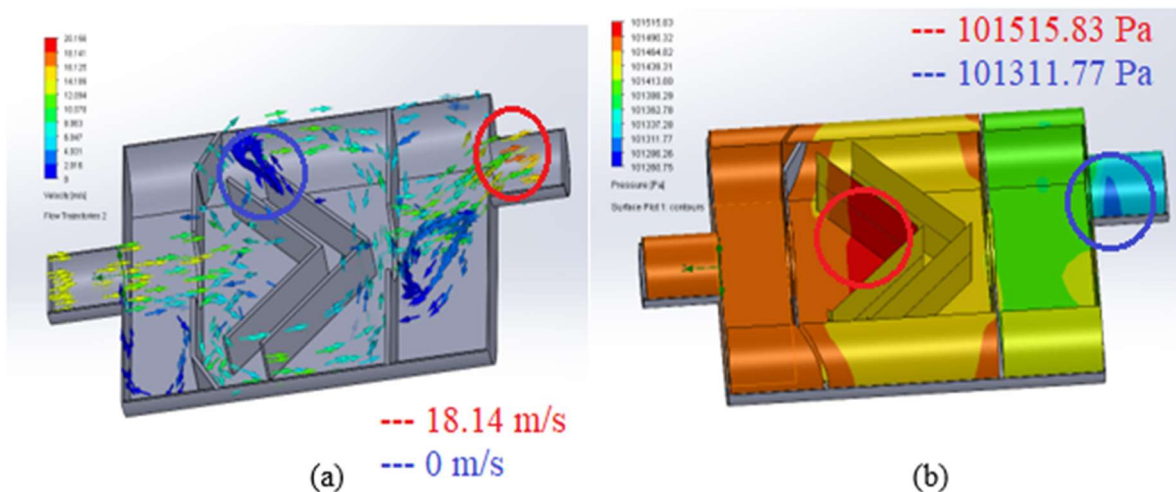


Fig. 63. Velocity trajectories and Pressure contours of design-1

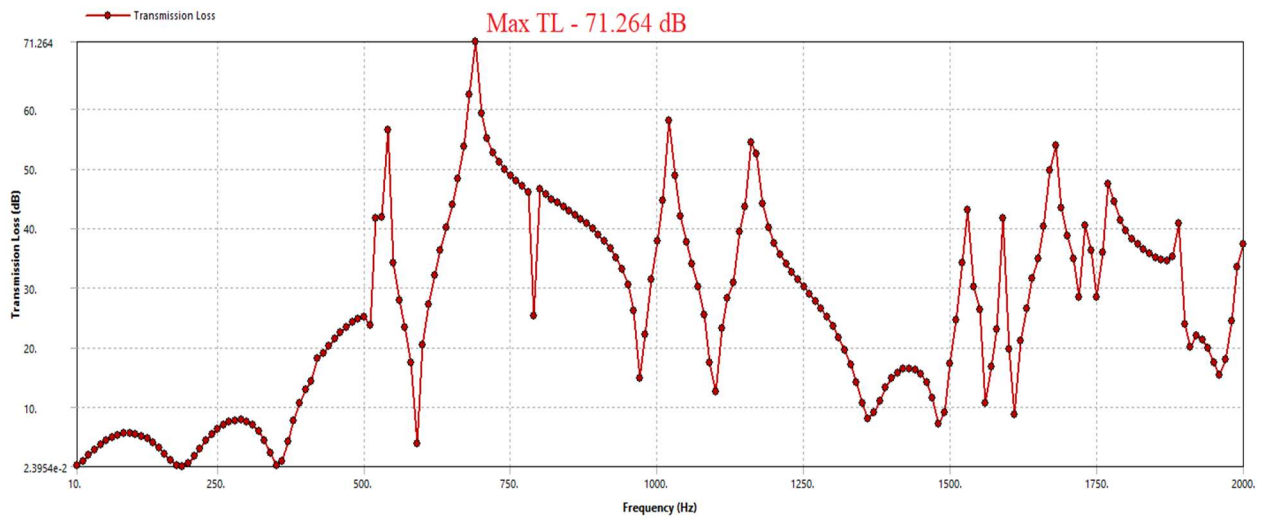


Fig. 64. Frequency Vs Transmission loss graph for design-1

Fig. 64 represents the frequency and transmission loss graph that was performed in Ansys software. The maximum transmission loss is 71.26 dB, and it is obtained at the frequency range of 690 Hz, and this is achieved due to the attenuation of the acoustics transmission in the V perforation plate in the expansion chamber.

Design-2.3

Design 2.3 was modelled with a baffle plate at either end of the expansion section with two baffles plates at the outlet end of the expansion chamber with a pipe as explained in the methodology section. Along with the baffle plates V-shaped perforation plates are placed between them. Once the computational domain is set up the simulation for this design is performed on Solidworks which is shown in fig.65 denotes the velocity trajectories and pressure contours. The exhaust gas is a laminar flow till it enters the muffler where the muffler design alters the flow is the exhaust gas further. The flow is altered due to the design of the muffler to create a controlled laminar flow pattern. As we can see the velocity decreases while the trajectory of the flow is diverted into two sections on a V-shaped perforation plate design of the muffler and decreases to a minimum between the V-shaped perforation plates. Proportional to the design of the muffler, the pressure of the flow is intense in the obstruction region where the V-shaped perforation plate is placed is clearly shown in the figure below. Further, the pressure slightly increases before entering the hole in the baffle plate and drops beyond the last baffle plate in the expansion chamber towards the outlet.

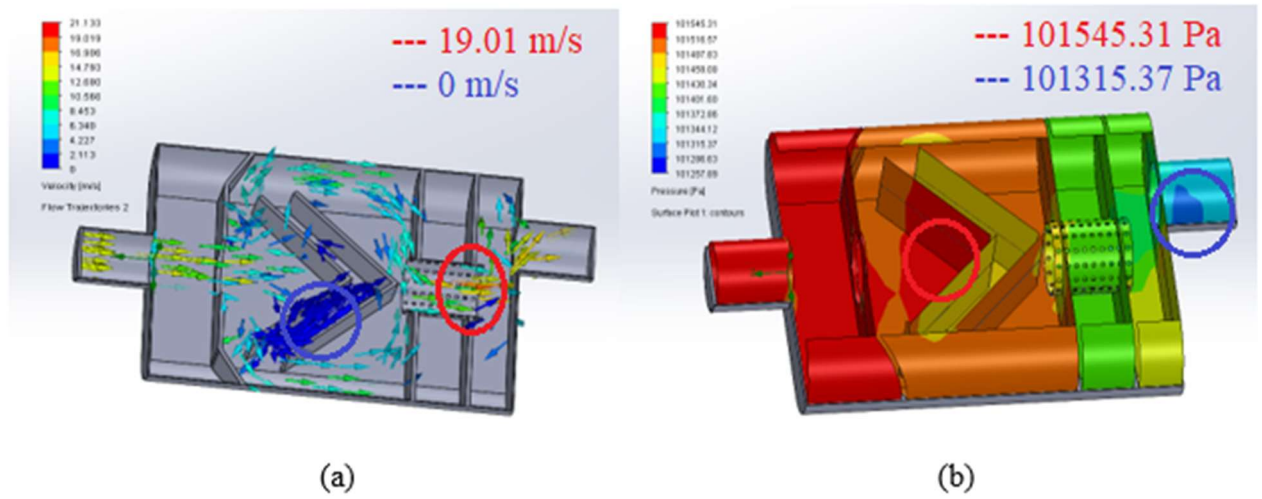


Fig. 65. Velocity trajectories and Pressure contours of design-1

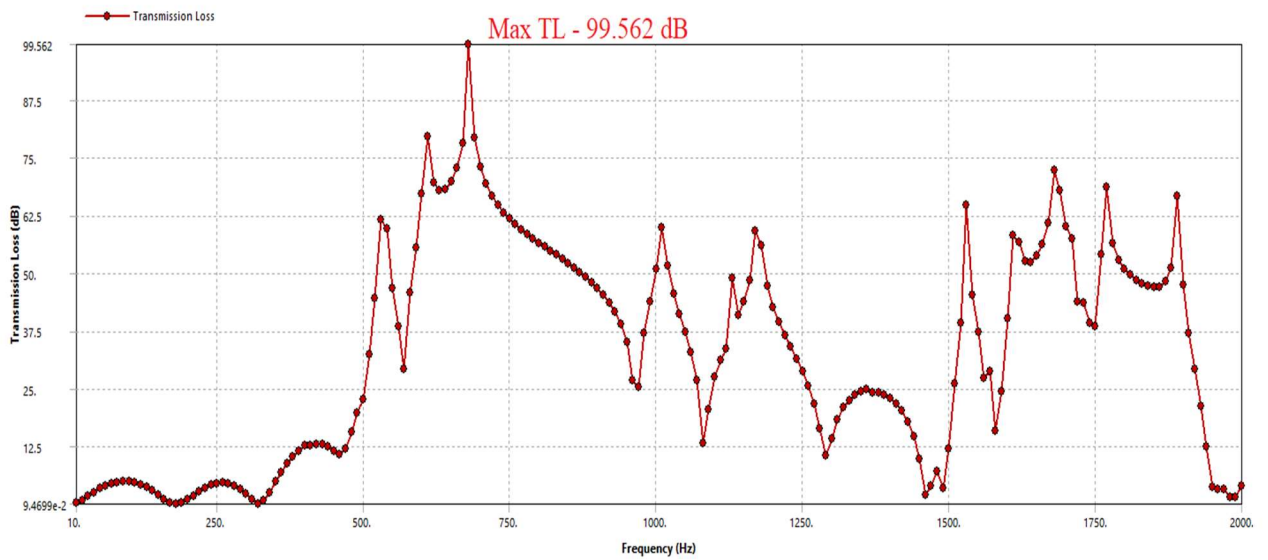


Fig. 66. Frequency Vs Transmission loss graph for design-1

Fig. 66 represents the frequency and transmission loss graph that was performed in Ansys software. The maximum transmission loss is 99.56 dB, and it is obtained at the frequency range of 680 Hz, and this is achieved due to the attenuation of the acoustics transmission in the V perforation plate in the expansion chamber.

Design-2.4

Design 2.4 was modelled with a baffle plate at either end of the expansion section with two baffles plates at the outlet end of the expansion chamber with a change in diameter of the pipe as explained in the methodology section. Along with the baffle plates V-shaped perforation plates are placed between them. Once the computational domain is set up the simulation for this design is performed on Solidworks which is shown in fig.67 denotes the velocity trajectories and pressure contours. The exhaust gas is a laminar flow till it enters the muffler where the muffler design alters the flow is the exhaust gas further. The flow is altered due to the design of the muffler to create a controlled laminar flow pattern. As we can see the velocity decreases while the trajectory of the flow is diverted into two sections on a V-shaped perforation plate design of the muffler and decreases to a minimum between the V-shaped perforation plates. Proportional to the design of the muffler, the pressure of the flow is intense in the obstruction region where the V-shaped perforation plate is placed is clearly shown in the figure below. Further, the pressure slightly increases before entering the hole in the baffle plate and drops beyond the last baffle plate in the expansion chamber towards the outlet.

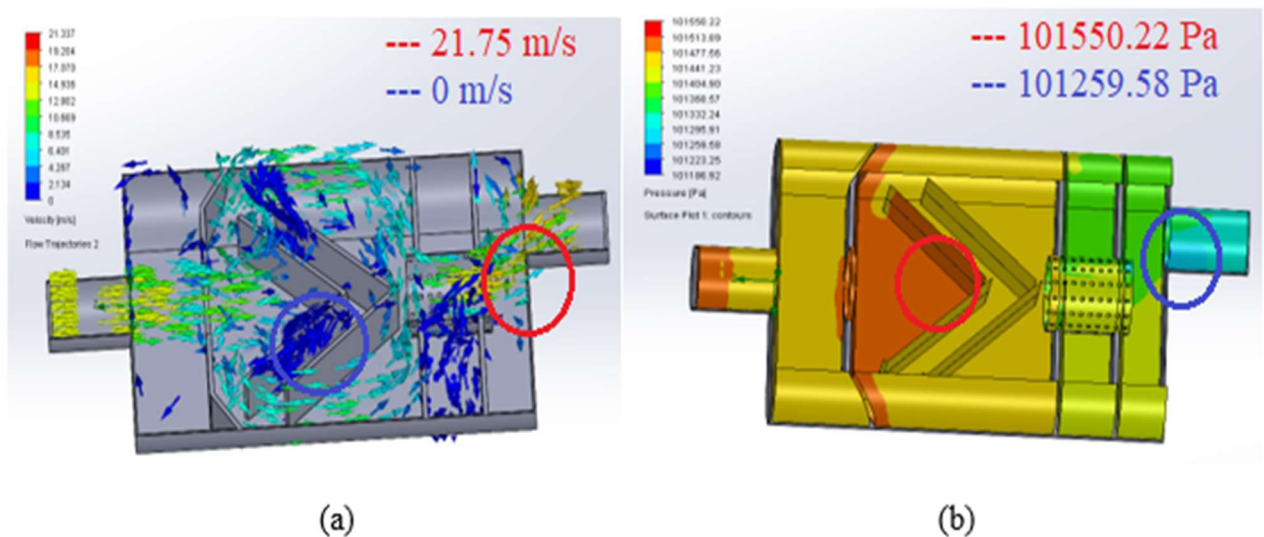


Fig. 67. Velocity trajectories and Pressure contours of design-1

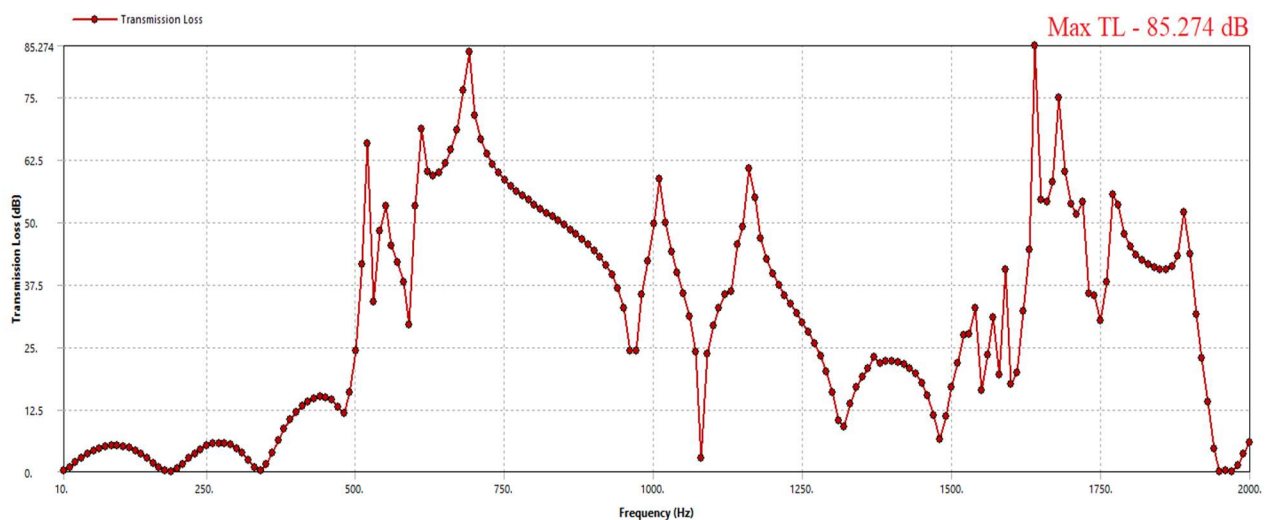


Fig. 68. Frequency Vs Transmission loss graph for design-1

Fig. 68 represents the frequency and transmission loss graph that was performed in Ansys software. The maximum transmission loss is 83.2 dB and 85.27 dB at the frequency range of 690 Hz and 1640 Hz respectively, this is achieved due to the attenuation of the acoustics transmission in the V perforation plate in the expansion chamber at 680 Hz and in the perforated pipe at 1640 Hz.

Design-3

Design 3 was modelled with three baffle plates placed equidistant in the expansion chamber with perforated pipes as mentioned in the methodology section. Once the computational domain is set up the simulation for this design is performed on Solidworks which is shown in fig.69 denotes the velocity trajectories and pressure contours. The exhaust gas is a laminar flow till it enters the muffler where the muffler design alters the flow is the exhaust gas further. The flow is altered due to the design of the muffler to create a controlled laminar flow pattern. As we can see the velocity decreases while the trajectory of the flow is diverted into two sections by the perforated pipes in the first baffle plate design of the muffler and decreases to a minimum between the two perforated pipes. With the complex combination of the convergence and divergence of the flow due to the baffle plates and perforation pipe, there is a fluctuation in the velocity. Proportional to the design of the muffler, the pressure of the flow is intense in the obstruction region where the baffle plate with two perforated pipes is placed as shown in the figure below. Further, the pressure drops drastically beyond the last baffle plate in the expansion chamber towards the outlet.

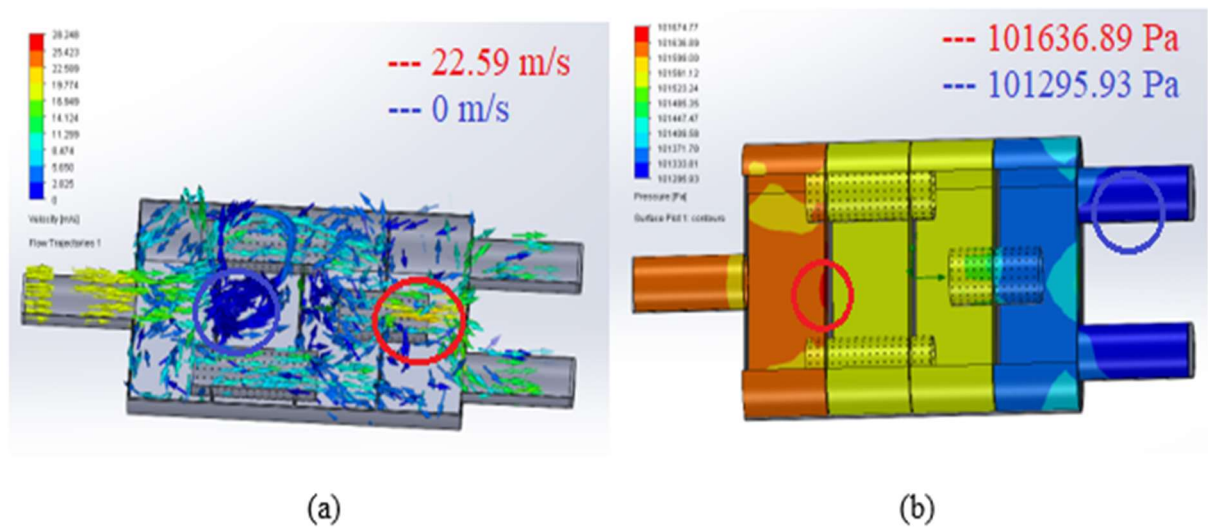


Fig. 69. Velocity trajectories and Pressure contours of design-1

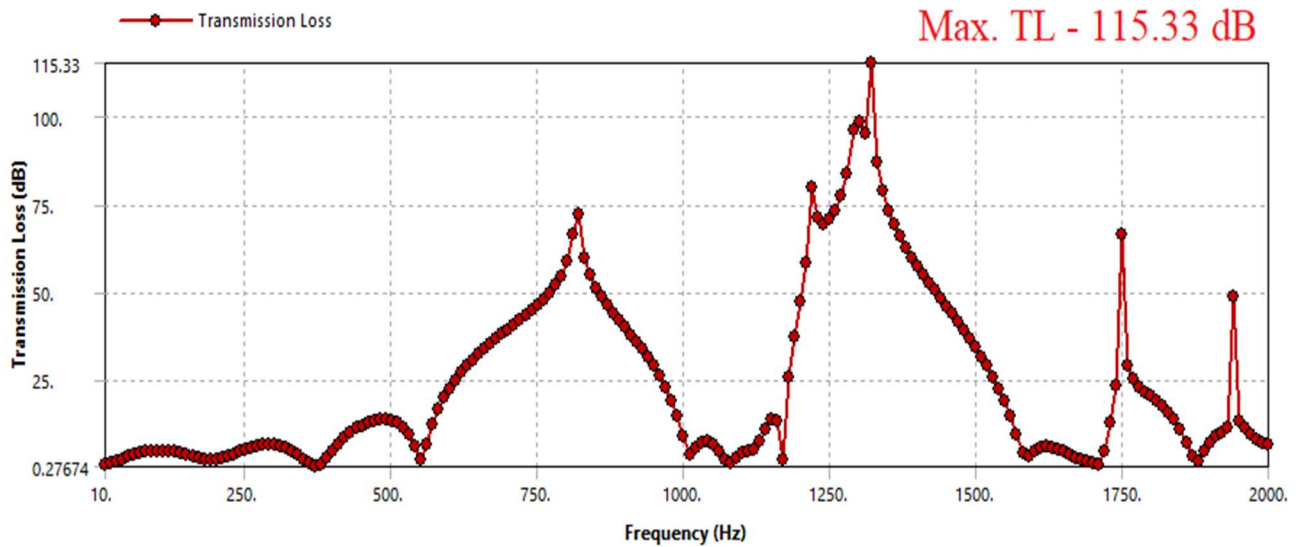


Fig. 70. Frequency Vs Transmission loss graph for design-1

Fig. 70 represents the frequency and transmission loss graph that was performed in Ansys software. The first peak of transmission loss is 72.04 dB at 820 Hz due to the acoustics loss in the vacuum chamber between the two divergent perforation pipes in the first baffle plate. The maximum transmission loss is 115.33 dB at 1320 Hz, this is achieved due to the attenuation of the acoustics transmission in the outlet perforation pipe in the baffle plate.

Design-3.1

Design 3.1 was modelled with three baffle plates placed equidistant in the expansion chamber with perforated pipes as mentioned in the methodology section while the diameter of the perforated pipe was changed from 70mm to 80mm. Once the computational domain is set up the simulation for this design is performed on Solidworks which is shown in fig.71 denotes the velocity trajectories and pressure contours. The exhaust gas is a laminar flow till it enters the muffler where the muffler design alters the flow is the exhaust gas further. The flow is altered due to the design of the muffler to create a controlled laminar flow pattern. As we can see the velocity decreases while the trajectory of the flow is diverted into two sections by the perforated pipes in the first baffle plate design of the muffler and decreases to a minimum between the two perforated pipes. With the complex combination of the convergence and divergence of the flow due to the baffle plates and perforation pipe, there is a fluctuation in the velocity. Proportional to the design of the muffler, the pressure of the flow is intense in the obstruction region where the baffle plate with two perforated pipes is placed as shown in the figure below. Further, the pressure drops beyond the last baffle plate in the expansion chamber towards the outlet.

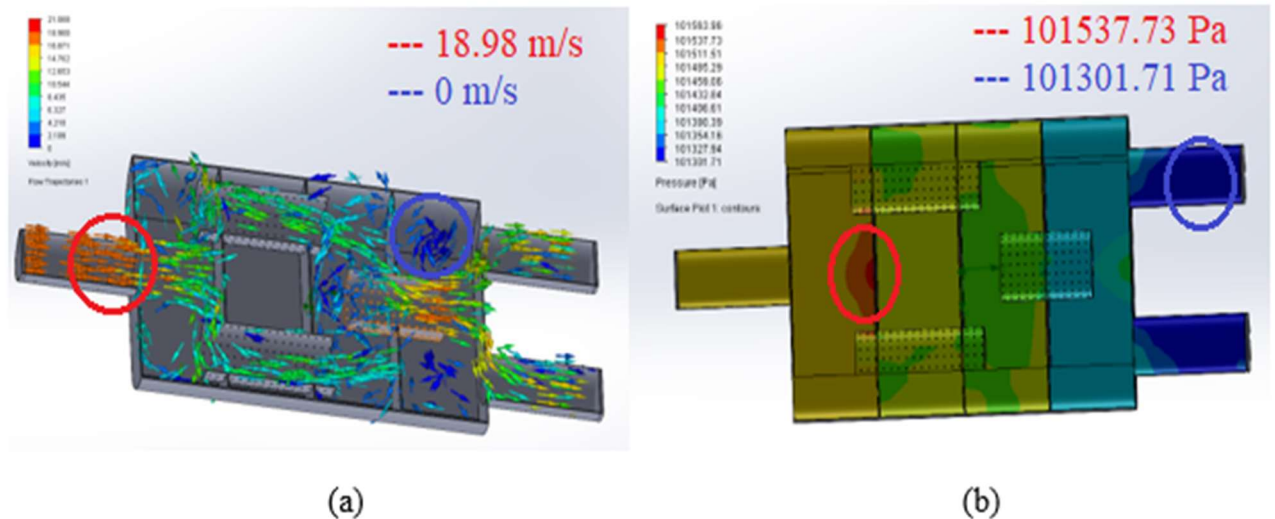


Fig. 71. Velocity trajectories and Pressure contours of design-1

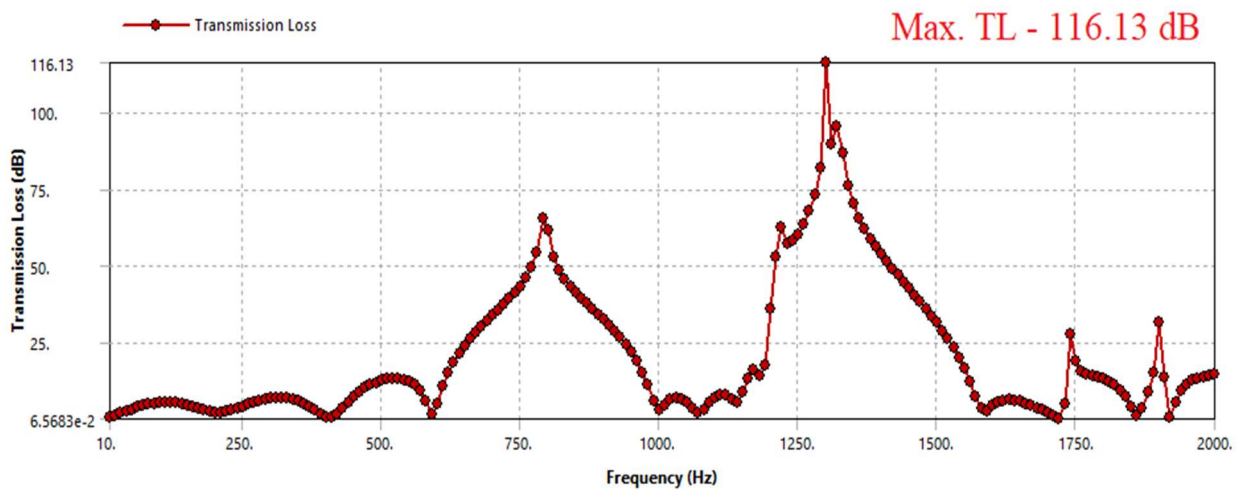


Fig. 72. Frequency Vs Transmission loss graph for design-1

Fig. 72 represents the frequency and transmission loss graph that was performed in Ansys software. The first peak of transmission loss is 65.31dB at 790 Hz due to the acoustics loss in the vacuum chamber between the two divergent perforation pipes in the first baffle plate. The maximum transmission loss is 116.13 dB at 1300 Hz, this is achieved due to the attenuation of the acoustics transmission in the outlet perforation pipe in the baffle plate.

Design-3.2

Design 3.2 was modelled with three baffle plates placed equidistant in the expansion chamber with perforated pipes as mentioned in the methodology section while the perforated pipe hole diameter was changed from 2 mm to 5 mm. Once the computational domain is set up the simulation for this design is performed on Solidworks which is shown in fig.73 denotes the velocity trajectories and pressure contours. The exhaust gas is a laminar flow till it enters the muffler where the muffler design alters the flow is the exhaust gas further. The flow is altered due to the design of the muffler to create a controlled laminar flow pattern. As we can see the velocity decreases while the trajectory of the flow is diverted into two sections by the perforated pipes in the first baffle plate design of the muffler and decreases to a minimum between the two perforated pipes. With the complex combination of the

convergence and divergence of the flow due to the baffle plates and perforation pipe, there is a fluctuation in the velocity. Proportional to the design of the muffler, the pressure of the flow is intense in the obstruction region where the baffle plate with two perforated pipes is placed as shown in the figure below. Further, the pressure drops drastically beyond the last baffle plate in the expansion chamber towards the outlet.

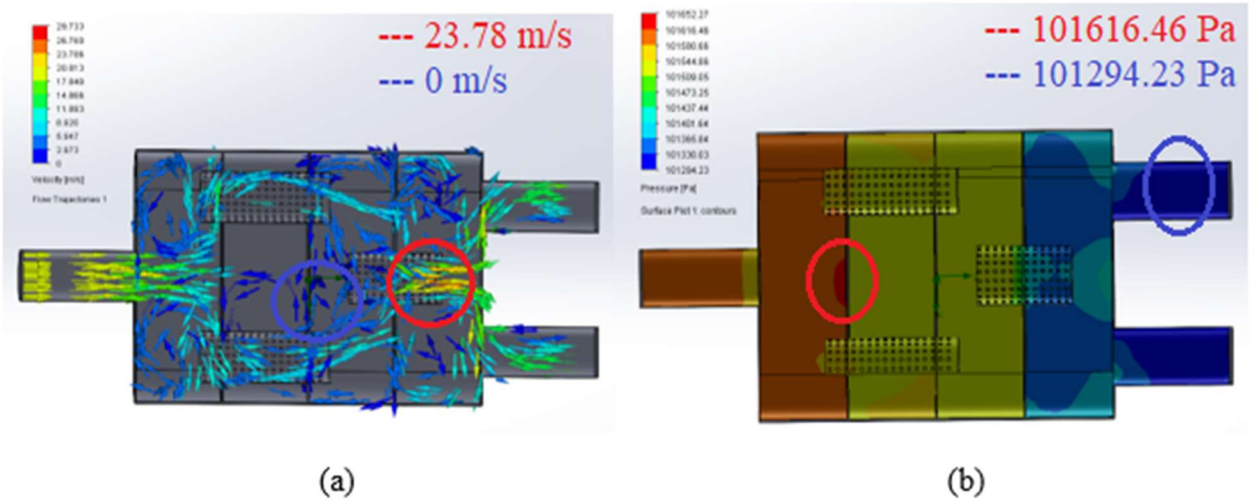


Fig. 73. Velocity trajectories and Pressure contours of design-1

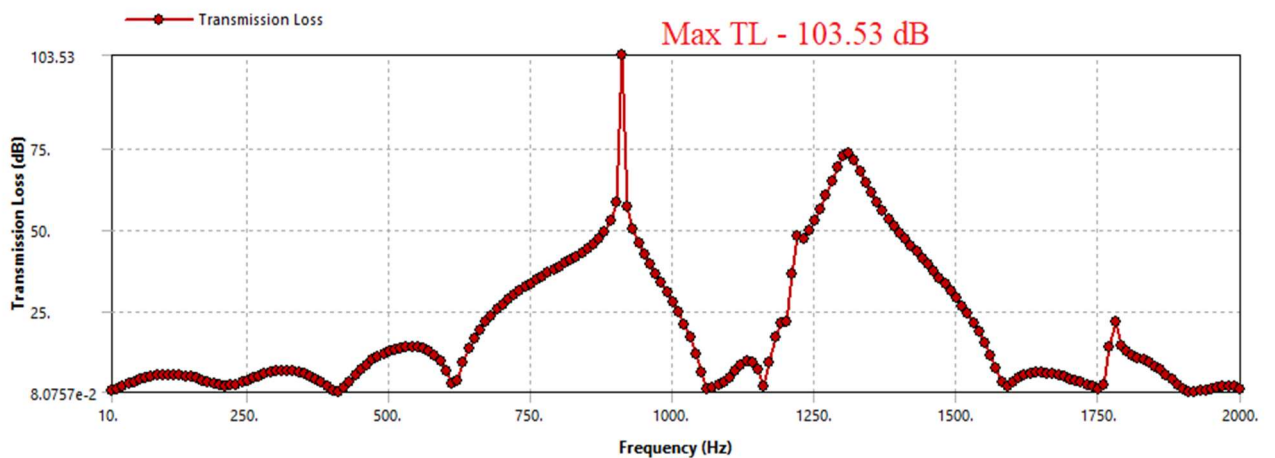


Fig. 74. Frequency Vs Transmission loss graph for design-1

Fig. 74 represents the frequency and transmission loss graph that was performed in Ansys software. The maximum transmission loss is 103.53 dB at 910 Hz due to the acoustics loss in the vacuum chamber between the two divergent perforation pipes in the first baffle plate. The second transmission loss peak is 73.50 dB at 1310 Hz, this is achieved due to the attenuation of the acoustics transmission in the outlet perforation pipe in the baffle plate.

Design-3.3

Design 3.3 was modelled with three baffle plates placed in the expansion chamber with perforated pipes as mentioned in the methodology section. Once the computational domain is set up the simulation for this design is performed on Solidworks which is shown in fig.75 denotes the velocity trajectories and pressure contours. The exhaust gas is a laminar flow till it enters the muffler where

the muffler design alters the flow is the exhaust gas further. The flow is altered due to the design of the muffler to create a controlled laminar flow pattern. As we can see the velocity decreases while the trajectory of the flow is diverted into two sections by the perforated pipes in the first baffle plate design of the muffler and decreases to a minimum between the two perforated pipes. With the complex combination of the convergence and divergence of the flow due to the baffle plates and perforation pipe, there is a fluctuation in the velocity. Proportional to the design of the muffler, the pressure of the flow is intense in the obstruction region where the baffle plate with two perforated pipes is placed as shown in the figure below. Further, the pressure drops drastically beyond the last baffle plate in the expansion chamber towards the outlet.

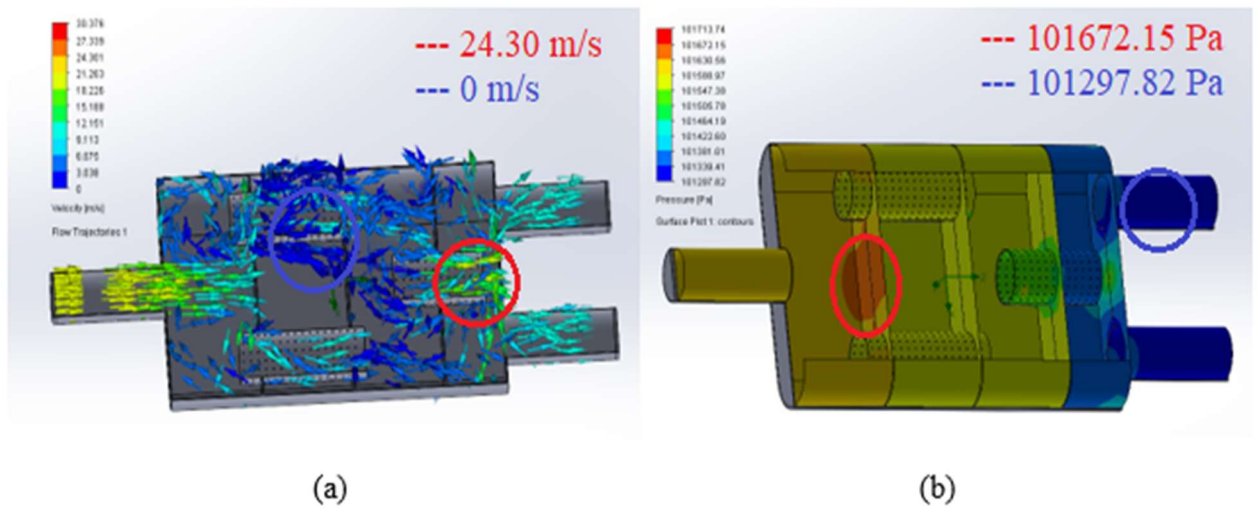


Fig. 75. Velocity trajectories and Pressure contours of design-1

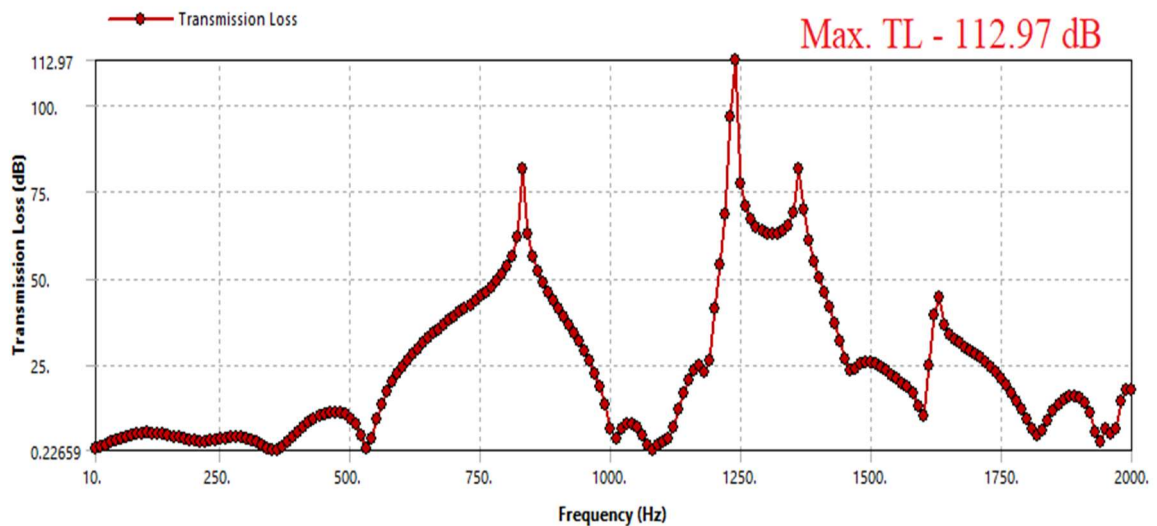


Fig. 76. Frequency Vs Transmission loss graph for design-1

Fig. 76 represents the frequency and transmission loss graph that was performed in Ansys software. The first peak of transmission loss is 81.29 dB at 830 Hz due to the acoustics loss in the vacuum chamber between the two divergent perforation pipes in the first baffle plate. The maximum

transmission loss is 112.97 dB at 1240 Hz, this is achieved due to the attenuation of the acoustics transmission in the outlet perforation pipe in the baffle plate.

Design-3.4

Design 3.4 was modelled with three baffle plates placed at a distance in the expansion chamber with perforated pipes as mentioned in the methodology section while the diameter of the perforated pipe was changed from 70mm to 80mm, as this contains all the design modifications of design 3. Once the computational domain is set up the simulation for this design is performed on Solidworks which is shown in fig.77 denotes the velocity trajectories and pressure contours. The exhaust gas is a laminar flow till it enters the muffler where the muffler design alters the flow is the exhaust gas further. The flow is altered due to the design of the muffler to create a controlled laminar flow pattern. As we can see the velocity decreases while the trajectory of the flow is diverted into two sections by the perforated pipes in the first baffle plate design of the muffler and decreases to a minimum between the two perforated pipes. With the complex combination of the convergence and divergence of the flow due to the baffle plates and perforation pipe, there is a fluctuation in the velocity. Proportional to the design of the muffler, the pressure of the flow is intense in the obstruction region where the baffle plate with two perforated pipes is placed as shown in the figure below. Further, the pressure drops beyond the last baffle plate in the expansion chamber towards the outlet.

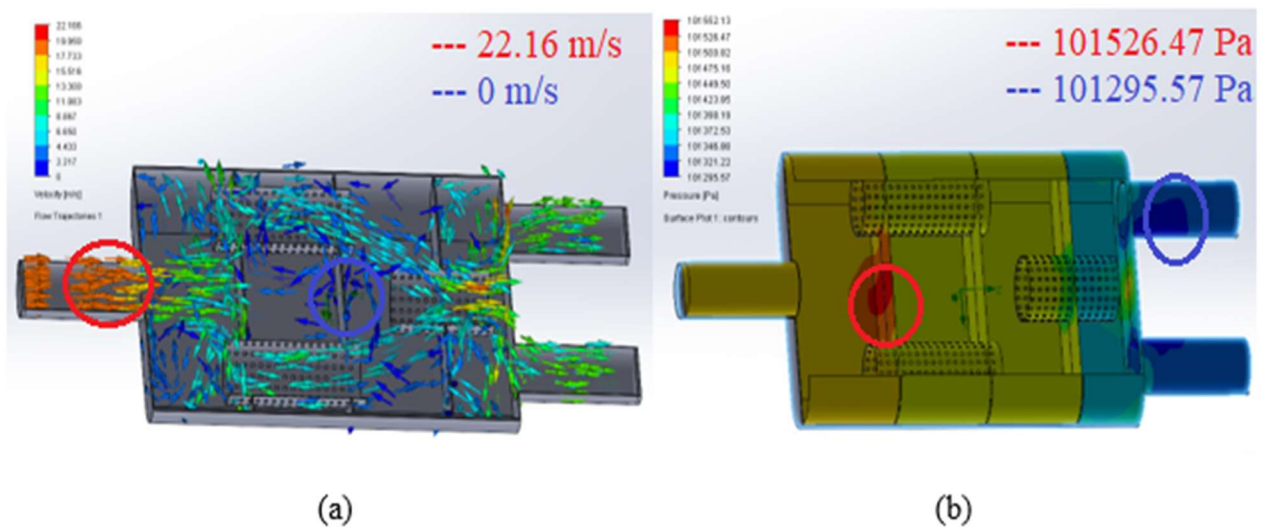


Fig. 77. Velocity trajectories and Pressure contours of design-1

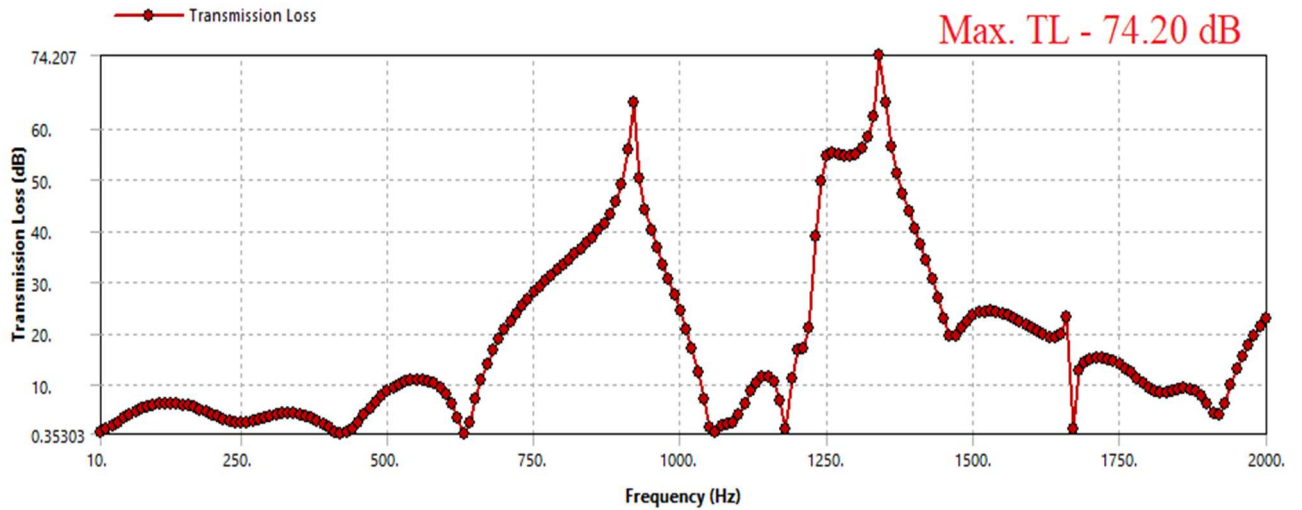


Fig. 78. Frequency Vs Transmission loss graph for design-1

Fig. 78 represents the frequency and transmission loss graph that was performed in Ansys software. The first peak of transmission loss is 65.04 dB at 920 Hz due to the acoustics loss in the vacuum chamber between the two divergent perforation pipes in the first baffle plate. The maximum transmission loss is 74.20 dB at 1340 Hz, this is achieved due to the attenuation of the acoustics transmission in the outlet perforation pipe in the baffle plate.

3.2. Discussions

The transmission loss vs frequency graph is plotted for each design variant of design 1 as shown in fig.79. The graph clearly explains that the transmission loss occurs at the places where the baffle plates are placed. Design 1.1 and 1.2 have baffle plates with different hole patterns placed in the mid of the expansion chamber. They exhibit similar attenuation properties as their peak transmission loss values are close numerical values at the same frequency range. While these baffle plates were incorporated in the muffler design, the transmission loss beyond the last baffle plate yielded maximum attenuation of 13.21 dB at 1380 Hz (design 1.3). Thus, from this design variation evaluation, it can be concluded that the position, shape, size, and pattern of an obstruction in the flow of gases induce loss in the transmission of the flow. For similar designs of the muffler with baffle plate, the transmission loss is low at low frequencies and is high at high frequencies.

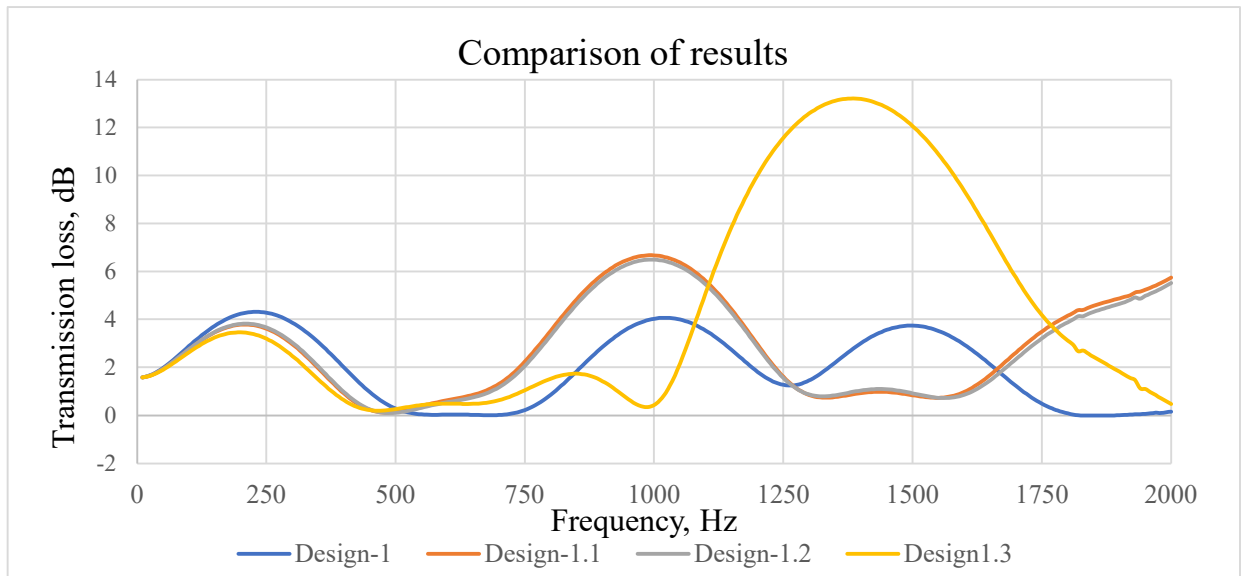


Fig. 79. Frequency vs Transmission loss comparison graph of design (1 – 1.3)

The input and output parameters of the simulation carried out in both Solidworks and Ansys are represented in table 25. Design 1.2 has the lowest backpressure value when compared to other designs. As transmission loss is a more impacting parameter of this study, design 1.3 has proven to have both considerably low value of backpressure and high transmission loss pertaining to be the best variant of design 1.

Table 25. Simulation parameters for design (1-1.3)

Design	Input				Output	
	In Solidworks		In ANSYS		Backpressure (kPa)	Max. TL (dB)
1	Volume flow rate (m ³ /s)	0.049	Surface Velocity (mm/s)	15345	0.015	4.31
1.1					0.0049	6.67
1.2					0.0048	6.49
1.3	Temp. (°C)	600			0.023	13.21

The transmission loss vs frequency graph is plotted for each design variant of design 2 as shown in fig.80. The graph clearly explains that the transmission loss occurs at the places where the V-shaped obstruction is placed. Design 2.1 – 2.4 has a combination of obstruction, baffle plate, and perforated pipe placed in the expansion chamber. They exhibit similar attenuation properties as their peak transmission loss values are close numerical values at the same frequency range. While the baffle plates, perforated pipe, and V obstruction were incorporated in the muffler design, the transmission loss beyond the first baffle plate yielded maximum attenuation of 99.56 dB at 680 Hz (design 2.3). Thus, from this design variation evaluation, it can be concluded that the position, shape, size, and pattern of obstruction, baffle plate, and perforation plate affect the flow and induce loss in the transmission of the flow. For similar designs of the muffler, the transmission loss is high at low frequencies and similar second peak attenuation is observed in the medium frequency range.

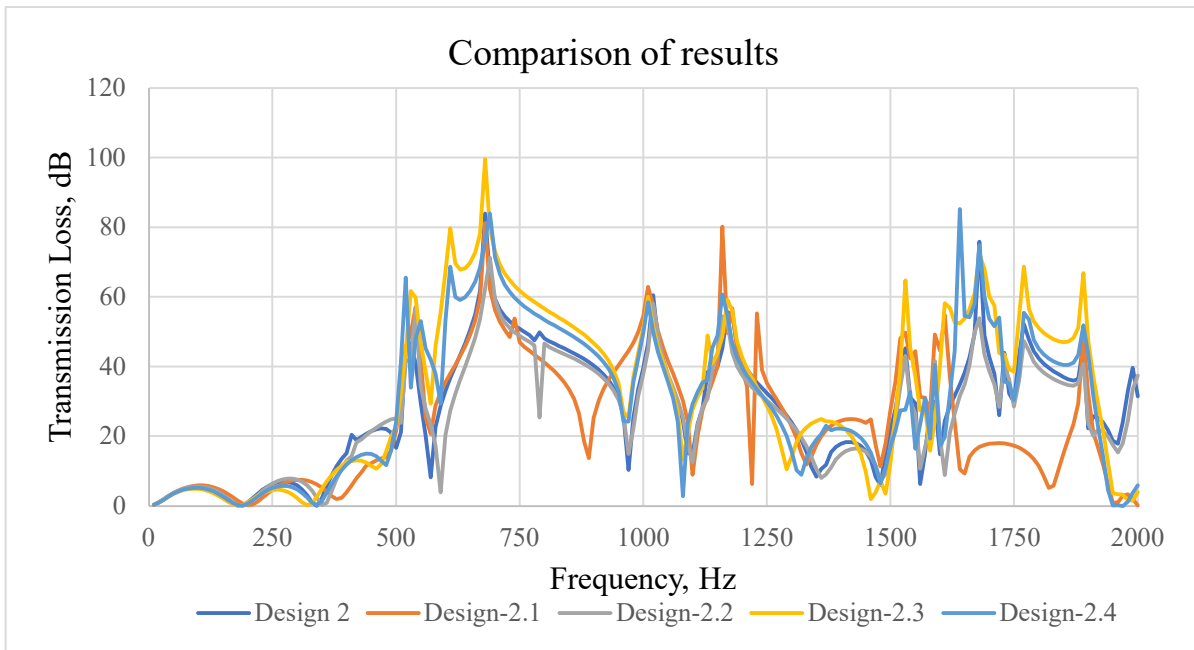


Fig. 80. Frequency vs Transmission loss comparison graph of design (2 – 2.4)

The input and output parameters of the simulation carried out in both Solidworks and Ansys are represented in table 26. Design 2.4 has the lowest backpressure value when compared to other designs. As transmission loss is a more impacting parameter of this study, design 2.3 has proven to have both considerably low value of backpressure and high transmission loss pertaining to be the best variant of design 2.

Table 26. Simulation parameters for design (2-2.4)

Design	Input		Output			
	In Solidworks	In ANSYS	Backpressure (kPa)	Max. TL (dB)		
2	Volume flow rate (m ³ /s)	0.059	Surface Velocity (mm/s)	13649	0.176	83.97
2.1					0.208	81.20
2.2	Temp. (°C)	600	Surface Velocity (mm/s)	13649	0.161	71.26
2.3					0.196	99.56
2.4					0.155	85.27

The transmission loss vs frequency graph is plotted for each design variant of design 3 as shown in fig.81. The graph clearly explains that the transmission loss occurs at the places where the last baffle plate with perforation pipe is placed. Design 3.1 – 3.4 has a combination of the baffle plate and perforated pipe placed in the expansion chamber. They exhibit similar attenuation properties as their peak transmission loss values are close numerical values at the same frequency range. While the baffle plates and perforated pipe were incorporated in the muffler design, the transmission loss beyond the last baffle plate yielded maximum attenuation of 116.13 dB at 1300 Hz (design 3.1). Thus, from this design variation evaluation, it can be concluded that the position, shape, size, and pattern of the baffle plate and perforation plate affect the flow of gases and induce loss in the transmission of

the flow. For similar designs of the muffler, the transmission loss is high at low frequencies and similar second peak attenuation is observed in the medium frequency range.

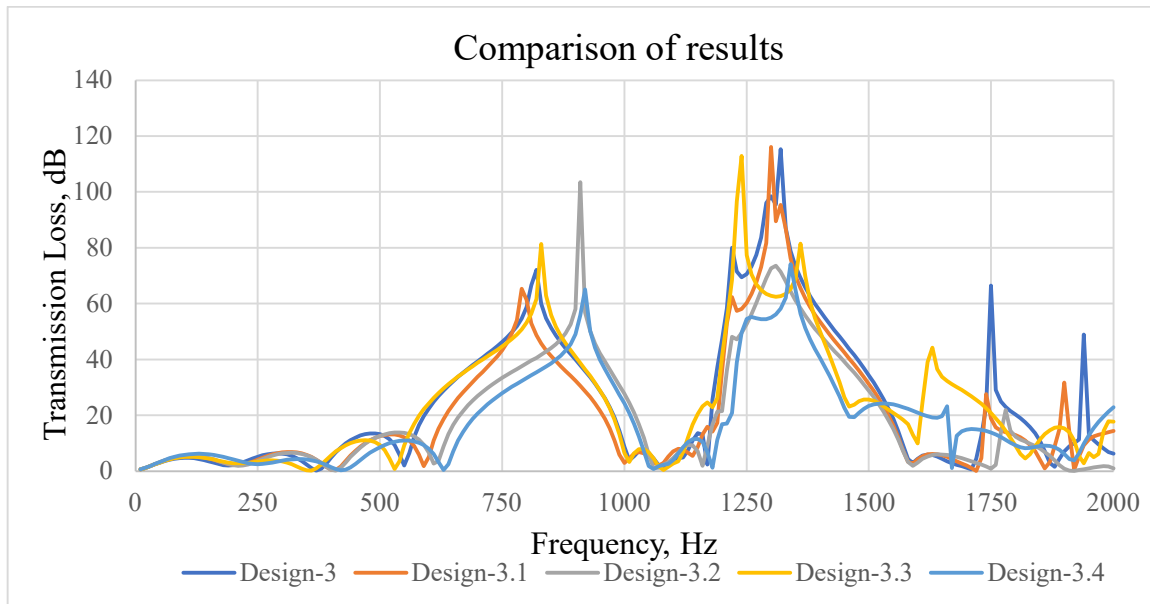


Fig. 81. Frequency vs Transmission loss comparison graph of design (3 – 3.4)

The input and output parameters of the simulation carried out in both Solidworks and Ansys are represented in table 27. Design 3.4 has the lowest backpressure value when compared to other designs.

Table 27. Simulation parameters for design (3-3.4)

Design	Input				Output	
	In Solidworks		In ANSYS		Backpressure (kPa)	Max. TL (dB)
3	Volume flow rate (m ³ /s)	0.066	Surface Velocity (mm/s)	18536	0.284	115.33
3.1					0.179	116.13
3.2	Temp. (°C)	600			0.264	103.53
3.3					0.284	112.97
3.4					0.166	74.207

As transmission loss is a more impacting parameter of this study, design 3.1 has proven to have both considerably low value of backpressure and high transmission loss pertaining to be the best variant of design 3.

Conclusions

1. Scientific papers were reviewed, to study the engine backpressure and transmission loss of the muffler. From the literature review, it is evident that the design of the muffler can be altered to gain the desired range of engine backpressure and acoustics loss by employing different types of obstructions to the expansion chamber. It was stated in numerous papers that reactive mufflers are effective under the low-frequency range.
2. A base muffler was designed. The analytical value of 15.43 at 650 Hz was the closest to the experimental values. The results from the comparison comply with each other. Hence this verifies the setup for the harmonic acoustics simulation that has to be carried out for the different muffler models to verify the significance of transmission loss based on the design modification parameter.
3. Three types of mufflers were designed with different types of design obstructions to stimulate transmission loss. The simulations were conducted, from which the backpressure was calculated using Solidworks.
4. Harmonic acoustics simulations were conducted that yielded a graph that represented the transmission loss of all the mufflers over a frequency range. These results were compared and analyzed for a particular muffler design with different obstructions parameters.
5. From the simulation results, a comparison study was created to understand the impact of the design obstructions inserted into the expansion chamber on transmission loss. This study represents that each obstruction creates a significant amount of acoustics loss. Design 1 yields the maximum transmission loss with the design 1.3 variant having 13.21 dB at 1380 Hz. Design 2 yields the maximum transmission loss with the design 2.3 variant having 99.56 dB at 680 Hz. Design 3 yields the maximum transmission loss with the design 3.1 variant having 116.13 dB at 1300 Hz. Irrespective of the shape of the expansion chamber the baffle plate and perforated pipes create an impact. But to conclude, the position, shape, and size of the obstructions and the design of the expansion chamber play a major role in impacting the transmission loss. From this comparison study, the divergence convergence concept along with the perforated pipes and baffle plates yielded the maximum amount of transmission loss at both low and high frequencies. Even though studies are stating the performance of reactive mufflers under low frequency, it can be seen that the design of the muffler and expansion chamber alters the transmission loss irrespective of the frequency range. Depending on the needs we can design the muffler and the expansion chamber to perform under a specific frequency range.

List of references

1. Behavior of transmission loss in muffler with the variation in absorption layer thickness. Ujjal Kalita, Abhijeet Pratap, Sushil Kumar. 4, s.l. : International Journal of scientific research and management (IJSRM), 2015, Vol. 3. 2656-2661.
2. Optimal Design and Fabrication of Exhaust Muffler. K.Sri Rama Murthy, Dr.Venkata Ramesh Mamilla. 3, s.l. : IJSART, March 2018, Vol. 4. 2395-1052.
3. Foryousolution.blogspot (2013). The history of car mufflers. [online] Available at: <http://foryousolution.blogspot.com/2013/10/the-history-of-car-mufflers.html> [Accessed day 12 April 2021].
4. Alchetron.com (2018) Milton Reeves Biography. [Online] Available at: <https://alchetron.com/Milton-Reeves> [Accessed day: 12 April 2021].
5. Edu.glogster.com 920140. Catalytic Converter [Online] Available at: <https://edu.glogster.com/glog/catalytic-converter/2dam3icjwgtg?=glogpedia-source> [Accessed day: 12 April 2021].
6. Idaoffice.org (2019). Car Mufflers. [online] Available at: <https://idaoffice.org/posts/car-mufflers/> [Accessed day: 12 April 2021].
7. Zia Ur Rahman Farooqi, Muhammad Sabir, Nukshab Zeeshan, Ghulam Murtaza, Muhammad Mahroz Hussain, and Muhammad Usman Ghani. Vehicular Noise Pollution: Its Environmental Implications and Strategic Control. [book auth.] Sezgin Ersoy and Tayyab Waqar. Autonomous Vehicle and Smart Traffic. London, United Kingdom: IntechOpen, 2020.
8. Danijela Miloradović, Jasna Glišović, and Jovanka Lukić. Regulations on-road vehicle noise – trends and future. Mobility & Vehicle Mechanics. 2017, Vol. 43.
9. Elena SANTIAGO CID CEN & CENELEC: “Work programme 2021 - European Standardization and related activities”, 2021, - CEN & CENELEC, Brussels.
10. The European Parliament and the Council of the European Union: “Regulation (EU) No. 540/2014 of the European Parliament and of the Council of 16 April 2014 on the sound level of motor vehicles and of replacement silencing systems and amending Directive 2007/46/EC and repealing Directive 70/157/EEC”, 2014, Official Journal of the European Union, L 158/131 - L 158/195.
11. Quazi Design and Optimization of Exhaust System for Internal Combustion Engines. Lalit Zipre, Prathmesh Aher, Prathmesh Jalgaonkar Mohammad Altaf Prof. T.Z. 5, s.l. : International Journal of Scientific & Engineering Research, 2008, Vol. 9. 2229-551.
12. Study on the Sound Quality of Steady and Unsteady Exhaust Noise. Sun, Falin Zeng and Sunmin. s.l. : Hindawi publications, 2018. 6205140.
13. A Prediction of Noise Reduction of Exhaust Muffler system. Hanida Abdullah, Aminudin Abu, Puziah Muhamad, Aung Lwin Moe, Asnizah Sahekhaini and Lee Kee Quen. s.l. : IEEE.
14. Design Principles for an Automotive Muffler. Dhamangaonkar, Vinod Sherekar and P. R. 4, Pune: Research India Publications, 2014, Vol. 9. 483-489.
15. An Approach to Reduce the Product Variants through Design of Hybrid Muffler for Commercial Vehicle Application. Mandal, Sanjoy Biswas and Goutam. s.l. : SAE International, 2013. 2013-26-0096.
16. General design principles for an automotive muffler. Potente, Daniel. Busselton: IJERT, 2005.

17. Muffler Design for Automotive Exhaust Noise Attenuation - A Review. Mr. Jigar H. Chaudhri, Prof. Bharat S. Patel, and Prof. Satis A. Shah. 1, s.l. : Int. Journal of Engineering Research and Applications, 2014, Vol. 4. 220-223.
18. Analysis of reactive muffler by experimental and numerical method. Sujata Sushant Tambe, and Prof Lagdive H.D. 8, s.l. : JETIR, 2017, Vol. 4. 2349-5162.
19. Acoustic behaviour analysis and optimal design of a multi-chamber reactive muffler. Longyang Xiang, Shuguang Zuo, Xudong Wu, Jun Zhang, Jingfang Liu. 13, china: SAGE Journals, 2016, Vol. 230. 1862-1870.
20. vibration and noise in reactive muffler: A study. Nitinkumar Anekar, Kalpana Girase, Shrikant Nimbalkar, and Santosh Sandanshiv. Pune: Engineering Research Publication and IJEAS, 2015.
21. Design and Fabrication of Reactive Muffler. International Journal of Chemical Science. Reddy, G.G. and Prakash, N. 2, 2016, Vol. 14. 1069-1076.
22. Absorption Materials Used In Muffler A Review. Ujjal Kalita, Abhijeet Pratap, and Sushil Kumar. 2, s.l. : International Journal of Mechanical and Industrial Technology, 2014, Vol. 2. 2348-7593.
23. An Investigation on Shape Optimization of Pressurized Inlet Diffuser in Steam Vent Silencer By Using Computational Fluid Dynamics. Rajgopal, Kiran K, Yeshwantraya Ashtagi. IJERT, 2014, Vol.4. 2248-9622
24. Effect of Liner Layer Properties on Noise Transmission Loss in Absorptive Mufflers. Mostafa Ranjbar, Maryam Alinagh. 2, Gazimagusa: Science Publishing Group, 2016, Vol. 1.
25. Design, Development and Analysis of Absorptive Muffler with Ammonia Pulsator for IC Engine. Jayashri P. Chaudhari, Amol B. Kakade. International Engineering Research Journal, 2014, vol.4.
26. Investigation of transmission loss in muffler by varying absorption material. Ujjal Kalita, Sushil Kumar, Kirti Singh. 6, s.l. : International Journal of Scientific & Engineering Research, 2017, Vol. 8. 2229-5518.
27. Applying Models in Fluid Dynamics. Heidelberg, Michael. s.l. : Taylor and Francis, 2006. 10.1080/02698590600641016.
28. Effect of perforated tube on transmission loss of muffler- A review. Abhijeet Pratap, Ujjal Kalita, Sushil Kumar. 3, s.l. : International Journal of Engineering Research and General Science, 2015, Vol. 3. 2091-2730.
29. Performance of Extended Inlet and Extended Outlet Tube on Single Expansion Chamber for Noise Reduction. Gupta, Amit Kumar. 1, s.l. : International Journal on Emerging Technologies, 2016, Vol. 7. 0975-8364.
30. Acoustical Transmission Loss Performance by Using Various Absorptive Material. Gupta, A., and Sachin Jha. s.l. : International Journal of Scientific & Technology Research, 2019, Vol. 8. 1419-1424.
31. Design optimization of hybrid muffler and acoustic transmission loss prediction. Sibin Babu, Akhildev VP, Jerin Sabu. 7, Kerala : IRJET, 2020, Vol. 7. 2395-0056.
32. Shape optimization of one-chamber mufflers with reverse flow ducts using a genetic algorithm. Chiu, Min-Chie. 1, Taiwan: Journal of Marine Science and Technology, 2010, Vol. 18. 2709-6998.

33. Boundary Element Analysis of Muffler Transmission loss with LS-DYNA. Zhe Cui, Yun Huang. s.l. : 12th international LS-DYNA users Conference, 2012.
34. Muffler Design by Noise Transmission Loss Maximization. Kermani, Milad. s.l. : Eastern Mediterranean University Institutional Repository, 2015.
35. Backpressure study in Exhaust Muffler of single cylinder diesel engine using CFD analysis. M, Puneetha C. G. Manjunath H and Shashidar. s.l. : Altair Technology Conference, 2015.
36. CFD Analysis of Back Pressure of Reactive Muffler. Suyog S. Mane Prof. S. Y. Bhosle and Prof. H. N. Deshpande 12, s.l. : International Journal of Innovations in Engineering Research and Technology, 2016, Vol. 3. 2394 – 3696.
37. CFD Analysis of exhaust manifold of multi-cylinder petrol engine for optimal geometry to reduce backpressure. Navadagi, V., & Sangamad, S. 3, s.l. : IJERT, 2014, Vol. 3. 2278-0181.
38. Muffler Design with Baffle Effect and Perforations on Transmission Loss. Kamarkhani, S., Karimyan, A., Kheybari, M., & Khanali, J. s.l. : The Journal of Engine Research, 2017.
39. CFD analysis on the effects of exhaust backpressure generated by four-stroke marine diesel generator after modification of silencer and exhaust flow design. Ridwan Saputra Nursal, Abdul Hadi Hashim, Nor Isha Nordin, Mohd Afandi Abdul Hamid and Mohd. 4, s.l. : ARPN, 2017, Vol. 12. 1819-6608.
40. Prediction of back pressure of muffler through results obtained b theory and CFD approach. Deshmukh, Yatik Nupur and Bersha. s.l. : International journal of current microbiology and applied sciences, 2020, Vol. 9. 2319-7706.
41. The Main Components of Vehicle Exhaust Gases and Their Effective Catalytic Neutralization. L. R. Sassykova, Y. A. Aubakirov, S. Sendilvelan, Zh. Kh. Tashmukhambetova, M. F. Faizullaeva³, K. Bhaskar, A. A. Batyrbayeva, R. G. Ryskaliyeva¹, B. B. Tyussyupova, A. A. Zhakupova and M. A. Sarybayev. 1, s.l. : Oriental Journal of Chemistry, 2019, Vol. 35. 10.13005/ojc/350112.
42. Acoustic Analysis of a Perforated-pipe Muffler Using Ansys. Ezzeddin. M. Milad, Dr. Mohamed. Jolgef. 19, 2017, Vol. 4.